Morphoelastic rods: Part II: Growing birods

Thomas Lessinnes, Derek E. Moulton, and Alain Goriely

Mathematical Institute, University of Oxford
E-mail: goriely@maths.ox.ac.uk

August 15, 2014

■ **Abstract** The general problem of determining the shape and response of two attached growing elastic Kirchhoff rods is considered. A description of the kinematics of the individual interacting rods is introduced. Each rod has a given intrinsic shape and constitutive laws, and a map associating points on the two rods is defined. The resulting filamentary structure, a growing birod, can be seen as a new filamentary structure. This kinematic description is used to derive the general equilibrium equations for the shape of the rods under loads, or equivalently, for the new birod. It is shown that, in general, the birod is not simply a Kirchhoff rod but rather, due to the internal constraints, new effects can appear. The two-dimensional restriction is then considered explicitly and the limit for small deformation is shown to be equivalent to the classic Timsohenko bi-metallic strip problem. A number of examples and applications are presented. In particular, the problem of two attached rods with intrinsic helical shape and uniform growth is computed in detail and a host of new interesting solutions and bifurcations are observed.

Contents

1 Introduction **3**

2 A single morphoelastic rod **5**
2.1 Kinematics . . . 5
2.1.1 Geometry of curves . . . 5
2.1.2 Kinematics of unshearable Kirchhoff rods . . . 6
2.1.3 Kinematics of growing rods . . . 7
2.2 Mechanics of morphoelastic rods . . . 8
2.3 Constitutive laws . . . 8
2.3.1 Diagonal constitutive laws . . . 9
2.3.2 Inextensible rods . . . 10

3 Morphoelastic birods: kinematics and mechanics **10**
3.1 Geometry of two attached morphoelastic rods . . . 10
3.1.1 Single contact point . . . 10
3.1.2 General geometric definition of a morphoelastic birod . . . 10
3.1.3 Examples . . . 12
3.1.4 The birod as one slender object . . . 14
3.2 Mechanics . . . 17

3.2.1 External loads . . . 17
3.2.2 Internal loads . . . 17
3.2.3 Mechanics of the birod and global quantities . . . 18

4 A birod constrained on the line **19**
4.1 Geometry of linear birods . . . 19
4.2 Constitutive laws and reference state . . . 19
4.2.1 Linear constitutive laws . . . 20
4.2.2 A neo-Hookean birod . . . 21
4.3 Application to tissue tension and differential growth stiffening . . . 21

5 Planar birods **23**
5.1 Geometry of planar birods . . . 23
5.2 Constitutive laws and reference state . . . 24
5.2.1 Extensible sub-rods with linear constitutive laws . . . 25
5.2.2 Extensible sub-rods with linear and diagonal constitutive laws . . . 26
5.2.3 Linear extensible-inextensible sub-rods . . . 27
5.3 Timoshenko's bimetallic strips . . . 27
5.4 Birings . . . 28
5.4.1 Trivial case . . . 28
5.4.2 Inversion of a ring . . . 29

6 3D birods **32**
6.1 Geometry of 3D birods . . . 32
6.2 Generalised moments for the 3D extensible birod . . . 35
6.3 Constitutive laws . . . 36
6.4 Unloaded birod and reference configuration . . . 37
6.5 Unloaded configuration with linear moments . . . 38

7 Homogeneous birods **40**
7.1 A mechanical analogy . . . 40
7.2 Inextensible sub-rods . . . 40
7.3 Identical sub-rods with free glue . . . 41
7.4 Explicit examples . . . 43

8 Conclusions **43**

A Normal frames and frame of directors **52**

B Geometry of the 3D birod as slender structure themselves **53**
B.1 Stretches $\alpha^{\pm}$ and angle θ . . . 54
B.2 Deriving the Darboux vectors of the sub-rods . . . 57

C The unloaded 2D ring **58**

D Constitutive laws for n, M and m for 3D extensible birod **59**
D.1 Constitutive law for $\mathbf{n}$ . . . 59
D.2 Constitutive law for $\mathbf{M}$ and $\mathbf{m}$ . . . 60
D.3 Constitutive laws for $\mathbf{m}^{\pm}$ in function of the kinematic variables of the birod . . . 60

E Linear approximation to the constitutive laws of 2D morphoelastic birods **62**

F Proof of (6.7) **63**

G Calculus for Section 6.2 **65**

H Linear constitutive laws for moments $\mathbf{m}^{\pm}$ **66**

I A computationally friendly version of the birod equilibrium equations **69**

1 Introduction

Within the wealth of structures and shapes found in the natural world, we encounter a great number of filamentary structures. These structures, such as polymers, roots, stems, axons, octopus' arms, elephant trunks, and tendrils, to name a few, can typically be described by a one dimensional representation. Also, at the macroscopic level, their response to external loads can often be accurately modeled by a theory of continuum elastic rods, as has been demonstrated for proteins and DNA [1, 2, 3, 4, 5, 6, 7, 8], plants [9, 10, 11, 12] and in many problems in physiology [13, 14, 15].

The key feature of many such biological filaments is their ability to grow and remodel depending on age and external conditions, a common feature in many three-dimensional processes [16, 17]. This continual growth and remodeling process can serve to accomplish a number of tasks, such as matching growth within an organ or an organism, moving, forming self attachments, or providing mechanical support against external forces. At the level of a rod, growth and remodeling is achieved by an increase in size, a change in reference shape, and evolution of material properties. Whereas a general theory of volumetric growth is, in principle, applicable to these structures, the reduction in geometry offered by the description of a one-dimensional object evolving in a three-dimensional space suggests that a general framework for growing elastic rods (*morphoelastic rods)* offers a simple and more fruitful alternative. This effort was initiated in the first installment of this series of papers [18], where it was shown that a self-contained theory of growing one-dimensional rods can be developed by integrating classical rod mechanics with the general prescription of multiplicative decomposition first proposed within the context of biology in [19]. The problem is then to understand the interplay between growth, geometry, and mechanics within a one-dimensional theory. Since no residual stress is generated through growth in a 1D structure, interesting effects only appear when the rod is constrained geometrically. In [18], the authors considered constraining a single rod, both through elastic attachment to a substrate, and by considering growth in a closed ring geometry. In this second installment, we consider the natural generalization of these problems where the growth of a rod is constrained by another (possibly growing) rod.

The problem of two growing rods forms the first step in understanding the behavior of multiple interacting filaments, a problem of great generality and applicability, as many biological filaments are composed of sub-filaments bundled together. For instance, cells in roots are often organised in files that wind around each other helically around a main core. It is the delicate mechanical balance between geometry and mechanical stress that dictates the shape and functional properties of the roots. At the microscopic level, plant cells are also built from multiple interacting cellulose microfibrils that wind-up along the cells [20]. Again, it is the organisation and interaction of these constituents that dictates the overall response [21, 22]. Flagella are another example of well-studied filaments whose structure and response derive from internal coupled sub-filaments organized in the near universal 7+2 pattern (seven microtubules on a circle with two internal microtubules) [23, 24, 25, 26]. Other examples include the microtubules of axons [27], the triple helix arrangement of arteries and veins in umbilical cord [28, 29], the collagen fibers in arteries [30, 31], and the muscle groups of octopus arms [32] and elephant trunks [33]. Typically in these systems the different sub-filaments grow (or equivalently contract by muscle action) and remodel

at different rates and therefore develop different unstressed configurations that are incompatible with the geometry of the structure. This incompatibility results both in residual stresses in the sub-filaments and in equilibrium configurations of the global structure in which the sub-filaments undergo large displacements. These two correlated phenomena illustrate how macro-filaments of complex shapes and mechanical properties are produced from comparatively simpler sub-filaments.

A general theory for the mechanics of interacting rods has been proposed in [34], where the word "birod" was coined to refer to 'two elastically interacting elastic strands'. This structure was motivated by the study of DNA. Similarly, a number of authors have looked at the mechanics of braids and plies by considering the interaction of two rods in frictionless contact (as typically occurs during the formation of plectoneme structures in the folding of a filament on itself) [35, 36, 37, 38, 39, 40, 41]. The main difference with a birod is that the two strands of the birod interact elastically while in a ply or braid the two strands are assumed to have a continuous zone of hard contact and are allowed to slide along one another. Here we study a different version of the birod where the two rods are "glued" together, this is similar to the original birod [34] as we assume that the strands are not allowed to slide and that there might be an elastic response to the change of angle between the tangents to the strands. However we also assume that like a ply [36], the distance between the centrelines of the strands is constant (a rigid constraint). The present study is therefore well suited to encompass birods for which the attachment mechanism is much stiffer than the elastic strands. In this sense it can be viewed as a limit case of the original birod [34]. Interestingly, these assumptions allow to show best how to introduce a new geometric representation of the structure together with a novel system of balance equations between ensuing generalised stresses. Applying these methods to the original birod would be a natural extension of our contribution.

The paper is organized as follows: In Sec. 2, we summarize the formalism and findings of part I [18]. Sec. 3 develops the kinematic description necessary for the birod and a derivation of the equilibrium equations for the birod. Under our geometrical assumptions, the birod has the same number of degrees of freedom as a single unshearable rod. We show that it is possible to define a single centerline and an orthogonal local frame for the birod. A natural question is whether a birod is equivalent to a Kirchhoff rod in the sense that there exists a definition of stresses and strains satisfying the Kirchhoff equation for a single rod with appropriate constitutive laws. We show that the answer to this question depends on the dimension of the embedding space. In 1D (rod on the line) and 2D (a planar rod), the equilibrium equations are equivalent to Kirchhoff equations for adequately defined global stresses. Furthermore, in the limit of small deformations, the planar case is equivalent to the the classical 1925 Timoshenko bi-metallic strip problem [42]. In 3D, in general the equilibrium equations differ from a Kirchhoff-like rod. In Sec. 4 and Sec. 5 we consider the one- and two-dimensional cases, computing explicitly the unloaded shape and constitutive laws. The 1D examples are used to develop intuition, then the 2D case opens the door to modeling a vast range of applications. Finally, the three-dimensional case is studied in Sec. 6 in full generality. Because the equilibrium equations are now different from Kirchhoff equations, the standard geometric description – in terms of a centreline and orthonormal frame of directors – is no longer adequate, and an alternative geometric approach is proposed. It naturally leads to a different set of global mechanical quantities and to a new set of equilibrium equations. Once again, the unloaded shape of the birod is computed as well as its constitutive laws, and the theory is illustrated with a few examples. The case where the material properties of both the strands and the glue are homogeneous is of particular importance and we study it in detail in Sec. 7. Extensions and conclusions are discussed in Sec. 8.

2 A single morphoelastic rod

In this section, we briefly summarise the notations and concepts introduced in [18], to describe the kinematics and geometry of a growing elastic rod.

2.1 Kinematics

2.1.1 Geometry of curves

A dynamical space curve $\mathbf{r}(R,T)$ is a continuously differentiable function of a material parameter R and time T with values in $\mathbb{R}^3$:

$$\mathbf{r} : [A,B] \times \mathbb{R} \to \mathbb{R}^3 : (R,T) \to \mathbf{r}(R,T), \tag{2.1}$$

where A and B denote the ends of the curve. At any time T, the arc length s is defined as

$$s = \int_A^R \left| \frac{\partial \mathbf{r}}{\partial \sigma}(\sigma,T) \right| \mathrm{d}\sigma. \tag{2.2}$$

To complete the geometrical description of a curve, we attach a local orthonormal basis (or frame). In part I [18], we used the standard Frenet frame. Here we complete this picture by introducing the *natural frame*, as first described in [43]. To define the natural frame, we parametrise the curve by its arc length s, assume that the function $\mathbf{r}(s,T)$ is C^2 with respect to its first variable, and set $A = 0$ without loss of generality (assuming finite length). We define $\mathbf{c}_3 = \frac{\partial \mathbf{r}}{\partial s}$ as the unit tangent vector to the curve. At $s = 0$, $\mathbf{c}_3(0,T)$ is completed by $\mathbf{c}_1(0,T)$ and $\mathbf{c}_2(0,T)$ so that $\{\mathbf{c}_1(0,T), \mathbf{c}_2(0,T), \mathbf{c}_3(0,T)\}$ forms a right handed orthonormal frame. This frame is defined up to an arbitrary phase and is transported along the curve by solving

$$\frac{\partial \mathbf{c}_i}{\partial s} = \mathbf{p} \times \mathbf{c}_i, \tag{2.3}$$

where $\mathbf{p}$ is defined by

$$\mathbf{p} := \mathbf{c}_3 \times \frac{\partial \mathbf{c}_3}{\partial s}. \tag{2.4}$$

The frame $\{\mathbf{c}_1(s,T), \mathbf{c}_2(s,T), \mathbf{c}_3(s,T)\}$ is a *natural frame* of the curve $\mathbf{r}$. As s spans $[0,l]$ (l being the total length of the curve), $\mathbf{r}$ spans the curve and the natural frame rotates about the direction $\mathbf{p}$ at a rate $|\mathbf{p}|$ per unit s. Note that the definition (2.4) does not depend on the choice of phase. Hence, $\mathbf{p}$ is a property of the curve itself and all natural frames have the same $\mathbf{p}$. Furthermore, $\mathbf{p}$ is everywhere orthogonal to $\mathbf{c}_3$ and can be written as:

$$\mathbf{p} = p_1 \mathbf{c}_1 + p_2 \mathbf{c}_2. \tag{2.5}$$

The pair (p_1, p_2) is called the *normal development* of the curve $\mathbf{r}$ [43]. As s spans $[0,l]$, the normal development draws a curve in $\mathbb{R}^2$. Although this new curve is defined up to a global rotation about the origin of $\mathbb{R}^2$ – corresponding to the arbitrary rotation in the definition of the frame at $s = 0$ – its shape provides much information about the geometry of the three-dimensional curve $\mathbf{r}$. The normal development is to normal frames what curvature and torsion are to the Frenet frame. Indeed, p_1 (resp. p_2) specifies the bending of the curve about $\mathbf{c}_1$ (resp. $\mathbf{c}_2$). After parameterisation of the normal development in polar coordinates (p,θ), the curvature κ and torsion τ of $\mathbf{r}$ are recovered as

$$\kappa = p = \sqrt{p_1^2 + p_2^2}, \tag{2.6}$$

$$\theta = \arctan \frac{p_2}{p_1}, \tag{2.7}$$

$$\tau = \frac{\partial \theta}{\partial s} = \frac{p_1\, \partial_s p_2 - p_2\, \partial_s p_1}{p_1^2 + p_2^2}. \tag{2.8}$$

2.1.2 Kinematics of unshearable Kirchhoff rods

An elastic rod is geometrically defined by a dynamic curve called the *centreline* $\mathbf{r}(R,T)$, equipped with a local frame of orthonormal vectors $\{\mathbf{d}_1(R,T),\mathbf{d}_2(R,T),\mathbf{d}_3(R,T)\}$ called the *frame of directors*. The role of this material frame is to keep track of the orientation of the cross section at every point along the centreline. By convention, $\mathbf{d}_3(s,T)$ is normal to the cross section at s, while $\mathbf{d}_1$ and $\mathbf{d}_2$ are tangent to it at the point contained in the centreline. A rod is *unshearable* if its cross-sections remain perpendicular to its centreline in all configurations so that $\mathbf{d}_3 = \mathbf{c}_3$. This is the case considered in this paper and no further mention of unshearability shall be required. The definition of the frame of directors is completed by specifying $\mathbf{d}_1$ as a material direction corresponding to the orientation of the cross section (e.g. along the width of the ribbon in Fig. 1). By orthonormality of the frame of directors, $\mathbf{d}_2 = \mathbf{d}_3 \times \mathbf{d}_1$. The components of any vector $\mathbf{a} = \mathsf{a}_1\mathbf{d}_1 + \mathsf{a}_2\mathbf{d}_2 + \mathsf{a}_3\mathbf{d}_3$ in this particular frame are denoted in the sans-serif fonts by the triplets $(\mathsf{a}_1,\mathsf{a}_2,\mathsf{a}_3)$.

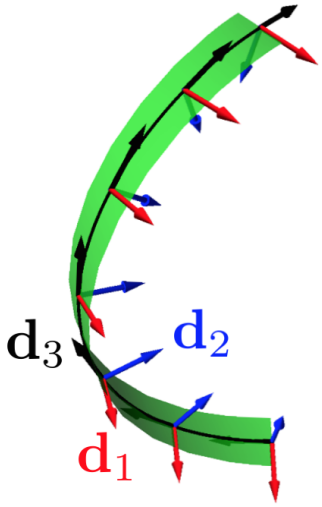

Figure 1: A rod (green online) with its centreline (black online) and local material frame drawn at a few points along the centreline: $\mathbf{d}_1$ (red online), $\mathbf{d}_2$ (blue online) and $\mathbf{d}_3$ (black online).

A *configuration* of a rod can be characterised (up to global translations and rotations) by two local quantities (four degrees of freedom): the *stretch* v and the *Darboux vector* $\mathbf{u}$ of the frame of directors. These quantities are defined (implicitly) by the following relations:

$$\frac{\partial \mathbf{r}}{\partial R} = v\ \mathbf{d}_3; \qquad \frac{\partial \mathbf{d}_i}{\partial R} = \mathbf{u}\times\mathbf{d}_i \quad (i=1,2,3). \tag{2.9}$$

Hence $v = \frac{\partial s}{\partial R}$ characterises the increase or decrease in arclength and $\mathbf{u}$ describes the rotation of the frame of directors: the frame rotates about axis $\mathbf{u}/|\mathbf{u}|$ by an amount $|\mathbf{u}|\mathrm{d}R$ over an infinitesimal displacement $\mathrm{d}R$. Once the functions v and $\mathbf{u}$ are specified, the configuration of the rod can be recovered, up to a global rigid body motion, by integrating (2.9). The curvature and torsion of the centreline can also be recovered from $\mathbf{u}$, giving (see Appendix A):

$$\kappa = \frac{1}{v}\sqrt{\mathsf{u}_1^2+\mathsf{u}_2^2} \quad \text{and} \quad \tau = \frac{1}{v}\left(\mathsf{u}_3 + \frac{\mathsf{u}_1\partial_R\mathsf{u}_2 - \mathsf{u}_2\partial_R\mathsf{u}_1}{\mathsf{u}_1^2+\mathsf{u}_2^2}\right). \tag{2.10}$$

Furthermore, u_1 and u_2 encodes the rate of bending of the centreline about $\mathbf{d}_1$ and $\mathbf{d}_2$ per unit R, while u_3 encodes the twist of the rod.

Note that the notion of a configuration does not involve motion, it is a purely geometric statement. The motion is described by taking a derivative of $\mathbf{r}$ by time T, and through the *spin vector* $\mathbf{w}$ implicitly defined by

$$\frac{\partial \mathbf{d}_i}{\partial T} = \mathbf{w} \times \mathbf{d}_i, \qquad i = 1, 2, 3. \tag{2.11}$$

Introducing the matrix $\mathbf{D} = \begin{pmatrix} \mathbf{d}_1 & \mathbf{d}_2 & \mathbf{d}_3 \end{pmatrix}$, the relations (2.9,2.11) can be written in matrix form $\partial_R \mathbf{D} = \mathbf{D}\mathbf{U}$; $\partial_T \mathbf{D} = \mathbf{D}\mathbf{W}$, with

$$\mathbf{U} = \begin{pmatrix} 0 & -\mathsf{u}_3 & \mathsf{u}_2 \\ \mathsf{u}_3 & 0 & -\mathsf{u}_1 \\ -\mathsf{u}_2 & \mathsf{u}_1 & 0 \end{pmatrix} \quad \text{and} \quad \mathbf{W} = \begin{pmatrix} 0 & -\mathsf{w}_3 & \mathsf{w}_2 \\ \mathsf{w}_3 & 0 & -\mathsf{w}_1 \\ -\mathsf{w}_2 & \mathsf{w}_1 & 0 \end{pmatrix}. \tag{2.12}$$

This form is useful as it allows one to define the Darboux and spin matrices explicitly

$$\mathbf{U} = \mathbf{D}^T \frac{\partial \mathbf{D}}{\partial R}, \quad \text{and} \quad \mathbf{W} = \mathbf{D}^T \frac{\partial \mathbf{D}}{\partial T}. \tag{2.13}$$

It is important to note that when modeling an actual slender structure as a Kirchhoff rod, a number of choices have to be made. First, the centreline has to be chosen. For a free rod, one may choose to define it through the centre of mass of the sections. With external attachments or constraints, however, alternative choices may work better. Similarly, a choice of orientation for the section-wise directors $\{\mathbf{d}_1, \mathbf{d}_2\}$ is required. In most cases, the directors will be chosen to lie along the principal axes of the distribution of Young's modulus in the rod (if the sections are constitutively uniform, this amounts to the principal axes of the second moments of area).

2.1.3 Kinematics of growing rods

We now turn our attention to the kinematics of growing rods, for which three special configurations play important roles: the initial configuration $\mathcal{B}_0$, the reference configuration $\mathcal{V}$ and the current configuration $\mathcal{B}$.

The *reference configuration* of an elastic rod is the configuration it assumes when stress free. The stretch $\hat{v}$ and Darboux vector $\hat{\mathbf{u}}$ corresponding to this configuration are denoted with a hat to emphasise their special status. It is often convenient to parameterise rods by their arc length in this state and we denote this quantity with an upper case S. Technically, we can designate one tip of the rod as the origin. Then S is defined as the (one-to-one) map between material points of the centreline and the arc length from the origin to the material point in the reference configuration. With this parameterisation, the reference state by definition has the property $\hat{v} = 1$ and is completely described by the definition of its Darboux vector $\hat{\mathbf{u}}$.

To proceed, we must clarify the notion of growth and maps evolving in time. We define a *morphoelastic rod* as an elastic rod whose reference configuration evolves on a growth time scale t that is slow in comparison to the time scale associated with the mechanical motion of the rod, associated with the time T. Only the latter gives rise to inertial terms in the balance of momenta, while the former changes the properties of the rod in quasi static fashion.

Having defined the slow (growth) time scale t, the *initial configuration* is the reference configuration at time $t = 0$. All quantities in this state are denoted by a subscript 0. In particular, we define S_0 as the (one-to-one) map between material points of the centreline and their reference arc-length in the initial configuration. Inverting this mapping and composing it with S leads to the definition of a one-to-one map Γ so that $S = \Gamma(S_0, t)$. With these definitions, the addition (or resorption) of new matter along the centreline is captured by the *growth factor* γ:

$$\gamma(S_0, t) = \frac{\partial \Gamma}{\partial S_0} = \frac{\partial S}{\partial S_0}, \tag{2.14}$$

where the second equality consists of a benign abuse of notations that amounts to identifying material points and their parameterisation by the associated arc-length in the initial configuration whereby S becomes a function of S_0 and t.

At any time t, the *current configuration* is defined as the shape assumed by the rod under the actual constraints and loads that are applied to it. Naturally, the material points of the centreline can also be parameterised by the corresponding *current arc length* s. We then define the *elastic stretch* of the rod as $\alpha = \frac{\partial s}{\partial S}$ and its *total stretch* by $\lambda = \frac{\partial s}{\partial S_0} = \alpha\gamma$. While α is a mechanical deformation, γ is the *growth stretch* as it encodes the elongation of the reference configuration purely due to growth. The total stretch λ contains information about both stretches. While λ is typically the easiest parameter to access experimentally, a mechanical description of the process requires separating growth from mechanical stretch.

Note the subtle difference between the geometric stretch $v = \frac{\partial s}{\partial R}$ defined in (2.9) for any parameterisation R of $\mathbf{r}$ and the elastic stretch $\alpha = \frac{\partial s}{\partial S}$. Both quantities are equal whenever the morphoelastic rod is parameterised by its reference arc length. Similarly, when studying morphoelastic rods, and unless otherwise specified, we always assume that $\mathbf{u}$ refers to the Darboux vector of the rod parameterised by its reference arc-length S, i.e. $\mathbf{u}$ is defined by

$$\frac{\partial \mathbf{d}_i}{\partial S} = \mathbf{u} \times \mathbf{d}_i.$$

In particular, considering the slow growth time t, a change in γ captures the elongation of the reference configuration as the rod grows, while a change in $\hat{\mathbf{u}}$ captures a change of reference shape.

2.2 Mechanics of morphoelastic rods

To describe the mechanics of rods, the geometric description of Sec. 2.1 must be completed by information regarding mass distribution in the cross sections. Following [44], we define the linear density of mass (ρA) and second moment of mass inertia $(\rho I)_{1,2}$ per unit R along the centreline $\mathbf{r}(R,T)$ as

$$(\rho A)(S) = \int_{\mathcal{S}} \rho(S, x_1, x_2)\mathrm{d}x_1\mathrm{d}x_2, \tag{2.15}$$

$$(\rho I)_1(S) = \int_{\mathcal{S}} \rho(S, x_1, x_2)x_2^2\mathrm{d}x_1\mathrm{d}x_2, \qquad (\rho I)_2(S) = \int_{\mathcal{S}} \rho(S, x_1, x_2)x_1^2\mathrm{d}x_1\mathrm{d}x_2, \tag{2.16}$$

where $\mathcal{S}$ is the section at S with points labelled (x_1, x_2) according to their location at $\mathbf{r}+x_1\mathbf{d}_1+x_2\mathbf{d}_2$, and ρ is the mass density per unit stress-free volume.

Finally, we define the resultant force $\mathbf{n}(R,T)$ and resultant moment of forces $\mathbf{m}(R,T)$ about $\mathbf{r}(R,T)$ applied by the material at $R' > R$ on the material at $R'' < R$. The balance of momenta yields [44]

$$\begin{aligned} &\frac{\partial \mathbf{n}}{\partial R} + \mathbf{f} = (\rho A)\frac{\partial^2 \mathbf{r}}{\partial T^2}, \\ &\frac{\partial \mathbf{m}}{\partial R} + \frac{\partial \mathbf{r}}{\partial R} \times \mathbf{n} + \mathbf{l} = (\rho I)_2\ \mathbf{d}_1 \times \frac{\partial^2 \mathbf{d}_1}{\partial T^2} + (\rho I)_1\ \mathbf{d}_2 \times \frac{\partial^2 \mathbf{d}_2}{\partial T^2}, \end{aligned} \tag{2.17}$$

where $\mathbf{f}$ and $\mathbf{l}$ are the external densities of forces and moments about $\mathbf{r}(S,T)$ applied on the rod per unit of R.

2.3 Constitutive laws

The system is completed with constitutive laws. We refer to part I [18] for a more detailed discussion. Here, we recall the assumption that there exist functions $\mathbf{K}$ and k relating the four strains

$\mathbf{u}-\hat{\mathbf{u}}$ and $v-\hat{v}$ to the four stresses that deliver work under their respective virtual displacements:

$$\mathbf{m} = \mathbf{K}(\mathbf{u}-\hat{\mathbf{u}}, v-\hat{v}), \tag{2.18}$$

$$\mathsf{n}_3 = k(\mathbf{u}-\hat{\mathbf{u}}, v-\hat{v}). \tag{2.19}$$

By definition of the reference configuration, it is required that $\mathbf{K}(\mathbf{0},0)=\mathbf{0}$ and $k(\mathbf{0},0)=0$ and that $(\mathbf{0},0)$ is the only simultaneous minimum of these functions. We assume that both functions derive from a convex and coercive energy-density function $W(\mathbf{u},v)$ that relates the strains $\mathbf{u}$ and v to the line density of mechanical energy stored in the rod with a unique minimum at $(\hat{\mathbf{u}},\hat{v})$.

2.3.1 Diagonal constitutive laws

It is often assumed that the tension depends solely on the stretch and the bending moment depends only on the curvature and twist, i.e. $\mathsf{n}_3 = k(v-\hat{v})$ and $\mathbf{m}=\mathbf{K}(\mathbf{u}-\hat{\mathbf{u}})$, in which case the constitutive laws are said to be *diagonal*. Because rods are slender bodies and provided that $|\mathbf{u}-\hat{\mathbf{u}}| \ll \delta$ where $1/\delta$ is the characteristic radius of the cross-section, a first order development of $\mathbf{K}$ about $\hat{\mathbf{u}}$ is found to be an excellent approximation for many problems. In this case, we have explicitly

$$\mathbf{m} = (EI)_1\ (\mathsf{u}_1-\hat{\mathsf{u}}_1)\,\mathbf{d}_1 + (EI)_2\ (\mathsf{u}_2-\hat{\mathsf{u}}_2)\,\mathbf{d}_2 + (\mu J)\ (\mathsf{u}_3-\hat{\mathsf{u}}_3)\,\mathbf{d}_3, \tag{2.20}$$

where the parameter (μJ) depends both on the shear modulus and the shape of the cross-section [45, 46, 47, 44] and

$$(EI)_1(S) = \int_{\mathcal{S}} E(S,x_1,x_2)\,x_2^2\,\mathrm{d}x_1\mathrm{d}x_2, \qquad (EI)_2(S) = \int_{\mathcal{S}} E(S,x_1,x_2)\,x_1^2\,\mathrm{d}x_1\mathrm{d}x_2, \tag{2.21}$$

where E is the Young's modulus at $\mathbf{r}(S)+x_1\mathbf{d}_1+x_2\mathbf{d}_2$ and where the centreline has been defined such that

$$\int_{\mathcal{S}} E(S,x_1,x_2)\,x_1\,\mathrm{d}x_1\mathrm{d}x_2 = 0, \qquad \text{and} \qquad \int_{\mathcal{S}} E(S,x_1,x_2)\,x_2\,\mathrm{d}x_1\mathrm{d}x_2 = 0. \tag{2.22}$$

Furthermore, the constitutive law (2.20) assumes that $(\mathbf{d}_1,\mathbf{d}_2)$ correspond to the principal directions of the distribution of E in each section. Also, note that if E is constant in the section then $(EI)_1 = EI_1$ and $(EI)_2 = EI_2$ where I_1 and I_2 are the second moment of area with respect to the axis along $\mathbf{d}_1$ and $\mathbf{d}_2$ respectively and going through the point $\mathbf{r}$.

If the stretch[1] is small, that is $|v-\hat{v}| \ll \hat{v}$, then a linear constitutive law for the tension is also found to be a suitable approximation in many situations (but higher stretches may require more refined constitutive laws, especially for biological tissues). In this case, the constitutive laws (2.18,2.19) become

$$\begin{pmatrix}\mathbf{m}\\ \mathsf{n}_3\end{pmatrix} = \mathcal{K}\begin{pmatrix}\mathbf{u}-\hat{\mathbf{u}}\\ v-\hat{v}\end{pmatrix}, \quad \text{where} \quad \mathcal{K} = \begin{pmatrix}(EI)_1 & 0 & 0 & 0\\ 0 & (EI)_2 & 0 & 0\\ 0 & 0 & (\mu J) & 0\\ 0 & 0 & 0 & (E\mathcal{A})\end{pmatrix} \tag{2.23}$$

and $(E\mathcal{A})$ is defined as

$$(E\mathcal{A}) = \int_{\mathcal{S}} E(S,x_1,x_2)\mathrm{d}x_1\mathrm{d}x_2. \tag{2.24}$$

Note that if the Young's modulus E is constant over a section, Eq. (2.24) reduces to $(E\mathcal{A}) = E\mathcal{A}$ where $\mathcal{A}$ is the area of the cross section of the rod.

[1] Note we use the term stretch to refer to either axial extension *or* compression.

2.3.2 Inextensible rods

It is sometimes useful to assume that the rods elongation under tensile forces is negligible. In those cases, the rod is said to be *inextensible*: the arc length between any two points R_1 and R_2 on the centreline is the same in all configurations and by definition: $v = \hat{v}$ (equal to unity if R is chosen to be the reference arc length). In such a case, the tensile stress n_3 is no longer known constitutively and the constitutive laws reduce to (2.18) alone.

3 Morphoelastic birods: kinematics and mechanics

Our aim is to develop a general framework to study the mechanics of morphoelastic birods. In this section, we introduce a number of conventions and definitions for the rest of the paper. In the next sections we consider the cases of birods embedded in 1D (Sec. 4) and 2D (Sec. 5) Euclidian spaces. The reduced dimensionality is instructive for the theory but is also applicable to several applications. We study the more general case of 3D birods in Sec. 6.

3.1 Geometry of two attached morphoelastic rods

As briefly outlined in the introduction, a birod consists of two morphoelastic rods, called *sub-rods*, which are attached to one-another along their length. We label the sub-rods by a sign '+' or '−' and all variables relating to either rod acquire the corresponding superscript. For instance, the sub-rods are parameterised by their reference arc-length S^+ and S^-. The attachment between the sub-rods is not trivial and needs to be fully specified.

3.1.1 Single contact point

We consider first the simplest case of two non-growing sub-rods with circular cross-sections of constant radii $a^\pm$. The construction of a birod is shown schematically in Fig 2. Define a curve on the surface of each subrod (Fig 2(a)), and then imagine twisting the rods so that the curves are aligned (Fig 2(b)). The next step is to "glue" the rods together, which requires defining a gluing map between material points of each rod (Fig 2(c)). In the absence of external loads, the glued birod (Fig 2(d)) relaxes to its reference state (Fig 2(e)).

Mathematically, this procedure defines unambiguously a contact line: referring to the green line in Fig 2(e)), this is a material curve $\mathbf{c}^+ = \mathbf{c}^-$ on the surface of both sub-rods that can be written

$$\mathbf{c}^\pm : [0, L^\pm] \to \mathbb{R}^3 : S^\pm \to \mathbf{r}^\pm + a^\pm \left[\cos\varphi^\pm(S^\pm)\mathbf{d}_1^\pm + \sin\varphi^\pm(S^\pm)\mathbf{d}_2^\pm\right]. \tag{3.1}$$

The functions $\varphi^\pm$ are the polar angles of the contact point in the local frame $(\mathbf{d}_1^\pm, \mathbf{d}_2^\pm)$ of its cross-section. The functions $\varphi^\pm$ can be defined in any configuration of the birod and are invariant under any elastic deformations.

The "gluing map" is a bijection between material points of the subrods, i.e. a map

$$G : [0, L^-] \to [0, L^+] : S^- \to S^+ = (\mathbf{c}^+)^{-1}(\mathbf{c}^-(S^-)). \tag{3.2}$$

Under our assumptions, G is invariant under any elastic deformation of the birod. However, as we will see in the next section, it can be modified when the sub-rods undergo growth.

3.1.2 General geometric definition of a morphoelastic birod

For sub-rods with general cross sections, the definition of a contact line is not always straightforward. Indeed, in many cases such as polygonal cross sections, the rods actually have a contact

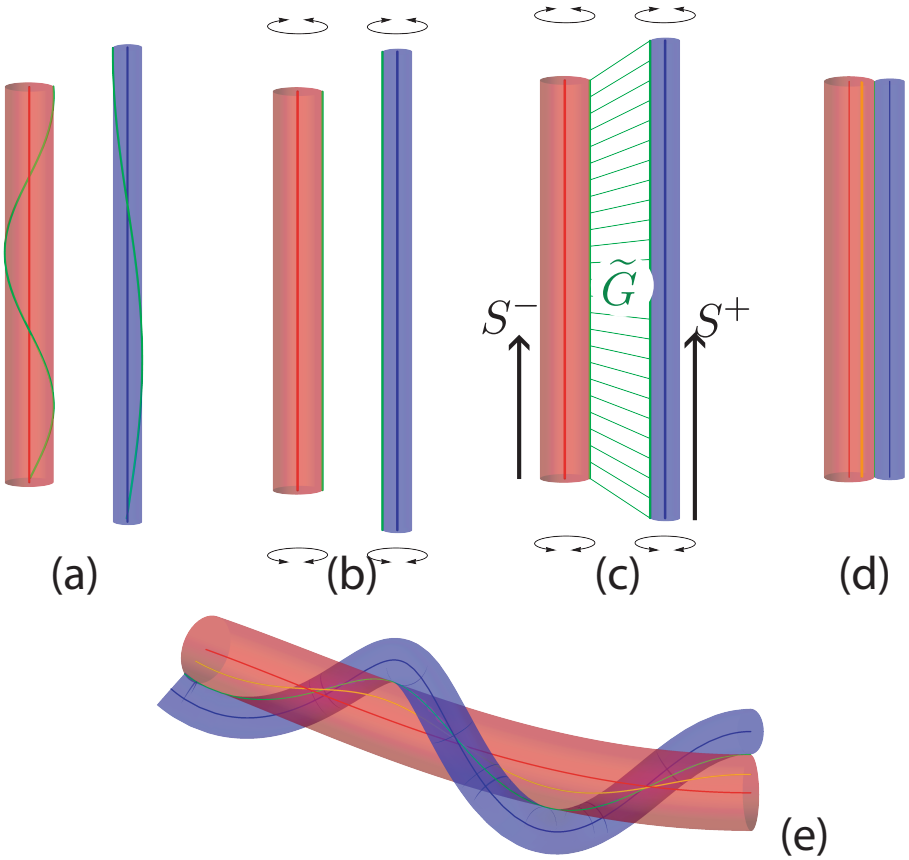

Figure 2: (a) The sub-rods in their reference states with the (material) contact line (green online). (b→d) A sequence of configurations showing the steps leading to a birod in a current configuration (e). Depending on the external loads, the birod of (d) could relax to elastically deform to a shape similar to (e)

surface. For this reason, we define geometrically an attachment between two sub-rods that does not rely on the shape of the section but is intrinsic to the configuration of the rods.

We start with two elastic sub-rods labelled by $+$ and $-$, with lengths $L_0^\pm$ and arclength parameters $S_0^\pm$ in an initial configuration. Each sub-rod is geometrically described by a space curve $\mathbf{r}^\pm$ and a director frame $\{\mathbf{d}_1^\pm, \mathbf{d}_2^\pm, \mathbf{d}_3^\pm\}$, with $\mathbf{d}_3^\pm$ along the tangent of their respective curves. A *morphoelastic birod* is defined by the two sub-rods and an attachment, characterised by the following:

- A *gluing function* G_0: that is, a continuous and monotonic map $G_0 : [0, L_0^-] \to [0, L_0^+]$ such that
$$G_0(S_0^-) = S_0^+. \tag{3.3}$$
- The *distance constraint*: the distance between paired points on the two sub-rods is uniform. That is $a_0 = |\mathbf{r}^-(S_0^-) - \mathbf{r}^+(G_0(S_0^-))|$[2] is independent of S_0^-.
- The *polar angle* $\varphi_0^- : [0, L_0^-] \to \mathbb{R}$ of the vector $\mathbf{r}^+ - \mathbf{r}^-$ in the local frame $(\mathbf{d}_1^-, \mathbf{d}_2^-)$
- The *polar angle* $\varphi_0^+ : [0, L_0^+] \to \mathbb{R}$ of the vector $\mathbf{r}^+ - \mathbf{r}^-$ in the local frame $(\mathbf{d}_1^+, \mathbf{d}_2^+)$.

[2]In most cases, we will try to avoid such cumbersome notations. Quantities such as $\mathbf{r}^-(S_0^-) - \mathbf{r}^+(G(S_0^-)) = (\mathbf{r}^- - \mathbf{r}^+ \circ G_0)(S_0^-)$ will simply be written as $\mathbf{r}^- - \mathbf{r}^+$ where the composition by G_0 at the adequate place is implicit.

These three maps and the distance constraint can evolve in the quasi-static evolution of the system (the slow growth time t) but they are not the result of a mechanical balance. Rather, they are kinematic constraints imposed on the two sub-rods. In the context of growth, t can be thought of as the time and we will talk of growing rods even though the kinematic description is valid for any other process that changes the intrinsic geometry or material parameters in time. The distance constraint is of great use in the mathematical treatment; while it reduces the generality of the approach, the system is still sufficiently general to model many systems with analytical treatment.

The growth of each sub-rod is specified by the growth maps $\Gamma^{\pm}$ (cf. Sec. 2.1.3) so that their reference arc lengths $S^{\pm}$ obey :

$$\begin{aligned} S^- &= \Gamma^-(S_0^-, t). \\ S^+ &= \Gamma^+(S_0^+, t). \end{aligned} \tag{3.4}$$

These growth functions define an evolving gluing function $G : [0, L^-] \to [0, L^+]$ such that

$$G(S^-) = \left(\Gamma^+ \circ G_0 \circ (\Gamma^-)^{-1}\right) = S^+. \tag{3.5}$$

By analogy with the definition (2.14) of a growth stretch γ for a single morphoelastic rod, we define the *relative growth stretch* g of the "+" rod with respect to the "−" rod as

$$g = \frac{\partial G}{\partial S^-}. \tag{3.6}$$

There is an interesting and important equivalence in the growth of birods. The gluing function G_0 specifies the sections of the two sub-rods that are connected. Each reference configuration can grow independently while remaining attached. An equivalent viewpoint is to consider two rods free to grow up to a time t and attach them by a gluing function at that time. Therefore, the attachment and growth processes commute in the sense that the mechanical equilibrium in the current configuration is independent of the order in which these two basic processes take place: rods can be glued then grown or, equivalently, first grown and then glued. In this context the growth stretch g really represents the differential growth between the two rods.

The polar angle maps $\varphi_0^{\pm}$ can also evolve under growth

$$\varphi^{\pm}(S^-, t) = {\varphi_0}^{\pm}(S^-) + \phi^{\pm}(S^-, t) \tag{3.7}$$

where the functions $\phi^{\pm}$ allow for an active change of the direction of the attachment as growth and remodelling occurs. The polar angle $\varphi^{\pm}(S^-, t)$ is an important quantity that will require further study when we model the process of mechanical attachment. Note that for systems where there is no active reorientation of the attachment, $\phi^{\pm} = 0$ and the maps $\varphi^{\pm}$ are fixed.

We also let the distance constraint evolve in time t, however while remaining uniform. That is, the distance $a(t) = |\mathbf{r}^- - \mathbf{r}^+|$ is independent of position.

Note that our definition of a birod implies that the point at $\mathbf{r}^+$ lies in the plane spanned by $(\mathbf{d}_1^-, \mathbf{d}_2^-)$. Similarly, the point $\mathbf{r}^-$ lies in the plane spanned by $(\mathbf{d}_1^+, \mathbf{d}_2^+)$.

3.1.3 Examples

To elucidate the role and practical use of the growth function, we briefly outline 3 examples of problems whose geometry can be well modelled within our framework.

Example 1: Timoshenko's bi-metallic strip. Consider two initially flat thermo-elastic strips bonded together in their unstressed configuration, each susceptible to thermal expansion and only allowed to deform in the plane perpendicular to their width (Fig. 3(a)). This classic problem was first described by Timsohenko in 1925 [42]. We can model the deformation of these bonded strips as a birod evolving in the plane with trivial polar angle $\varphi^{\pm} = \frac{\pi}{2}$ and distance $2a$ taken as the sum of the strip thickness. We identify the temperature t_0 as the temperature at which both plates of initial length L_0 are flat and initially bonded. We assume that the strips have different thermal expansion coefficients c^+ and c^-. Hence, when the plates are brought to a new temperature t (such that $|t - t_0| \ll t_0$), their reference lengths become $L^{\pm} = L_0\,[1 + c^{\pm}(t - t_0)]$ and we compute

$$g(t - t_0) = \frac{L^+}{L^-} = \frac{1 + c^+(t - t_0)}{1 + c^-(t - t_0)}. \tag{3.8}$$

We will return to this example in Sec. 5.3, where we compute the mechanical equilibrium of a bi-metallic strip and recover Timoshenko's result in the limit of small deflections.

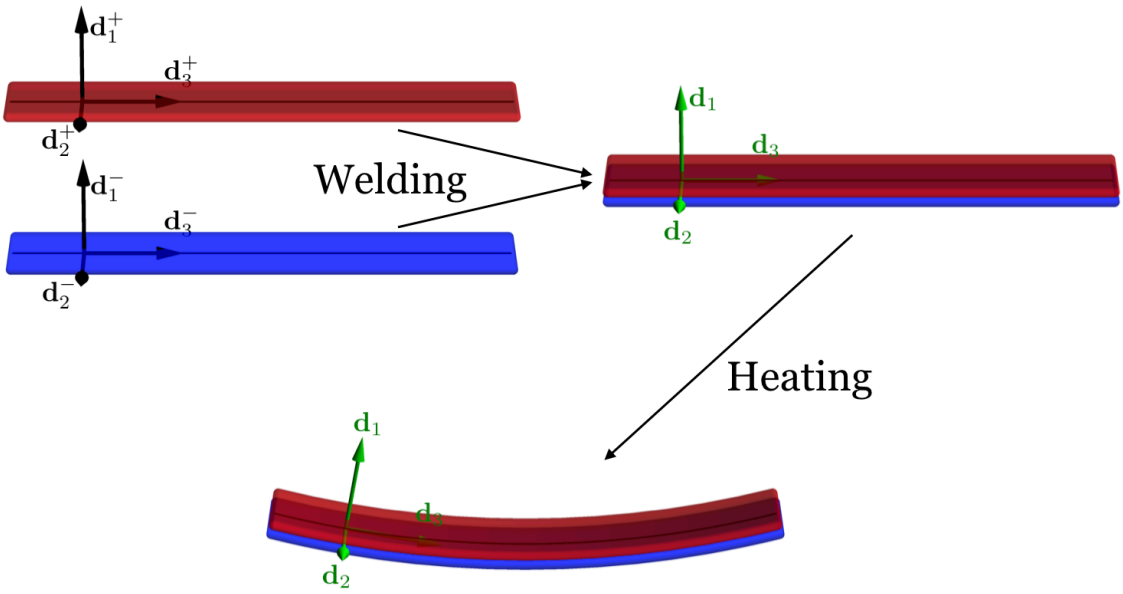

Figure 3: Bi-metallic strips can be modelled within the framework of morphoelastic birods by considering the deformation of the centrelines of each strips as they are bonded through welding and deform by thermal expansion.

Example 2: Uniform growth in 3D A simple example in 3D is to consider initially two rods of circular cross section and diameter a but of different lengths such that the gluing function and one of the polar angle functions are linear. Then we have

$$S_0^+ = G_0(S_0^-) = \frac{L_0^+}{L_0^-} S_0^-, \quad \varphi_0^- = 0, \quad \varphi_0^+ = \omega S_0^-, \quad a_0 = a. \tag{3.9}$$

In this case, the mechanical structure obtained by the attachment is equivalent to a structure where the "+" rod is first twisted so that the helical curve traced by the polar angle φ_0^+ becomes a straight line, then compressed (or extended) uniformly by an amount $1/g_0 = \frac{L_0^-}{L_0^+}$, and then glued to the "-" rod. In the case where $\omega = 0$, so that no twisting is required, the structure might be thought of as an idealised model of a plant with one filament growing at a different rate. A natural question is

whether the resulting structure forms a planar or non-planar (e.g. helical) shape. We consider this explicitly in Sec. 7.2.

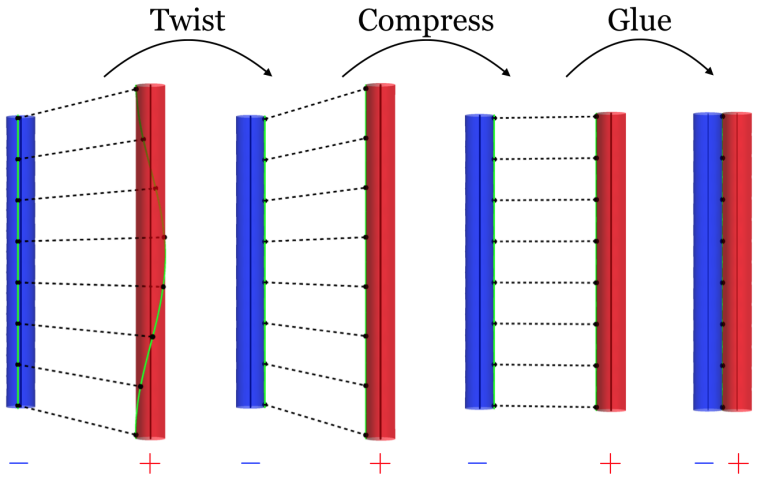

Figure 4: Uniform growth of a twisted rod. Here one rod is grown uniformly and attached along a helical path to a second rod. This is equivalent to specifying the initial length of both rods, and linear gluing and polar angle functions.

Example 3: A ladder with rigid spokes. The interesting design proposed in [48] can also be modelled within the framework of (non-growing) birods. In this system, two elastic flanges are connected by a number of rigid spokes (see Fig. 5). The spokes insure that the flanges stay at a constant distance a from one another. Since the length of the spokes is much larger than the thickness of the flanges, the structure may adopt shapes for which $|a\mathbf{u}^{\pm}| > 1$ while still satisfying the condition $|a^{\pm}\mathbf{u}^{\pm}| \ll 1$ so that each flange can be treated as a Kirchhoff rod. This particular structure leads to a number of interesting non-trivial mechanical equilibria studied in details [48]. We will show how these solutions can also be recovered within our framework in Sec. 7.3.

3.1.4 The birod as one slender object

When attaching two rods to create a birod, the resulting object is also a slender structure. It is therefore a natural question to ask whether its mechanical response is equivalent to that of a single elastic Kirchhoff rod. Such an upscaling would require two parts: first the definition of a single centreline and frame of directors, and second, the mechanical balance of the birod as a single structure. We consider the definition of a birod centreline and frame of directors in this section, and defer consideration of forces and moments to the subsequent section.

Consider the birod in Fig. 6. We define the centreline of the birod as a curve lying between the centrelines of the two sub-rods, that is

$$\mathbf{r} = (1-\beta)\,\mathbf{r}^{-} + \beta\,\mathbf{r}^{+}, \tag{3.10}$$

where $\beta \in [0,1]$ is an arbitrary constant.

A note regarding parameterization. *With two rods that are each independently growing and changing arclength, we are confronted with numerous choices for how to parameterize any given curve/vector. The key point is that all maps are one-to-one, so for instance while the curve above could easily be parameterized by S^{-}, since $S^{+} = G(S^{-})$, it could also be parameterised by S^{+} using the inverse of G, or S_0^{+} for that matter. Parameterization is irrelevant when referring to the curve*

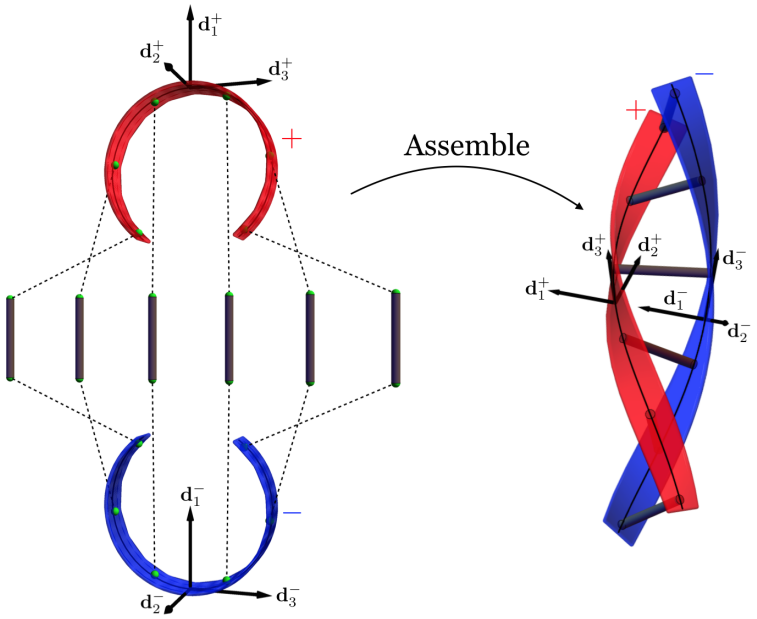

Figure 5: Left: An interesting structure can be generated by taking two rods with intrinsic curvature (flanges) and constraining their distances (spokes). Right: The assembled structure is a ladder that can be modeled as a continuous birod as explained in the main text.

itself. It is only when considering reference states, and defining quantities such as elastic stretch – which requires taking a derivative with respect to a reference arclength – that care must be taken. For notational simplicity, we try to avoid making a particular choice of parameterization except when needed.

Along these lines, it is important to define a reference arclength of the birod, which we do below, but we remark that the birod centreline could be written in any of the parameterizations.

Let us assume the existence of a *reference configuration* for the birod (the exact definition of which depends on the dimension of the embedding space and is therefore postponed to Sections 4, 5 and 6). The arc length along the curve $\mathbf{r}$ in this configuration is called the *reference arc length of the birod* S. This defines a bijective map $G^- : [0, L] \to [0, L^-]$ between S and S^- defined by

$$\left(G^-\right)^{-1} : S^- \to S = \int_0^{S^-} \left| \frac{\partial \mathbf{r}_{\text{ref}}(\sigma, t)}{\partial \sigma} \right| \mathrm{d}\sigma, \tag{3.11}$$

where $\mathbf{r}_{\text{ref}}$ is the centreline of the birod in its reference state (defined up to a rigid body motion). The mapping G^+ from the birod to the + rod is obtained by

$$G^+ = G \circ G^-. \tag{3.12}$$

It is useful to define the growth stretch of each rod with respect to the centreline as

$$g^\pm = \frac{\partial G^\pm}{\partial S}. \tag{3.13}$$

Any scalar function $\widetilde{\chi}$ of S^- or S^+ can be expressed as a function χ of S by the composition

$$\chi = \widetilde{\chi} \circ G^\pm, \tag{3.14}$$

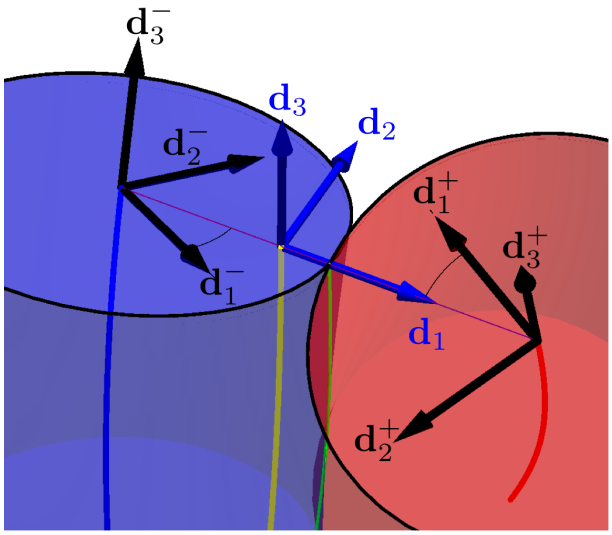

Figure 6: Details of the centrelines and director bases in a birod. The left (blue online) and right (red online) curves are the centrelines of the sub-rods shown with their local frames. Note the line along $\mathbf{d}_1$ connecting one point $\mathbf{r}^-$ to its associated point $\mathbf{r}^+$ in the + rod. The middle vertical curve (yellow online) is the centreline of the rod shown with its own frame.

and by application of the chain rule to (3.14), we have

$$\frac{\partial \chi}{\partial S} = g^{\pm} \frac{\partial \widetilde{\chi}}{\partial S^{\pm}}. \tag{3.15}$$

Also, differentiating (3.12), we obtain

$$g = \frac{\partial S^+}{\partial S^-} = \frac{g^+}{g^-}.$$

It is important to note that while the map G is prescribed geometrically (Sec. 3.1.2), the maps $G^{\pm}$ require the definition of a reference state. This reference state is the solution of a mechanical problem, namely, determining the shape of the birod in the absence of loads, a computation treated explicitly in Sections 4, 5, and 6.

We can now define the frame of directors attached to the birod. As before, we start by defining $\mathbf{d}_3$ as the unit tangent to $\mathbf{r}$ and we define $\mathbf{d}_1$ as the unit vector pointing from $\mathbf{r}^-$ to $\mathbf{r}^+$. We will only consider here the case where this vector is uniquely defined.[3] This implies the relations

$$\mathbf{r}^+ = \mathbf{r}^- + a\,\mathbf{d}_1 \quad \text{and similarly,} \quad \mathbf{r} = \mathbf{r}^- + a\beta\ \mathbf{d}_1 = \mathbf{r}^+ - a(1-\beta)\ \mathbf{d}_1. \tag{3.16}$$

Since $\mathbf{d}_1$ is perpendicular to $\mathbf{d}_3$ (cf. note at the end of (3.1.2)), we now have the orthonormal birod director frame

$$\mathbf{d}_3 = \frac{\frac{\partial \mathbf{r}}{\partial S}}{|\frac{\partial \mathbf{r}}{\partial S}|}, \qquad \mathbf{d}_1(S,T) = \frac{\mathbf{r}^+ - \mathbf{r}^-}{|\mathbf{r}^+ - \mathbf{r}^-|}, \qquad \mathbf{d}_2 = \mathbf{d}_3 \times \mathbf{d}_1. \tag{3.17}$$

As before, any vector $\mathbf{a}(S)$ can be written in the birod frame as $\mathbf{a}(S) = \mathsf{a}_1\mathbf{d}_1 + \mathsf{a}_2\mathbf{d}_2 + \mathsf{a}_3\mathbf{d}_3$.

Having defined a birod centreline and local frame, all associated strains can be easily defined. The *birod stretch* α and *birod Darboux vector* $\mathbf{u}$ are defined by

$$\alpha(S,t) = \left|\frac{\partial \mathbf{r}}{\partial S}\right|; \qquad \frac{\partial \mathbf{d}_i}{\partial S} = \mathbf{u} \times \frac{\partial \mathbf{d}_i}{\partial S}. \tag{3.18}$$

[3] In the case where one rod is inside another rod so that their centrelines coincide, the vector $\mathbf{d}_1$ is not uniquely defined. In this case $\mathbf{d}_1$ can be chosen conveniently either along $\mathbf{d}_1^+$ or $\mathbf{d}_1^-$.

As we shall see, one further geometric quantity of importance is the angle θ between the tangent vectors to the centrelines of the sub-rods

$$\theta = \mathrm{Sign}\Big[\mathbf{d}_1 \cdot \left(\mathbf{d}_3^- \times \mathbf{d}_3^+\right)\Big] \ \arccos\left(\mathbf{d}_3^- \cdot \mathbf{d}_3^+\right). \tag{3.19}$$

This angle is given explicitly in terms of α and $\mathbf{u}$ in Appendix B.

3.2 Mechanics

Starting from the Kirchhoff equations of both the sub rods, we now deduce balance equations for the birod as a whole. Each sub rod is subject to resultant forces $\mathbf{n}^\pm$ and moments $\mathbf{m}^\pm$ as defined in Sec. 2.2. These quantities obey the Kirchhoff equations (2.17). We focus here on static equilibria, i.e. we omit the time-dependent term (related to inertial effects)[4] The static Kirchhoff equations for the sub-rods are

$$\frac{\partial \mathbf{n}^\pm}{\partial S^\pm} + \frac{\mathbf{f}^\pm}{g^\pm} + \frac{\mathbf{F}^\pm}{g^\pm} = 0, \tag{3.20}$$

$$\frac{\partial \mathbf{m}^\pm}{\partial S^\pm} + \frac{\partial \mathbf{r}^\pm}{\partial S^\pm} \times \mathbf{n}^\pm + \frac{\mathbf{l}^\pm}{g^\pm} \mp c^\pm \mathbf{d}_1 \times \frac{\mathbf{f}^\pm}{g^\pm} + \frac{\mathbf{L}^\pm}{g^\pm} = 0, \tag{3.21}$$

where $c^+ = a(1-\beta)$ and $c^- = a\beta$. Note that in this formulation we have decomposed the body loads into external loads $\mathbf{F}^\pm$ and $\mathbf{L}^\pm$ and the internal loads $\mathbf{f}^\pm$ and $\mathbf{l}^\pm$ due to the interaction between the sub-rods. Specifically, $(\mathbf{F}^\pm/g^\pm)$ and $(\mathbf{L}^\pm/g^\pm)$ are forces and moments about the centrelines of either sub rod per unit reference arc length $S^\pm$.

3.2.1 External loads

The external forces $(\mathbf{F}^\pm/g^\pm)$ and moments $(\mathbf{L}^\pm/g^\pm)$ result in forces $\mathbf{F}^\pm$ and moments $\mathbf{L}^\pm$ per unit reference arc length S of the birod. It is therefore natural to define the resultant external force $\mathbf{F}$ and moment $\mathbf{L}$ about the centreline of the birod as

$$\mathbf{F} = \mathbf{F}^+ + \mathbf{F}^-, \tag{3.22}$$

$$\mathbf{L} = \mathbf{L}^+ + \mathbf{L}^- + c^+ \mathbf{d}_1 \times \mathbf{F}^+ - c^- \mathbf{d}_1 \times \mathbf{F}^-. \tag{3.23}$$

The last two terms in (3.23) account for the fact that $\mathbf{F}^\pm$ are applied at the centrelines of the sub-rods and therefore produce moments with respect to the centreline of the birod. In general, the difference of external moments can also produce work. Therefore, we define

$$\check{L}_1 = \left(\mathbf{L}^+ - \mathbf{L}^-\right) \cdot \mathbf{d}_1. \tag{3.24}$$

3.2.2 Internal loads

As a result of the attachment, internal stresses are local in the sense that the interaction between the two rods is only done through the paired cross sections. However, a pair of attached cross sections may have multiple points of contact. Hence, in general, they exert on each other a system of forces and moments which can be reduced to a resultant force and moment about an arbitrary point which we choose as $\mathbf{r}(S)$.[5] With this choice $(\mathbf{f}^\pm/g^\pm)$ and $(\mathbf{l}^\pm/g^\pm)$ are the linear densities of

[4] For static equilibrium it might seem more natural to use non-partial derivatives. However, since a key idea in our formulation is growth – which although occurring on a slow time scale, nevertheless gives quantities a quasi-static time component – we shall continue to use partial derivatives.

[5] Note that the choice of location of the point at which the resultant moments and forces are defined does not change the form of the resulting equations.

force and moment about $\mathbf{r}$ per unit reference arc length $S^{\pm}$ applied by the '$\mp$' rod on the '$\pm$' rod. Rescaling to the unit of reference arc length of the birod, we define $\mathbf{f} = \mathbf{f}^{+}$ and $\mathbf{l} = \mathbf{l}^{+}$ respectively as the force and moment applied by the $-$ rod on the $+$ rod per unit reference length of the birod. By application of the principle of action-reaction, the $+$ rod applies densities of forces $-\mathbf{f}$ and moments $-\mathbf{l}$ on the $-$ rod.

3.2.3 Mechanics of the birod and global quantities

The system (3.20,3.21), expressed in terms of the arc length parameter of the birod, S, is

$$\begin{aligned} &\left(\mathbf{n}^{\pm}\right)' \pm \mathbf{f} + \mathbf{F}^{\pm} = 0, \\ &\left(\mathbf{m}^{\pm}\right)' + \mathbf{r}^{\pm\prime} \times \mathbf{n}^{\pm} \pm \mathbf{l} - c^{\pm}\mathbf{d}_1 \times \mathbf{f} + \mathbf{L}^{\pm} = 0, \end{aligned} \tag{3.25}$$

where $(\ )' = \frac{\partial(\ )}{\partial S}$. We can now define $\mathbf{N}$ and $\mathbf{M}$ as the total resultant force and moment about the centreline as

$$\mathbf{N} = \mathbf{n}^{+} + \mathbf{n}^{-}, \tag{3.26}$$

$$\mathbf{M} = \mathbf{m}^{+} + \mathbf{m}^{-} + c^{+}\mathbf{d}_1 \times \mathbf{n}^{+} - c^{-}\mathbf{d}_1 \times \mathbf{n}^{-}. \tag{3.27}$$

The definitions (3.26,3.27), together with the individual Kirchhoff equations for the sub-rods (3.25), and the relations (3.22,3.23), lead to the following balance equations for the forces and moments in the birod first derived in [34]

$$\mathbf{N}' + \mathbf{F} = 0, \tag{3.28}$$

$$\mathbf{M}' + \mathbf{r}' \times \mathbf{N} + \mathbf{L} = 0. \tag{3.29}$$

We note that these equations have the form of the Kirchhoff equations. However, in general they are not sufficient to establish the mechanical balance. Indeed, as already discussed, a variation of the angle θ between the tangents of the sub-rods may produce work. To account for this effect, we introduce the difference of forces and moments applied at each section

$$\mathbf{n} = \mathbf{n}^{+} - \mathbf{n}^{-} \tag{3.30}$$

$$\mathbf{m} = \left(\mathbf{m}^{+} + c^{+}\mathbf{d}_1 \times \mathbf{n}^{+}\right) - \left(\mathbf{m}^{-} - c^{-}\mathbf{d}_1 \times \mathbf{n}^{-}\right). \tag{3.31}$$

The specific form of interaction between the sub-rods is such that the balance of forces and moments (3.28,3.29) is completed by a single equation expressing the notion that the moment about $\mathbf{d}_1$ on the $+$ sub-rod must equal the moment about $\mathbf{d}_1$ of the $-$ rod (as derived in Appendix D), that is

$$(\mathbf{m}') \cdot \mathbf{d}_1 + (\mathbf{r}' \times \mathbf{n}) \cdot \mathbf{d}_1 + 2\mathsf{l}_1 + \check{L}_1 = 0. \tag{3.32}$$

This extra equation introduces an extra mechanical quantity in the theory – l_1, the $\mathbf{d}_1$ component of the internal moment $\mathbf{l}$ – in addition to the traditional resultant force and moment $\mathbf{N}$ and $\mathbf{M}$. An extra constitutive equation for l_1 will therefore be needed.

Solving balance equations for these three mechanical quantities is considerably simpler than solving the Kirchhoff equations of both sub-rods. In part, the internal constraints $\mathbf{f}$, l_2 and l_3, which ensure the cohesion of the paired cross sections, do not need to be computed. Accordingly, instead of solving the 12 first order differential equations (3.20-3.21), we reduce the problem to only solving (3.28,3.29,3.32), and in a geometry that is natural for the entire macroscopic structure.

Having established the basic equations for the geometry and mechanical balance of a birod, we need to obtain the constitutive laws of this new structure, based on both the material response of the attached sub-rods and the attachment. The constitutive laws for the birod contain both the

unstressed state (the state that the birod takes in the absence of loads) and its material response away from that state. We develop these ideas in an instructive manner with increasing complexity by first restricting the rod in 1D (linear rods), then 2D (planar rods), and finally 3D (general rods). In the first two cases, the geometry is sufficiently simple to allow for explicit expressions for the birod and as such we give a full analysis.

4 A birod constrained on the line

In this section we treat the simplest case where both sub-rods are twistless and restricted to a straight line (i.e. they can expand and contract in length but not bend or twist).

4.1 Geometry of linear birods

If the birod and sub-rods are constrained to a line (taken to be the z-axis so that $\mathbf{d}_3^\pm = \mathbf{d}_3 = \mathbf{e}_z$), then $\mathbf{u} = \mathbf{0}$ and we can choose without loss of generality a director basis with $\mathbf{d}_1^\pm$ and $\mathbf{d}_2^\pm$ along the x and y axis, respectively. For the kinematics, we choose $\varphi^\pm \equiv 0$, $\mathbf{d}_i = \mathbf{d}_i^\pm$, and $a = 0$. The geometry of the 1D birod is then completely specified by $\alpha(S,t) = \frac{\partial r}{\partial S}$; in particular Eq. (3.16) reduces to

$$\mathbf{r} = \mathbf{r}^+ = \mathbf{r}^-. \tag{4.1}$$

Taking a derivative of (4.1) by S leads to two equations relating the configuration of the 1D birod (fully described by the function α) to that of the sub-rods (characterized by $\alpha^\pm$):

$$\alpha = \alpha^\pm g^\pm; \quad g = \frac{g^+}{g^-}. \tag{4.2}$$

4.2 Constitutive laws and reference state

The 1D case is particularly well suited to demonstrate the derivation of constitutive laws. This is typically a three step process. First, a general law is formed from the constitutive laws of the subrods; however, these involves the functions $g^\pm$, still unknown at this stage. Second, the reference state is defined such that the stresses vanish, and this relation is inverted to determine g^- and $g^+ = gg^-$. Third, the substitution of $g^\pm$ in the constitutive laws obtained at the first step provides a constitutive law relating directly the stress to the relevant geometrical quantity. We also note that the 1D case could be easily computed from energy considerations but that the goal here is to show how we can apply the ideas outlined in the previous sections.

We assume general constitutive laws for the tensions in both sub-rods:

$$\mathsf{n}_3^\pm = k^\pm(\alpha^\pm). \tag{4.3}$$

where the functions $k^\pm$ derive from convex potentials (possibly different) that have a minimum at 1 and with $k^\pm(1) = 0$.

Step 1: A general constitutive law. By definition of the tension N_3 in the birod given by (3.26) and using the fact that $\mathbf{d}_3^\pm = \mathbf{d}_3$, we obtain the constitutive law for the birod:

$$\mathsf{N}_3 = \mathsf{n}_3^+ + \mathsf{n}_3^- = k^+(\alpha^+) + k^-(\alpha^-). \tag{4.4}$$

Since $\alpha^+ = \frac{\alpha}{gg^-}$ and $\alpha^- = \frac{\alpha}{g^-}$, and g^- is not apriori known, this is only a formal law at this point.[6]

[6]Recall that $g^- = \frac{\partial S}{\partial S^-}$ describes the stretch from the reference length of the '-' rod to the reference length of the birod, so is not known until the birod reference state has been determined. While the quantity $g = \frac{\partial S^+}{\partial S^-}$ *is* known apriori, it cannot be expressed as a function of S without knowing the reference state of the birod.

Step 2: The reference configuration of the birod. In 1D, we define the *reference configuration* of the birod as the configuration that satisfies $\mathsf{N}_3 = 0$. In this configuration, $\alpha = 1$, the substitution of which in (4.4) leads to

$$k^+\left(\frac{1}{gg^-}\right) + k^-\left(\frac{1}{g^-}\right) = 0. \tag{4.5}$$

If there exists a solution of this equation for g^-, then it is unique as it is the (unique) root of a monotonically decreasing function.[7] Then we obtain g^- as a function of all other parameters appearing in the equation.

Remembering that $g^- = \frac{\partial S^-}{\partial S}$, the reference arc length parameter S and total length L are given by

$$S = \int_0^{S^-} \frac{1}{g^-(\sigma,t)}\mathrm{d}\sigma, \quad L = \int_0^{L^-} \frac{1}{g^-(\sigma,t)}\mathrm{d}\sigma. \tag{4.6}$$

Eq. (4.6) can then be inverted to obtain g^- as a function of S.

Step 3: The constitutive law. Once S^- is known as a function of S, all functions appearing in (4.4) are known as a function of S. This relation then provides a general constitutive law for the birod in terms of the birod variables $\alpha(S,t), g(S,t), g^-(S,t)$. In the next subsections we illustrate the theory with particular choices of constitutive law.

4.2.1 Linear constitutive laws

Step 1. Let the sub rods have linear constitutive laws

$$\mathsf{n}_3^\pm = k^\pm\ (\alpha^\pm - 1), \tag{4.7}$$

where $k^\pm$ are constants. The general constitutive law for the bi-rod is then

$$N_3(\alpha) = k^+\left(\frac{\alpha}{gg^-} - 1\right) + k^-\left(\frac{\alpha}{g^-} - 1\right). \tag{4.8}$$

Step 2. At $\alpha = 1$, $N_3(1) = 0$ is easily solved to obtain

$$g^- = \frac{1}{g}\ \frac{k^+ + gk^-}{k^+ + k^-}. \tag{4.9}$$

The arc length of the birod is $S = (k^+ + k^-)^{-1}\int_0^{S^-} \frac{k^+ + g(\sigma,t)k^-}{g(\sigma,t)}d\sigma$. If g is constant along the rod, i.e. a constant length differential, then the length of the birod is $L = gL^-\frac{k^+ + gk^-}{k^+ + k^-}$.

Step 3. Substituting (4.9) in (4.8), we obtain a linear constitutive law for the birod

$$\mathsf{N}_3 = (k^+ + k^-)\ \ (\alpha - 1)\,. \tag{4.10}$$

[7] The existence of a solution is not guaranteed as the constitutive laws for the subrods may have a vertical asymptote, preventing them from reaching a certain strain. In the case where the functions $k^\pm$ are continuous on the positive axis, a solution is guaranteed.

4.2.2 A neo-Hookean birod

Step 1. In many biological application, tissues operate in large deformation. In these cases, it is necessary to use non-linear constitutive laws. The simplest of such laws comes from the uniaxial response of a neo-Hookean material, which reads

$$\mathsf{n}_3^{\pm} = \mu^{\pm}\left(\alpha^{\pm 2} - \frac{1}{\alpha^{\pm}}\right), \tag{4.11}$$

where $\mu^{\pm}$ are constants. The corresponding Young's moduli are $E^{\pm} = 3\mu^{\pm}/\mathcal{A}^{\pm}$ (with $\mathcal{A}^{\pm}$ the areas of the rods sections). The general constitutive law is then

$$N_3(\alpha) = \mu^{+}\left(\frac{\alpha^2}{(gg^{-})^2} - \frac{gg^{-}}{\alpha}\right) + \mu^{-}\left(\frac{\alpha^2}{(g^{-})^2} - \frac{g^{-}}{\alpha}\right). \tag{4.12}$$

Step 2. At $\alpha = 1$, $N_3(1) = 0$ is solved to obtain

$$g^{-} = \sqrt[3]{\frac{1 + \frac{1}{g^2}\frac{\mu^{+}}{\mu^{-}}}{1 + g\frac{\mu^{+}}{\mu^{-}}}}. \tag{4.13}$$

Step 3. The constitutive law for the birod is obtained by substituting this last expression into (4.12), which after simplification, reads

$$\mathsf{N}_3 = \mu\left(\alpha^2 - \frac{1}{\alpha}\right), \qquad \mu = \mu^{-}\sqrt[3]{1 + \frac{1}{g^2}\frac{\mu^{+}}{\mu^{-}}}\left(1 + g\frac{\mu^{+}}{\mu^{-}}\right)^{2/3}. \tag{4.14}$$

We have obtained the interesting result that a birod made of two neo-Hookean sub-rods is itself neo-Hookean with an elastic stiffness that can be re-written symmetrically as $\mu = \mu^{+}g^{+} + \mu^{-}g^{-}$. That is, the stiffness of the birod is a linear combination of the effective stiffnesses of the sub-rods $\mu^{\pm}$ weighted by the amount of sub-rods material per unit arc length of the birod $g^{\pm}$. By contrast, the linear constitutive laws of Sec. 4.2.1 lead to a direct sum $k^{+} + k^{-}$ in Eqn. (4.10) that does not take this correction into account. The effective Young's modulus of the birod is then

$$E = 3\frac{\mu^{+}g^{+} + \mu^{-}g^{-}}{\mathcal{A}^{+} + \mathcal{A}^{-}}. \tag{4.15}$$

4.3 Application to tissue tension and differential growth stiffening

Many biological structures, such as arteries, roots, and stems, are composed of multiple tubular structures growing at different rates [49]. A natural problem is to understand the change of material properties resulting from axial differential growth. For deformation along the axis, the response of a two-layer cylinder is equivalent to that of a 1D birod. The effective Young's modulus (4.15) provides the overall axial response of this structure. In Fig. 7, we show that for any g different from 1, the Young's modulus of the birod increases, indicating that the structure stiffens whenever there is axial differential growth (the result remains valid even when $\mu^{+}/\mu^{-} \neq 1$).

We can use this idea to revisit the problem of the growth of rhubarb as discussed in [50, 51]. When the stalk of a rhubarb of length L is peeled, it can be easily observed that the peeled skin is shorter than the original stalk ($L^{+} < L$) and that the pith is longer than the original stalk $L^{-} > L$ (see Fig. 8(a)). These experimental observations suggest that the rhubarb stalk can be mechanically modelled as a composite beam made of a pith in compression surrounded by a skin in tension. Furthermore, in principle, uniaxial tension tests can be performed on both the skin and

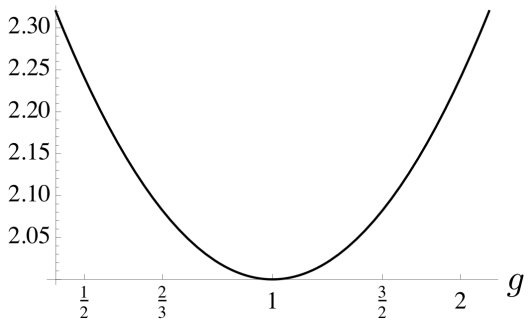

Figure 7: A log-linear plot of the elastic stiffness μ in (4.14) as a function of g in the case $\mu^+/\mu^- = 1$. We observe that the elastic stiffness of the birod can be increased as a result of differential growth.

the pith so that infinitesimal Young's moduli $E^\pm$ of both components are known. We assume that the differential growth between pith and skin is uniform, so that g and g^- are independent of arc length. This assumption implies that $g = \frac{L^+}{L^-}$ and $g^\pm = \frac{L^\pm}{L}$. For the purpose of this computation, we suppose that $L^\pm$ and the material parameters are known while L is unknown. We further assume that the pith is a neo-Hookean rod, so that

$$\mathsf{n}_3^- = \mu^-(\alpha^{-2} - \frac{1}{\alpha^-}), \tag{4.16}$$

whereas the skin is a Fung rod[52]:

$$\mathsf{n}_3^+ = \mu^+ \left(\alpha^{+2} - \frac{1}{\alpha^+}\right) e^{\nu\left(\alpha^{+2}+2/\alpha^+-3\right)}. \tag{4.17}$$

Within our framework, we have, as before:

Step 1. The general law is

$$N_3(\alpha) = \mu^+ \left(\frac{\alpha^2}{(gg^-)^2} - \frac{gg^-}{\alpha}\right) e^{\nu\left(\frac{\alpha^2}{(gg^-)^2}+2\frac{gg^-}{\alpha}-3\right)} + \mu^- \left(\frac{\alpha^2}{(g^-)^2} - \frac{g^-}{\alpha}\right). \tag{4.18}$$

Step 2. At $\alpha = 1$, $N_3(1) = 0$ is solved to obtain g^- or equivalently L as a function of all the parameters. This is a transcendental equation for which a single solution exists.

Step 3. Once L is known, the constitutive law for the birod is obtained as

$$N_3(\alpha) = \mu^+ \left(\frac{\alpha^2 L^2}{(L^+)^2} - \frac{L^+}{\alpha L}\right) e^{\nu\left(\frac{\alpha^2 L^2}{(L^+)^2}+2\frac{L^+}{\alpha L}-3\right)} + \mu^- \left(\frac{\alpha^2 L}{(L^-)^2} - \frac{L^-}{\alpha L}\right). \tag{4.19}$$

The Young's modulus is obtained as $E = (\frac{\partial N_3}{\partial \alpha}|_{\alpha=1})/(\mathcal{A}^+ + \mathcal{A}^-)$, where $(\mathcal{A}^+ + \mathcal{A}^-)$ is the cross-sectional area of the birod. An example of the increase of effective Young's modulus as a function of axial differential growth is shown in Fig. 8(b))

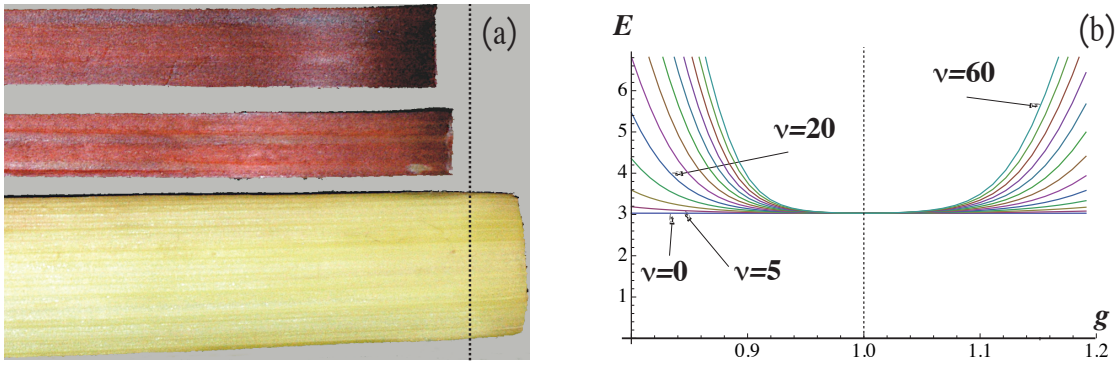

Figure 8: (a) Peeled rhubarb stalk and skin. The skin contracts whereas the pith elongates, indicative of the state of tension and compression of both parts (dotted line indicates length before peeling). (b) Effective Young's modulus of a rhubarb stalk in function of $g = L^+/L^-$, here we chose $\mathcal{A}^+ + \mathcal{A}^- = 1$, $\mu^+/\mu^- = 0.01$. We observe a dramatic increase of stiffness with increasing values of the strain-stiffening parameter ν.

5 Planar birods

5.1 Geometry of planar birods

We now consider the case of a 2D birod, i.e. when the birod is twistless and constrained so that the centreline $\mathbf{r}$ lies in a plane. We take $\mathbf{d}_2^\pm$ normal to the plane (along $\mathbf{e}_z$). In this case, the three frames $\{\mathbf{d}_1^\pm, \mathbf{d}_2^\pm, \mathbf{d}_3^\pm\}$ and $\{\mathbf{d}_1, \mathbf{d}_2, \mathbf{d}_3\}$ are aligned.[8] In particular, we have

$$\frac{\partial \mathbf{d}_i}{\partial S} = \frac{\partial S^\pm}{\partial S}\frac{\partial \mathbf{d}_i^\pm}{\partial S^\pm} \tag{5.1}$$

and the Darboux vector of the birod, $\mathbf{u} = \mathsf{u}_2\,\mathbf{d}_2$, is related to the Darboux vectors of the sub-rods $\mathbf{u}^\pm = \mathsf{u}_2^\pm \mathbf{d}_2^\pm = \mathsf{u}_2^\pm \mathbf{d}_2$ by

$$\mathsf{u}_2 = \mathsf{u}_2^\pm g^\pm. \tag{5.2}$$

The derivative of (3.16) by S^- and of (3.10) by S together with (5.2) imply

$$\begin{cases} \mathsf{u}_2 = g^- \dfrac{\alpha^- - \alpha^+ g}{a}, \\ \alpha = g^- \left[(1-\beta)\alpha^- + \beta\alpha^+ g\right], \end{cases} \quad \text{or, equivalently,} \quad \begin{cases} \alpha^- = \dfrac{1}{g^-}(\alpha + a\beta\mathsf{u}_2), \\ \alpha^+ g = \dfrac{1}{g^-}\left[\alpha - a(1-\beta)\mathsf{u}_2\right]. \end{cases} \tag{5.3}$$

Therefore, once the gluing function g is defined and the maps $g^\pm$ are known, a configuration of the planar birod is entirely determined by two generalised strains given by the global stretch α and curvature u_2. All other geometric variables can be obtained from (5.2,5.3).

Note that we still have the arbitrary parameter $\beta \in [0,1]$ that describes the position of the birod centreline with respect to the sub-rods. However, in any configuration, α^-, α^+ and g are independent of β while α, $\mathbf{u}$, g^- and g^+ depend on it. This reflects the fact that the former quantities are intrinsic to the individual sub-rods, while the latter are intrinsic to the birod and thus depend on how its centreline is defined. Hence, the constitutive laws will depend also on β and some judicious choices can be made depending on the application.

[8] Indeed, since the birod is in the plane perpendicular to $\mathbf{d}_2^+ = \pm\mathbf{d}_2^-$ and we parameterise the sub-rods so that $\mathbf{d}_2^+ = \mathbf{d}_2^-$. For the birod, $\mathbf{d}_1$ is orthogonal to $\mathbf{d}_3^+$, $\mathbf{d}_3^-$ and $\mathbf{d}_3$. Since sub-rods and birod have the same orientation, $\mathbf{d}_3^+ = \mathbf{d}_3^- = \mathbf{d}_3$, which in turn implies $\mathbf{d}_1^+ = \mathbf{d}_1^- = \mathbf{d}_1$. Hence the three frames $\{\mathbf{d}_1^\pm, \mathbf{d}_2^\pm, \mathbf{d}_3^\pm\}$ and $\{\mathbf{d}_1, \mathbf{d}_2, \mathbf{d}_3\}$ are aligned.

5.2 Constitutive laws and reference state

In order to find the constitutive laws (CL) and reference state of the planar birod, we follow the strategy developed in the previous section. First, we obtain a general constitutive law by substituting the constitutive laws of the sub-rods in (3.26,3.27). Second, the reference state is computed by solving $\mathbf{N} = \mathbf{0}$ and $\mathbf{M} = \mathbf{0}$ for g^- and $\hat{\mathsf{u}}_2$. Third, once the reference state is know, the birod's CL can be written as a function of the birod strain parameters α and u_2.

Step 1: The general constitutive laws. Assuming both sub-rods are extensible, their constitutive laws are

$$\mathsf{n}_3^{\pm} = k^{\pm}(\alpha^{\pm}, \mathsf{u}_2^{\pm}), \tag{5.4}$$
$$\mathbf{m}^{\pm} = K^{\pm}(\alpha^{\pm}, \mathsf{u}_2^{\pm})\ \mathbf{d}_2. \tag{5.5}$$

Upon using (5.2,5.3) to express $\alpha^{\pm}$ and $\mathsf{u}_2^{\pm}$ as functions of α and u_2, and with the definitions (3.26,3.27), the general law for the birod is of the form

$$\begin{aligned} \mathsf{N}_3 &= k(\alpha, \mathsf{u}_2\ ;\ \hat{\mathsf{u}}_2, g^-), \\ \mathsf{M}_2 &= K(\alpha, \mathsf{u}_2\ ;\ \hat{\mathsf{u}}_2, g^-), \end{aligned} \tag{5.6}$$

where $k = k^+ + k^-$ and $K = K^+ + K^-$.

Step 2: The reference state. In the reference state of the birod, $\mathbf{N} = \mathbf{0}$, $\mathbf{M} = \mathbf{0}$, $\alpha = 1$ and $\mathsf{u}_2 = \hat{\mathsf{u}}_2$, where $\hat{\mathsf{u}}_2$ describes the reference curvature of the birod. Therefore, g^- and $\hat{\mathsf{u}}_2$ are found by solving the equations

$$\begin{aligned} k(1, \hat{\mathsf{u}}_2\ ;\ \hat{\mathsf{u}}_2, g^-) &= 0, \\ K(1, \hat{\mathsf{u}}_2\ ;\ \hat{\mathsf{u}}_2, g^-) &= 0. \end{aligned} \tag{5.7}$$

Step 3: The constitutive law and the planar birod equations. For each particular solution found in Step 2, (5.8) provides a constitutive law for the birod. The full system for the birod is then

$$\begin{aligned} &\mathbf{r}' = \alpha \mathbf{d}_3, \\ &\mathbf{N}' + \mathbf{F} = \mathbf{0}, \\ &\mathbf{M}' + \mathbf{r}' \times \mathbf{N} + \mathbf{L} = \mathbf{0}, \\ &\mathsf{N}_3 = k(\alpha, \mathsf{u}_2\ ;\ \hat{\mathsf{u}}_2, g^-), \\ &\mathsf{M}_2 = K(\alpha, \mathsf{u}_2\ ;\ \hat{\mathsf{u}}_2, g^-). \end{aligned} \tag{5.8}$$

Hence in the planar case, the birod *is* a Kirchhoff elastic rod, as its configuration under load is fully specified by a planar system of elastic rod equations with no extra stress variables. As usual, it is often convenient to let $\mathbf{r} = [x, y, 0]$, $\mathbf{N} = [n_x, n_y, 0]$, $\mathbf{M} = [0, 0, m]$ and define θ as the angle between the tangent vector $\mathbf{d}_3 = [\cos\theta, \sin\theta, 0]$ and the x-axis. Then $\mathsf{u}_2 = \frac{\partial \theta}{\partial S}$ and the system can be written

$$\begin{aligned} &x' = \alpha\cos\theta, \quad y' = \alpha\sin\theta \\ &n_x' + f_x = 0, \quad n_y' + f_y = 0 \\ &m' + \alpha\cos\theta n_y - \alpha\sin\theta n_x + l = 0, \\ &n_x\cos\theta + n_y\sin\theta = k(\alpha, \theta'), \\ &m = K(\alpha, \theta'), \end{aligned} \tag{5.9}$$

where $\mathbf{F} = [f_x, f_y, 0]$ and $\mathbf{L} = [0, 0, l]$. This constitutes 7 equations for the unknowns $\{x, y, n_x, n_y, \alpha, \theta, m\}$, to be complemented with 6 boundary conditions.

The properties of the birod are derived from its constitutive laws, i.e. the form of solutions of (5.7). In the remainder of this section, we perform steps 1 and 2 explicitly for a number of typical linear cases. Interesting behavior can emerge through the interaction of linear subrods. Of course, many biological applications rely on the interplay between differential growth and non-linear constitutive laws, such as the rhubarb stalk discussed in Sec. 4.3. The resulting structures tend to have highly non-linear constitutive laws and the program highlighted above must be followed for each specific systems. Yet, it is sometimes enough to know the response of the system to small deformations of the composite structure (i.e. to linearise the theory about its non-linear equilibrium). The interested reader can find this calculation in App. E for arbitrary constitutive laws.

5.2.1 Extensible sub-rods with linear constitutive laws

Here we apply the general method outlined above to the particular case where both sub-rods obey linear constitutive laws. In this case, they can be easily written in matrix notation for the generalised stresses and strains

$$\mathbf{z}^{\pm} = \begin{pmatrix} \mathsf{n}_3^{\pm} \\ \mathsf{m}_2^{\pm} \end{pmatrix}, \quad \mathbf{x}^{\pm} = \begin{pmatrix} \alpha^{\pm} \\ \mathsf{u}_2^{\pm} \end{pmatrix}; \qquad \mathbf{x} = \begin{pmatrix} \alpha \\ \mathsf{u}_2 \end{pmatrix}, \quad \mathbf{z} = \begin{pmatrix} \mathsf{N}_3 \\ \mathsf{M}_2 \end{pmatrix}. \tag{5.10}$$

With these notations, the constitutive laws are

$$\mathbf{z}^{\pm} = \mathbf{K}^{\pm} \left(\mathbf{x}^{\pm} - \hat{\mathbf{x}}^{\pm} \right), \quad \hat{\mathbf{x}}^{\pm} = \begin{pmatrix} 1 \\ \hat{\mathsf{u}}_2^{\pm} \end{pmatrix}, \tag{5.11}$$

where $\mathbf{K}^{\pm}$ are 2×2 matrices.

Step 1. Since $\mathbf{M}$ and $\mathbf{N}$ are linearly dependent on $\mathsf{n}_3^{\pm}$ and on $\mathbf{m}^{\pm}$ the constitutive laws of the birods given by (3.27,3.26) are also linear. Rewriting (5.2,5.3) in matrix form, we have

$$\mathbf{x}^{\pm} = \frac{1}{g^{\pm}} \mathbf{M}^{\pm} \mathbf{x}; \quad \text{with} \quad \mathbf{M}^{+} = \begin{pmatrix} 1 & -a(1-\beta) \\ 0 & 1 \end{pmatrix} \quad \text{and} \quad M^{-} = \begin{pmatrix} 1 & a\beta \\ 0 & 1 \end{pmatrix}. \tag{5.12}$$

With these two matrices, we can write the general form of the constitutive law for the birod as

$$\mathbf{z} = \left(\mathbf{M}^{+}\right)^{T} \mathbf{z}^{+} + \left(\mathbf{M}^{-}\right)^{T} \mathbf{z}^{-}. \tag{5.13}$$

Using (5.11,5.12) in (5.13) then gives

$$\mathbf{z} = \frac{1}{g^{-}} \mathbf{K} \mathbf{x} - \mathbf{v}; \tag{5.14}$$

with

$$\mathbf{K} = \left[\left(\mathbf{M}^{+}\right)^{T} \frac{\mathbf{K}^{+}}{g} \mathbf{M}^{+} + \left(\mathbf{M}^{-}\right)^{T} \mathbf{K}^{-} \mathbf{M}^{-} \right], \quad \mathbf{v} = \left[\left(\mathbf{M}^{+}\right)^{T} \mathbf{K}^{+} \hat{\mathbf{x}}^{+} + \left(\mathbf{M}^{-}\right)^{T} \mathbf{K}^{-} \hat{\mathbf{x}}^{-} \right]. \tag{5.15}$$

Step 2. In the reference state of the birod, $\mathbf{z} = 0$ (since $\mathbf{N} = \mathbf{0}$ and $\mathbf{M} = \mathbf{0}$) and $\mathbf{x} = \hat{\mathbf{x}}$. In this configuration, (5.14) gives $\mathbf{v} = \frac{1}{g^{-}} \mathbf{K} \hat{\mathbf{x}}$, which can be written

$$\begin{pmatrix} v_1 & -K_{12} \\ v_2 & -K_{22} \end{pmatrix} \begin{pmatrix} g^{-} \\ \hat{\mathsf{u}}_2 \end{pmatrix} = \begin{pmatrix} K_{11} \\ K_{21} \end{pmatrix}. \tag{5.16}$$

This is a linear system for g^{-} and $\hat{\mathsf{u}}_2$. Its solution provides the information on both the length of the reference state of the birod as well as its reference curvature.

Step 3. Once g^- and $\hat{\mathsf{u}}_2$ are known, from (5.14) the linear constitutive law for the birod is simply

$$\mathbf{z} = \frac{1}{g^-}\mathbf{K}(\mathbf{x} - \hat{\mathbf{x}}). \tag{5.17}$$

5.2.2 Extensible sub-rods with linear and diagonal constitutive laws

It is of interest to further restrict our attention to the most commonly used constitutive laws: those for which there is no coupling between stretch and curvature. In this case, $K_{12}^{\pm} = K_{21}^{\pm} = 0$ and we can easily obtain explicit expression of $\hat{\mathsf{u}}_2$, g^- and K

$$a\hat{\mathsf{u}}_2 = \frac{\kappa(1-g) + \rho\delta(g+\kappa)}{\rho(g+h)(1+\kappa) + \kappa(1+\rho\delta) - \beta[\kappa(1-g) + \rho\delta(g+\kappa)]}, \tag{5.18}$$

$$g^- = \frac{1+\kappa/g}{1+\kappa} + a\hat{\mathsf{u}}_2\frac{\beta - (1-\beta)\kappa/g}{1+\kappa}, \tag{5.19}$$

where we have introduced the ratio of elastic stifnesses: $\kappa = K_{11}^+/K_{11}^-$, the ratio of bending stiffnesses $h = K_{22}^+/K_{22}^-$, the squared ratio of the persistence length of one of the rod to the thickness of the birod $\rho = K_{22}^-/(K_{11}^- a^2)$, and $\delta = (a\hat{\mathsf{u}}_2^- + h\, a\hat{\mathsf{u}}_2^+)$ measuring the total effect of the reference curvature of the sub-rods.

The constitutive laws of the birod can then be explicitly written as

$$\begin{pmatrix} \mathsf{N}_3 \\ \mathsf{M}_2 \end{pmatrix} = \mathbf{K}\begin{pmatrix} \alpha - 1 \\ \mathsf{u}_2 - \hat{\mathsf{u}}_2 \end{pmatrix}, \tag{5.20}$$

where

$$\mathbf{K} = \frac{K_{11}^-}{g^-}\begin{pmatrix} 1+\kappa/g & a\beta - a(1-\beta)\kappa/g \\ a\beta - a(1-\beta)\kappa/g & a\beta^2 + a\frac{\kappa}{g}(1-\beta)^2 + (1+\frac{h}{g})\rho a \end{pmatrix}. \tag{5.21}$$

If the sub-rods are furthermore uniform and uniformly glued so that $K^{\pm}$ and g are independent of S, the modelling parameter $\beta = \frac{\kappa}{g+\kappa} = \frac{K_{11}^+}{gK_{11}^- + K_{11}^+}$ can be chosen such that $\beta - (1-\beta)\kappa/g = 0$, in which case the birod has diagonal constitutive laws.

In the simplest case of uniformly glued rods of the same length and with no growth, i.e. $g = 1$, a simple formula arises. Indeed, we find

$$\mathsf{N}_3 = k(\alpha - 1), \tag{5.22}$$

$$\mathsf{M}_2 = K(\mathsf{u}_2 - \hat{\mathsf{u}}_2), \tag{5.23}$$

$$\tag{5.24}$$

where

$$k = k^+ + k^- \tag{5.25}$$

$$K = K^- + K^+ + a^2\frac{k^- k^+}{k} \tag{5.26}$$

$$\hat{\mathsf{u}}_2 = \frac{K^-\hat{\mathsf{u}}_2^- + K^+\hat{\mathsf{u}}_2^+}{K}. \tag{5.27}$$

We see that the axial stiffness of the birod is simply the sum of the stiffnesses of the individual rods, as we found in the 1D case, similarly with the bending stiffness but with an extra term that accounts for compression/extension of the individual rods when bending, and the intrinsic curvature comes as a weighted sum of $\hat{\mathsf{u}}_2^+$ and $\hat{\mathsf{u}}_2^-$.

5.2.3 Linear extensible-inextensible sub-rods

There is a further simplification that is particularly relevant in numerous applications. If the elastic stiffness of one of the sub-rod is much larger than the other, then it is reasonable to model it as inextensible. We then have the case of a birod with one extensible and one inextensible sub-rod (note that the case where both are inextensible is possible but amounts then to a purely geometric exercise as no axial extension is possible). We assume that the $-$ rod is inextensible while the the $+$ rod is extensible. The constitutive laws of the sub-rods are then

$$\mathsf{n}_3^+ = k^+(\alpha^+, \mathsf{u}_2^+), \tag{5.28}$$
$$\mathbf{m}^+ = K^+(\alpha^+, \mathsf{u}_2^+)\ \mathbf{d}_2, \tag{5.29}$$
$$\mathbf{m}^- = K^-(\mathsf{u}_2^-)\ \mathbf{d}_2, \tag{5.30}$$

Since the $-$ rod is inextensible, we can use it as a centreline (that is we choose $\beta = 0$). As a consequence n_3^- does not appear in the definition (3.27) of $\mathbf{M}$. Furthermore, $s = S^-$, so $g^- = 1$, thus $\alpha = 1$ and the birod itself is inextensible (in particular there is no constitutive law for N_3). With this choice, Equations (5.2,5.3) become

$$\mathsf{u}_2^- = \mathsf{u}_2; \qquad \mathsf{u}_2^+ = \frac{\mathsf{u}_2}{g}; \qquad \alpha^+ = \frac{1}{g}(1 - a\mathsf{u}_2). \tag{5.31}$$

Assuming linear constitutive laws of the form

$$\mathsf{n}_3^+ = k^+(\alpha^+ - 1); \qquad \mathsf{m}_2^+ = K^+(\mathsf{u}_2^+ - \hat{\mathsf{u}}_2^+); \qquad \mathsf{m}_2^- = K^-(\mathsf{u}_2^+ - \hat{\mathsf{u}}_2^+), \tag{5.32}$$

and following the same steps as in the previous cases, the constitutive law for the birod is

$$\mathsf{M}_2 = K(\mathsf{u}_2 - \hat{\mathsf{u}}_2), \tag{5.33}$$

with

$$K = \frac{1}{g}\left[K^+ + gK^- + a^2k^+\right], \qquad \hat{\mathsf{u}}_2 = \frac{g(K^+\mathsf{u}_2^+ + K^-\mathsf{u}_2^-) + ak^+(1-g)}{K^+ + gK^- + a^2k^+}. \tag{5.34}$$

5.3 Timoshenko's bimetallic strips

In his seminal paper [42], Timoshenko studied the mechanics of two metallic strips welded along their length. In particular, the different coefficients of thermal expansion ($t^\pm$) of the strips imply that the bilayer bends under changes of temperature, as shown in Fig 6. In this section, we show how Timoshenko's result can be recovered in the limit of small deformations. Recalling the discussion of Sec. 3.1.3 we have

$$g = \frac{1 + c_t^+(t - t_0)}{1 + c_t^-(t - t_0)} \qquad \text{so that} \qquad 1 - g = \frac{(c_t^- - c_t^+)(t - t_0)}{1 + c_t^-(t - t_0)}. \tag{5.35}$$

Defining

$$m = \frac{a^-}{a^+} \qquad \text{and} \qquad n = \frac{E^-}{E^+}, \tag{5.36}$$

Timoshenko found that the radius of curvature of a bi-metallic strip of thickness $2a$ (Equation (4) in [42]) is

$$\hat{\mathsf{u}}_{\text{Timo}} = \frac{6(c_t^+ - c_t^-)(t - t_0)(1 + m)^2}{2a\left(3(1+m)^2 + (1 + mn)\left(m^2 + \frac{1}{mn}\right)\right)} \tag{5.37}$$

With the definitions (5.36), the non-dimensional parameters κ, h, ρ and δ defined in Sec. **??** become

$$\kappa = mn, \quad h = nm^3, \quad \rho = \frac{1}{3}\frac{1}{(1+m)^2} \quad \text{and} \quad \delta = 0. \tag{5.38}$$

The last equality in (5.38) expresses that the individual strips are straight in their own reference configuration.

Substituting (5.38) in (5.18) leads to

$$a\hat{\mathsf{u}}_2 = \frac{3(1-g)(m+1)^2}{\left(\frac{g}{mn}+m^2\right)+3\left(1-\beta(1-g)\right)(1+m)^2}. \tag{5.39}$$

Assuming small thermal dilatation, $\epsilon = c_t^-(T-T_0) \ll 1$, (5.35) can be expanded as $g = 1+(1-c_t^+/c_t^-)\epsilon + O(\epsilon^2)$. Accordingly, (5.39) becomes

$$\hat{\mathsf{u}}_2 = \frac{1}{2a}\frac{6(1+m)^2\left(1-\frac{c_t^+}{c_t^-}\right)}{3(1+m)^2+\left(\frac{1}{mn}+m^2\right)}\,\epsilon + O(\epsilon^2), \tag{5.40}$$

which matches (5.37) to first order in $\epsilon = c_t^-(t-t_0)$. Note that here and in general, we find a non-linear dependence of $\hat{\mathsf{u}}_2$ on g for large deformations. This is not relevant for the case of bimetallic strips but crucial to many biological systems.

5.4 Birings

Multi-layered tubular structures abound in biology, often deriving counterintuitive mechanical properties through mismatched reference states of the constitutive layers. The mechanical behavior can sometimes be understood through consideration of a cross-section, for instance measuring the opening angle of a cut ring of artery is used to infer residual stress [53]. As a simple example to demonstrate our framework in such a setting, we consider here birings, that is a birod constructed of planar subrods that each have constant intrinsic curvature $\hat{\mathsf{u}}_2^\pm$. We work under the assumption that the sub-rods have linear and diagonal constitutive laws so that the intrinsic curvature and constitutive laws follow Equations (5.18)-(5.21) with $\beta = \frac{\kappa}{g+\kappa}$.

Since each sub-rod is a (portion of) a circular ring, it is intuitive to think in terms of their radii in their reference state, $R^\pm$. It follows that

$$g = \frac{\partial S^+}{\partial S^-} = \frac{R^+}{R^-}, \qquad \hat{\mathsf{u}}_2^\pm = \frac{1}{R^\pm}. \tag{5.41}$$

5.4.1 Trivial case

We first verify the validity of (5.18) in the trivial case in which the two subrods perfectly fit together in their reference state. That is, suppose

$$R^- = R^+ + a. \tag{5.42}$$

Here, we have placed the minus rod on the "outside" so that $\mathbf{d}_1$ points inward. Then, if we choose the natural orientation, fixed in the x-y plane, so that increasing arclength corresponds to travelling the circle in a counterclockwise direction, $\mathbf{d}_3$ points in the circumferential direction and $\mathbf{d}_2 = \mathbf{e}_z$. Here, the sub-rods reference configurations being compatible with one another, "gluing" the rods to create the birod should have no effect, i.e. creating the birod should not deform the subrods or

create any stress. To see that this is indeed the case, note that the radius of curvature of the birod is $r = 1/\hat{\mathfrak{u}}_2$, and the radii of curvature of the subrods are, from (3.16),

$$r^- = r + \text{Sign}(\hat{\mathfrak{u}}_2)\, a\beta, \quad r^+ = r - \text{Sign}(\hat{\mathfrak{u}}_2)\, a(1-\beta). \tag{5.43}$$

After some algebraic manipulation[9], it is easily found that $r^- = R^-$ and $r^+ = R^+$, as expected.

The more interesting case is when the subrods have mismatched curvatures. Formula (5.43) still holds, but now it will not generally be true that $r^\pm = R^\pm$, instead the radii in the birod will be determined by a competition between bending and stretching in each subrod. Before we analyse this, we must clarify an important point regarding boundary conditions. Note that the reference state of the birod is such that no force or moment is applied at the ends of the rod. Thus, while we might naturally associate birings with a closed circle, a closed ring implies a closed boundary condition, and this is not assumed in the birod formulation. In other words, the reference state of the biring is such that the centreline forms *part* of a circle, but it is not necessarily a closed circle and the ends are not attached.

5.4.2 Inversion of a ring

As an intuitive example, consider the inversion of a ring, a process seen, for example, in the accretionary growth of a seashell [54]. Two closed elastic rings sit in a reference stress-free state such that the outside edge of the smaller ring aligns with the inside edge of the larger ring. Now stretch the smaller ring outside the larger ring and glue them together. What will be the radius of this closed biring?

To answer this in terms of the birods formulation, we first remove the closed boundary condition. Imagine a 3 step process (see Fig 9A) where we first (i) invert and glue to form the biring, then (ii) cut the rings to remove the closed geometry and form the biring reference state, and finally (iii) glue the ends back together to form the closed biring.[10]

The subrings. To describe the biring, we use the same orientation as in the trivial case, and thus label the outside rod the minus rod. Then we have

$$R^- = R^+ - a,$$

which underscores the inversion: the outside rod has the smaller reference radius.

The open biring.

Equation (5.18) gives the curvature of the open, "cut" biring. In Fig 9B we plot $\hat{\mathfrak{u}}_2$ as a function of E^+, the Youngs modulus of the plus rod. Fig 9C shows the reference open biring at the marked points. Here we are assuming circular cross-sections with equal radii $a^+ = a^- = a/2$, so that

$$k^\pm = E^\pm \pi (a^\pm)^2, \quad K^\pm = E^\pm \pi (a^\pm)^4/4. \tag{5.44}$$

As $E^+ \to 0$, $\hat{\mathfrak{u}}_2 \to \hat{\mathfrak{u}}_2^-$ and $\beta \to 0$. This is as expected, and simply reflects the fact that as the stiffness of the plus rod vanishes, the birod sits at the steady state of the minus rod. Conversely, as $E^+ \to \infty$, $\hat{\mathfrak{u}}_2 \to \hat{\mathfrak{u}}_2^+$ and $\beta \to 1$. Between these extremes, $\hat{\mathfrak{u}}_2(E^+)$ has an intriguing shape. There are two points at which $\hat{\mathfrak{u}}_2 = 0$, and a region where $\hat{\mathfrak{u}}_2 < 0$. Where $\hat{\mathfrak{u}}_2 = 0$, the reference state of the birod is actually flat. This means that two rods that naturally curve in the same direction

[9] For which it is useful to use the fact that (5.42) can be rewritten $\frac{a}{R^-} = 1 - g$.

[10] Experimentally, of course the cutting step is unnecessary. We include it here as it is natural from the theoretical point of view to first find the reference state, which requires removing the closed geometry restriction.

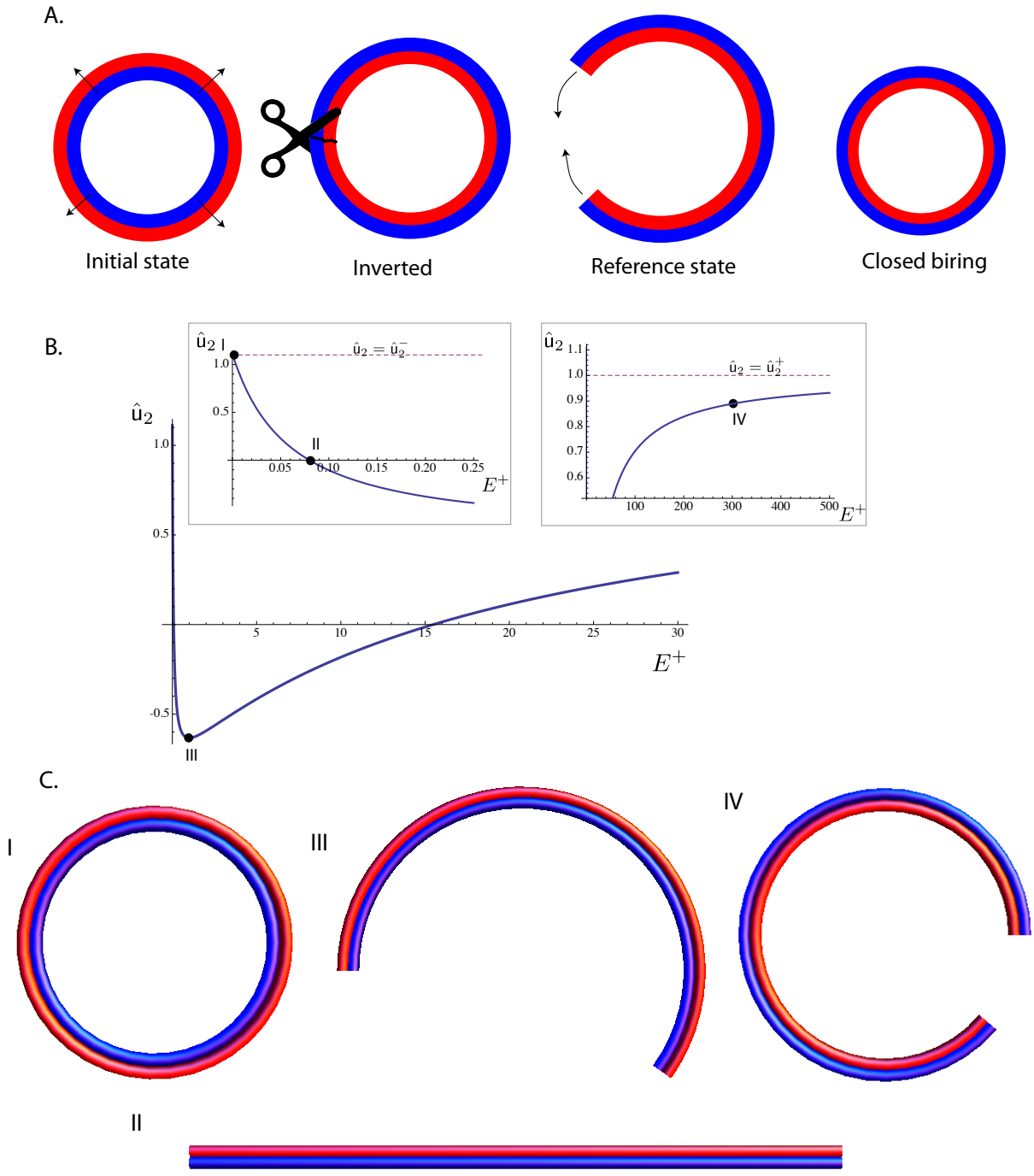

Figure 9: A: Depiction of three step process to form the inverted closed biring. B: Reference curvature $\hat{u}_2$ of the open biring as a function of stiffness E^+. Other parameters are $E^- = 1$, $a = 0.1$, $R^+ = 1.0$, $R^- = 0.9$. C: Reference state of the biring at the points I-IV of B.

are glued together and the result is a straight rod. Even more surprising, in the region $\hat{\mathsf{u}}_2 < 0$ the two rods bend the opposite direction of their reference state! To understand this, imagine that the minus rod is a string, i.e. that it only resists stretching, not bending (indeed, bending stiffness scales with radius to the fourth and can be negligible for small E). By opening the birod, the minus rod (which has been stretched to be glued) reduces its stretching; at the same time this can reduce the compressive stress of the plus rod. Of course, opening comes at the cost of bending energy. That $\hat{\mathsf{u}}_2$ can be zero or negative reflects the fine balance between bending and stretching energy in the system.

Closed biring. To form the everted ring, we must close the birod by joining the ends. To determine the radius of the closed biring, the key observation is that the length of the centreline of the birod is the same in the open and closed configurations. This is a consequence of the following statement, which we prove in Appendix C: *If a planar rod with constant intrinsic curvature and linear and diagonal constitutive laws is closed into a ring, there is no change in length, that is the deformation is such that $\alpha = 1$.*

Since the biring we are considering is mechanically equivalent to a single rod with linear and diagonal constitutive laws, the above result holds, and the radius of the closed biring is simply $r_{\text{ring}} = L/2\pi$, where L is the length of the open biring. Since $g^- = \frac{\partial S^-}{\partial S}$, we have

$$L = \frac{L^-}{g^-} = \frac{2\pi R^-}{g^-},$$

with g^- satisfying

$$\frac{1}{g^-} = 1 + \beta(g - 1).$$

It follows that the reference curvature of the biring, which we denote $\hat{\mathsf{u}}_{2_{\text{ring}}}$, satisfies

$$\hat{\mathsf{u}}_{2_{\text{ring}}} = g^- \hat{\mathsf{u}}_2^-, \tag{5.45}$$

It is easy to see that $\hat{\mathsf{u}}_{2_{\text{ring}}}$ is bounded between $\hat{\mathsf{u}}_2^-$ and $\hat{\mathsf{u}}_2^-$. Moreover, it only depends on the stretching stiffnesses and the length mismatch of the subrods. This highlights the notion that when a closed ring deforms to another closed ring, the deformation is purely one of stretching. This can be understood via a simple calculation: if a ring with reference radius R is deformed to one of radius r, then $\hat{\mathsf{u}}_2 = 1/R$, $\alpha = r/R$ and the geometric curvature $\kappa = 1/r$, and thus

$$\mathsf{u}_2 = \alpha\kappa = \frac{r}{R}\frac{1}{r} = \frac{1}{R} = \hat{\mathsf{u}}_2 \tag{5.46}$$

is unaffected. Thus, any deformation in which the biring remains closed and circular is purely stretching; on the other hand, if the biring is cut from its reference state it will open up, a deformation that will be purely bending.

We make one final remark regarding birings. There is an interesting consequence of the fact that closing a rod into a ring requires no stretching energy. Suppose we take two straight subrods of equal length but different thickness and glue them together to form a birod (again choosing β so that the birod is diagonal), which in this case will be straight in its reference state. Now form a ring by attaching the ends. There are two ways this can be done: the thick rod can be on the inside or on the outside of the ring. The point is that either way, the length of the birod centreline does not change, and thus the biring radius is the same, even though the subrods will have different radii in either case. Also, the energy is exactly equal in both cases. Similar arguments can be made to show that if the straight birod is clamped and a compressive force is applied until a buckling

occurs, the two directions of buckling, which are not symmetric in terms of the individual subrods, are equivalent in terms of the birod – the energy is the same and the system has no preference to buckle one direction or the other.

6 3D birods

In 3D, the tangents $\mathbf{d}_3^\pm$ to the sub-rods are not aligned in general (cf. Eq. (3.19) and Fig. 6). Hence the definition $\mathbf{N} = \mathbf{n}^+ + \mathbf{n}^-$ mixes components of $\mathbf{n}^\pm$ with components that are not known constitutively so that we cannot derive directly a constitutive law for N_3. Similarly, the definition of a moment $\mathbf{M}$ for the birod depends $\mathbf{n}^\pm$ and include components which are not known constitutively (see App.D for details). Therefore, unlike the 1D and 2D case where one could derive a constitutive law for the birod forces and moments, in 3D the equation for the birod cannot be simply written as a Kirchhoff equation. The key to develop a theory of birod is therefore to identify the correct generalised strains and the associated generalised stresses as proposed in the next Section.

6.1 Geometry of 3D birods

We use the definition of the sub-rods as given in Sec. 3.1.2 and summarised in Fig. 10. However, in Sec. **??**, we defined a centreline and a right-handed orthonormal frame of directors for the birod itself and showed how it could be characterised by 4 geometric degrees of freedom α and $\mathbf{u}$. Here we propose an alternative geometric description of the structure. We introduce a non-orthonormal frame and use four different geometric parameters: α^+, α^-, θ and $\mathcal{U}$. In particular, the definition of a centreline of the birod is no longer required. We therefore assume that sections of the birod are now labelled by a material parameter R (which depends on the particular problem of interest and can be different from the unloaded arc length S). The definitions of Sec. **??** remain valid after replacing S by R. In particular, there exist one-to-one mappings $G^\pm$ such that $S^\pm = G^\pm(R,t)$ which implies that $G^+ = G \circ G^-$ and we have

$$g^+ = \frac{\partial G^+}{\partial R}; \qquad g^- = \frac{\partial G^-}{\partial R}, \tag{6.1}$$

while $g = \frac{\partial G}{\partial S^-}$ as before. Note that while g is a physical quantity that encodes the differential growth between the two sub-rods, the functions $g^\pm$ actually relate the (arbitrary) parameterisation R of the birod to the reference arc-lengths $S^\pm$ of the sub-rods. In particular one of these latter functions (say g^-) may be chosen *ad libitum* as that (modelling) choice is equivalent to making a choice of parameterisation R. The other function is then given by $g^+ = gg^-$ according to the chain rule.

The unit vector $\mathbf{d}_1$ is defined, as before, as the vector (see Fig. 6) pointing from $\mathbf{r}^-$ to $\mathbf{r}^+$ as given (3.17). By definition of $\varphi^\pm$ in Sec. 3.1.2, we have

$$\mathbf{d}_1 = \cos\varphi^-\mathbf{d}_1^- + \sin\varphi^-\mathbf{d}_2^- = -\cos\varphi^+\mathbf{d}_1^+ - \sin\varphi^+\mathbf{d}_2^+, \tag{6.2}$$
$$\mathbf{d}_3^- \times \mathbf{d}_1 = -\sin\varphi^-\mathbf{d}_1^- + \cos\varphi^-\mathbf{d}_2^-, \tag{6.3}$$
$$\mathbf{d}_3^+ \times \mathbf{d}_1 = \sin\varphi^+\mathbf{d}_1^+ - \cos\varphi^-\mathbf{d}_2^+. \tag{6.4}$$

The frames $\{\mathbf{d}_i^\pm\}$ of the sub-rods are recovered from $\mathbf{d}_1$, $\mathbf{d}_3^\pm$ and $\varphi^\pm$:

$$\begin{aligned}
\begin{pmatrix}\mathbf{d}_1^- & \mathbf{d}_2^- & \mathbf{d}_3^-\end{pmatrix} &= \begin{pmatrix}\mathbf{d}_1 & \mathbf{d}_3^- \times \mathbf{d}_1 & \mathbf{d}_3^-\end{pmatrix}\ \mathbf{R}(\mathbf{d}_3^-, -\varphi^-),\\
\begin{pmatrix}\mathbf{d}_1^+ & \mathbf{d}_2^+ & \mathbf{d}_3^+\end{pmatrix} &= \begin{pmatrix}\mathbf{d}_1 & \mathbf{d}_3^+ \times \mathbf{d}_1 & \mathbf{d}_3^+\end{pmatrix}\ \mathbf{R}(\mathbf{d}_3^+, \varphi^+ + \pi),
\end{aligned} \tag{6.5}$$

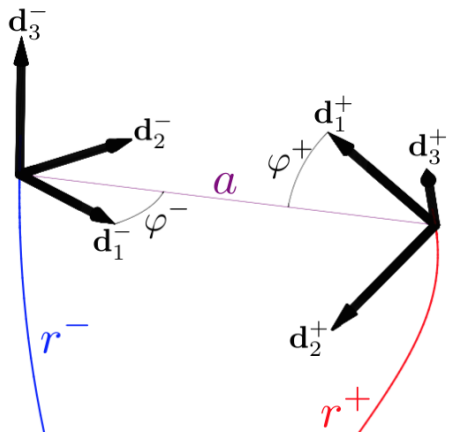

Figure 10: A summary of the key geometric quantities defining a birod from Sec. 3.1.2.

where $\mathbf{R}(\mathbf{d}, \alpha)$ indicates a right handed rotation around the vector $\mathbf{d}$ by an angle α. The frames $\mathbf{D}^\pm = \begin{pmatrix} \mathbf{d}_1^\pm & \mathbf{d}_2^\pm & \mathbf{d}_3^\pm \end{pmatrix}$ are related by the following sequence of rotations (see Fig. 10):

$$\mathbf{D}^+ = \mathbf{D}^- \ \ \mathbf{R}(\mathbf{d}_3^-, \varphi^-) \ \ \mathbf{R}(\mathbf{d}_1, \theta) \ \ \mathbf{R}(\mathbf{d}_3^+, -\varphi^+ - \pi), \tag{6.6}$$

From these definitions, it follows that (see Appendix F)

$$g^+\mathbf{u}^+ = g^-\mathbf{u}^- + \left(\varphi^-\right)' \mathbf{d}_3^- + \theta' \mathbf{d}_1 - \left(\varphi^+\right)' \mathbf{d}_3^+, \tag{6.7}$$

where $(\ )'$ denotes derivations w.r.t. R.

We equip the birod with the non-orthonormal frame $\{\mathbf{d}_1, \mathbf{d}_3^-, \mathbf{d}_3^+\}$. Although, this implies that we will also have to keep track of the dual basis, we will see in the next two sub-sections that this choice is natural and leads to a complete description of the birod. Since we need the dual basis, it is practical to use upper and lower indices. For this reason we introduce the following vectors

$$\mathbf{c}_1 = \mathbf{d}_1, \qquad \mathbf{c}_+ = \mathbf{d}_3^+, \qquad \mathbf{c}_- = \mathbf{d}_3^-, \tag{6.8}$$

$$\mathbf{c}^1 = \mathbf{d}_1, \qquad \mathbf{c}^+ = -\mathbf{d}_1 \times \mathbf{d}_3^-, \qquad \mathbf{c}^- = \mathbf{d}_1 \times \mathbf{d}_3^+. \tag{6.9}$$

According to (I.28), we have

$$\begin{aligned} \mathbf{c}^\mp &= -\sin\varphi^\pm \mathbf{d}_1^\pm + \cos\varphi^\pm \mathbf{d}_2^\pm, \\ \mathbf{c}^1 &= \mp(\cos\varphi^\pm \mathbf{d}_1^\pm + \sin\varphi^\pm \mathbf{d}_2^\pm), \end{aligned} \tag{6.10}$$

so that

$$\begin{aligned} \mathbf{d}_1^\pm &= -\sin\varphi^\pm \mathbf{c}^\mp \mp \cos\varphi^\pm \mathbf{c}^1, \\ \mathbf{d}_2^\pm &= \cos\varphi^\pm \mathbf{c}^\mp \mp \sin\varphi^\pm \mathbf{c}^1. \end{aligned} \tag{6.11}$$

We define θ as the oriented angle from $\mathbf{c}_- = \mathbf{d}_3^-$ to $\mathbf{c}_+ = \mathbf{d}_3^+$ such that $\mathbf{d}_3^- \times \mathbf{d}_3^+ = \sin\theta\, \mathbf{d}_1$ (this definition is equivalent to (3.19)). We note the following identities

$$\mathbf{c}^1 \cdot \mathbf{c}^\pm = 0, \qquad \mathbf{c}^+ \cdot \mathbf{c}^- = -\cos\theta, \tag{6.12}$$

$$\mathbf{c}_1 \times \mathbf{c}^\pm = \pm \mathbf{c}_\mp, \qquad \mathbf{c}^+ \times \mathbf{c}^- = -\sin\theta \mathbf{c}^1, \tag{6.13}$$

$$\mathbf{c}_\pm \cdot \mathbf{c}^\mp = 0, \qquad \mathbf{c}_\pm \cdot \mathbf{c}^\pm = -\sin\theta, \tag{6.14}$$

$$\mathbf{c}^\pm \times \mathbf{c}_\pm = \pm\cos\theta \mathbf{d}_1, \qquad \mathbf{c}^\pm \times \mathbf{c}_\mp = \pm \mathbf{d}_1. \tag{6.15}$$

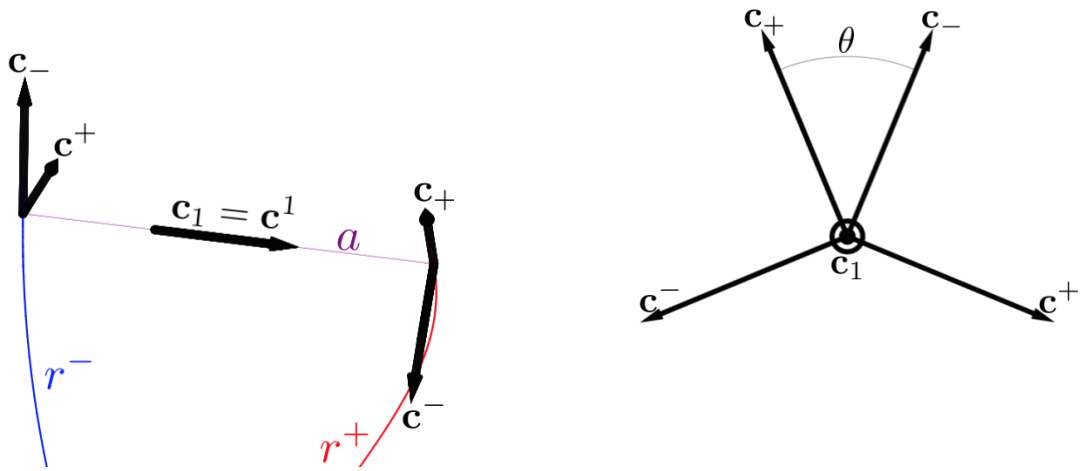

Figure 11: An alternative way to frame a birod: Non-orthonormal birod frame superposed on the sub-rods (left) and the same frame projected on a plane perpendicular to $\mathbf{c}_1$ (right). The right panel can be used to easily infer the relations (6.13-6.19).

For any vector $\mathbf{v}$, there exists six[11] scalars $\{\mathsf{v}_1, \mathsf{v}_+, \mathsf{v}_-\}$ and $\{\mathsf{v}^1, \mathsf{v}^+, \mathsf{v}^-\}$ defined as

$$\mathsf{v}_\pm = -\mathbf{v}\cdot\mathbf{c}_\pm, \qquad \mathsf{v}^\pm = -\mathbf{v}\cdot\mathbf{c}^\pm, \qquad \mathsf{v}^1 = \mathsf{v}_1 = \mathbf{v}\cdot\mathbf{d}_1. \tag{6.16}$$

Whenever $\theta \neq 0$,

$$\mathbf{v} = \mathsf{v}_1\ \mathbf{c}^1 + \mathsf{v}_+\ \frac{\mathbf{c}^+}{\sin\theta} + \mathsf{v}_-\ \frac{\mathbf{c}^-}{\sin\theta} = \mathsf{v}^1\ \mathbf{c}_1 + \mathsf{v}^+\ \frac{\mathbf{c}_+}{\sin\theta} + \mathsf{v}^-\ \frac{\mathbf{c}_-}{\sin\theta}. \tag{6.17}$$

In particular,

$$\begin{cases} \mathbf{c}_- = \dfrac{-\mathbf{c}^+\cos\theta - \mathbf{c}^-}{\sin\theta}, \\ \mathbf{c}_+ = \dfrac{-\mathbf{c}^+ - \mathbf{c}^-\cos\theta}{\sin\theta}, \end{cases} \quad \text{and} \quad \begin{cases} \mathbf{c}^- = \dfrac{-\mathbf{c}_- + \mathbf{c}_+\cos\theta}{\sin\theta}, \\ \mathbf{c}^+ = \dfrac{-\mathbf{c}_+ + \mathbf{c}_-\cos\theta}{\sin\theta}. \end{cases} \tag{6.18}$$

By taking the scalar product of (6.17) by $\mathbf{c}_-$, $\mathbf{c}_+$, $\mathbf{c}^-$ and $\mathbf{c}^+$, we obtain relations between the components in the two basis:

$$\begin{cases} -\mathsf{v}_- = \dfrac{\mathsf{v}^+\cos\theta + \mathsf{v}^-}{\sin\theta}, \\ -\mathsf{v}_+ = \dfrac{\mathsf{v}^+ + \mathsf{v}^-\cos\theta}{\sin\theta}, \end{cases} \quad \text{and} \quad \begin{cases} -\mathsf{v}^- = \dfrac{\mathsf{v}_- - \mathsf{v}_+\cos\theta}{\sin\theta}, \\ -\mathsf{v}^+ = \dfrac{\mathsf{v}_+ - \mathsf{v}_-\cos\theta}{\sin\theta}. \end{cases} \tag{6.19}$$

The construction (6.16,6.17) is not quite standard (usually, the sines would be included within the definitions of the components v_α). However, it insures that for a vector $\mathbf{v}$, the components v_α and v^β are well defined even when $\theta \to 0$. The presence of $\sin\theta$ may be a problem as $\theta \to 0$. To circumnavigate this problem, we will occasionally mix the basis $\{\mathbf{c}_1, \mathbf{c}_-, \mathbf{c}_+\}$ and its dual and express vectors as linear combinations of the right-handed orthnormal bases $\{\mathbf{c}_1, \mathbf{c}^+, \mathbf{c}_-\}$ or $\{\mathbf{c}_1, \mathbf{c}_+, \mathbf{c}^-\}$.

Next we compute the evolution of the new bases along the length of the birod. We start with

$$\mathbf{c}^{1\prime} = \mathbf{d}_1' = \left(\cos\varphi^-\mathbf{d}_1^- + \sin\varphi^-\mathbf{d}_2^-\right)' = \left(g^-\mathbf{u}^- + \left(\varphi^-\right)'\mathbf{d}_3^-\right)\times\mathbf{d}_1, \tag{6.20}$$

$$\mathbf{c}^{+\prime} = \left(-\mathbf{d}_1\times\mathbf{d}_3^-\right)' = \left(-\sin\varphi^-\mathbf{d}_1^- + \cos\varphi^-\mathbf{d}_2^-\right)' = \left(g^-\mathbf{u}^- + \left(\varphi^-\right)'\mathbf{d}_3^-\right)\times\mathbf{c}^+, \tag{6.21}$$

$$\mathbf{c}^{-\prime} = \left(\mathbf{d}_1\times\mathbf{d}_3^+\right)' = \left(-\sin\varphi^+\mathbf{d}_1^+ + \cos\varphi^+\mathbf{d}_2^+\right)' = \left(g^+\mathbf{u}^+ + \left(\varphi^+\right)'\mathbf{d}_3^+\right)\times\mathbf{c}^-, \tag{6.22}$$

[11] note however that $\mathsf{v}_1 = \mathsf{v}^1$ since $\mathbf{d}_1$ is always perpendicular to $\mathbf{d}_3^\pm$.

where we use, $(\ )' = \partial_R(\ )$ indicates derivative by R at constant T. By defining

$$\boldsymbol{\mathcal{U}} = g^- \mathbf{u}^- + \left(\varphi^-\right)' \mathbf{d}_3^- + \frac{\theta'}{2}\mathbf{c}^1, \tag{6.23}$$

and substituting (6.7) in (6.22), we obtain

$$(\mathbf{c}^\alpha)' = \left(\boldsymbol{\mathcal{U}} - \sigma_\alpha \ \frac{\theta'}{2}\mathbf{c}^1\right) \times \mathbf{c}^\alpha, \tag{6.24}$$

where Greek indices run through $\{1, +, -\}$ and $\sigma_\alpha = \pm$ if $\alpha = \pm$ and 0 if $\alpha = 1$; no summation implied in RHS. Similarly, we have

$$(\mathbf{c}_\alpha)' = \left(\boldsymbol{\mathcal{U}} + \sigma_\alpha \ \frac{\theta'}{2}\mathbf{c}_1\right) \times \mathbf{c}_\alpha. \tag{6.25}$$

Eqs. (6.24,6.25) show that the vector $\boldsymbol{\mathcal{U}}$ plays the role of the Darboux vector for the non-orthogonal basis $\{\mathbf{c}^1, \mathbf{c}^+, \mathbf{c}^-\}$ and $\{\mathbf{c}_1, \mathbf{c}_+, \mathbf{c}_-\}$. Next, taking the derivative by S of $\mathbf{r}^+ - \mathbf{r}^- = a\mathbf{d}_1$, we obtain

$$\alpha^+ g^+ \mathbf{c}_+ - \alpha^- g^- \mathbf{c}_- = a\, \boldsymbol{\mathcal{U}} \times \mathbf{c}^1 = a\ \left(\mathcal{U}_+ \frac{\mathbf{c}^+}{\sin\theta} + \mathcal{U}_- \frac{\mathbf{c}^-}{\sin\theta}\right) \times \mathbf{c}^1 = a\ \left(\mathcal{U}_- \frac{\mathbf{c}_+}{\sin\theta} - \mathcal{U}_+ \frac{\mathbf{c}_-}{\sin\theta}\right). \tag{6.26}$$

Projecting (6.26) on $\mathbf{c}^\pm$ leads to

$$a\mathcal{U}_\pm = \sin\theta\ \alpha^\mp g^\mp, \tag{6.27}$$

and therefore

$$\boldsymbol{\mathcal{U}} = \mathcal{U}\, \mathbf{c}^1 + \frac{g^-}{a}\left(\alpha^- \mathbf{c}^+ + \alpha^+ g \mathbf{c}^-\right), \tag{6.28}$$

where $\mathcal{U} = \boldsymbol{\mathcal{U}} \cdot \mathbf{c}_1$. The main advantage of using non-orthogonal bases is that a birod, through Eq. (6.28), can be completely parameterised[12] by the four scalar functions $\alpha^+(R)$, $\alpha^-(R)$, $\theta(R)$ and $\mathcal{U}(R)$ which gives a directly relevant description of the structure: the stretches in both strands, the angle between the strands and the bending of the structure about the common chord. Furthermore, the projection of (3.29) on the dual base $\{\mathbf{c}^1, \mathbf{c}^+, \mathbf{c}^-\}$ leads (see App. G) to the natural definition of generalised stresses for which it is possible to write explicit constitutive laws (see App. H) in function of $\alpha^\pm$, θ and $\mathcal{U}$.

6.2 Generalised moments for the 3D extensible birod

We start again from the equilibrium equation for each sub-rods, namely

$$\begin{aligned}
&\left(\mathbf{n}^+\right)' + \mathbf{f} + \mathbf{F}^+ = 0,\\
&\left(\mathbf{n}^-\right)' - \mathbf{f} + \mathbf{F}^- = 0,\\
&\left(\mathbf{m}^\pm\right)' + \mathbf{r}^{\pm\prime} \times \mathbf{n}^\pm \pm \mathbf{l} - c^\pm \mathbf{d}_1 \times \mathbf{f} + \mathbf{L}^\pm = 0,
\end{aligned} \tag{6.29}$$

where $(\ )' = \frac{\mathrm{d}(\ )}{\mathrm{d}R}$ and the density of external loads $\mathbf{F}^\pm$ and $\mathbf{L}^\pm$ and internal loads $\mathbf{f}$ and $\mathbf{l}$ are defined per unit R. Instead of defining $\mathbf{N}$ and a global moment $\mathbf{M}$ for which we were not able to find explicit constitutive laws (cf. App. D), we define the three forces obtained by projecting $\mathbf{N}$ on

[12] Since (6.24,6.25,6.28) can be integrated to find the local basis $\{\mathbf{c}_1, \mathbf{c}_-, \mathbf{c}_+\}$. The local frames of sub-rods are then given by (6.5) and their centrelines are found by integrating $(\mathbf{r}^\pm)' = \alpha^\pm g^\pm \mathbf{c}_\pm$.

the $\mathbf{c}_1, \mathbf{c}_+, \mathbf{c}_-$ basis and six generalised moments that are naturally associated with our kinematic description, namely:

$$\begin{aligned} \mathsf{P}^1 &= (\mathbf{m}^+ + \mathbf{m}^-) \cdot \mathbf{c}^1, & \mathsf{Q}_1 &= (\mathbf{m}^+ - \mathbf{m}^-) \cdot \mathbf{c}_1, \\ \mathsf{P}^+ &= -(\mathbf{m}^+ + \mathbf{m}^- - a\,\mathbf{d}_1 \times \mathbf{n}^-) \cdot \mathbf{c}^+ = -(\mathbf{m}^+ + \mathbf{m}^-) \cdot \mathbf{c}^+ - a\mathsf{n}_3^-, & \mathsf{Q}_+ &= -\mathbf{m}^- \cdot \mathbf{c}_+, \\ \mathsf{P}^- &= -(\mathbf{m}^+ + \mathbf{m}^- + a\,\mathbf{d}_1 \times \mathbf{n}^+) \cdot \mathbf{c}^- = -(\mathbf{m}^+ + \mathbf{m}^-) \cdot \mathbf{c}^- - a\mathsf{n}_3^+, & \mathsf{Q}_- &= -\mathbf{m}^+ \cdot \mathbf{c}_-. \end{aligned} \tag{6.30}$$

The four scalars $\mathsf{P}^\pm$, Q_1 and P^1 are the moments of force conjugated to virtual displacements of $\alpha^\pm$, θ and $\mathcal{U}$ (respectively). Furthermore, the 6 moments defined in (6.30) naturally arise when projecting (3.29) on the basis $\{\mathbf{c}^1, \mathbf{c}^+, \mathbf{c}^-\}$ (see App. G). Finally, it is useful to note (see App. I) that P^1 is the component along $\mathbf{c}^1$ of the total moment about any point on the common chord, P^+ (resp. P^-) is the component along $\mathbf{c}^+$ (resp. $\mathbf{c}^-$) of the total moment about $\mathbf{r}^+$ (resp. $\mathbf{r}^-$). We find, after some straightforward algebra (see App. G), the following system

$$(\mathsf{N}_1)' = \frac{g^-}{a}\left(\alpha^- \mathsf{N}_- - \alpha^+ g \mathsf{N}_+\right) - \mathsf{F}_1, \tag{6.31}$$

$$(\mathsf{N}_-)' = \left(\mathcal{U} - \frac{\theta'}{2}\right)\left(\frac{\mathsf{N}_+ - \mathsf{N}_- \cos\theta}{\sin\theta}\right) - \frac{g^-}{a}(\alpha^- - \alpha^+ g\cos\theta)\mathsf{N}_1 - \mathsf{F}_-, \tag{6.32}$$

$$(\mathsf{N}_+)' = -\left(\mathcal{U} + \frac{\theta'}{2}\right)\left(\frac{\mathsf{N}_- - \mathsf{N}_+ \cos\theta}{\sin\theta}\right) + \frac{g^-}{a}(\alpha^- \cos\theta - \alpha^+ g)\mathsf{N}_1 - \mathsf{F}_+, \tag{6.33}$$

$$(\mathsf{P}^1)' = \frac{g^-}{a}\left(\alpha^+ g \frac{\mathsf{P}^+ + \mathsf{P}^- \cos\theta - a\mathsf{N}_-}{\sin\theta} - \alpha^- \frac{\mathsf{P}^- + \mathsf{P}^+ \cos\theta - a\mathsf{N}_+}{\sin\theta}\right) - \mathsf{H}^1, \tag{6.34}$$

$$(\mathsf{P}^-)' = \frac{g^-}{a}\alpha^-\left(\mathsf{P}^1 \sin\theta - a\mathsf{N}_1\cos\theta\right) + \left(\frac{\theta'}{2} + \mathcal{U}\right)\frac{\mathsf{P}^+ + \mathsf{P}^- \cos\theta - a\mathsf{N}_-}{\sin\theta} - \mathsf{H}^-. \tag{6.35}$$

$$(\mathsf{P}^+)' = \frac{g^-}{a}\alpha^+ g(a\mathsf{N}_1\cos\theta - \mathsf{P}^1\sin\theta) + \left(\frac{\theta'}{2} - \mathcal{U}\right)\frac{\mathsf{P}^- + \mathsf{P}^+ \cos\theta - a\mathsf{N}_+}{\sin\theta} - \mathsf{H}^+, \tag{6.36}$$

$$\begin{aligned}(\mathsf{Q}_1)' = \frac{g^-}{a}&\left(\alpha^+ g \frac{\mathsf{P}^+ + \mathsf{P}^- \cos\theta - a\mathsf{N}_-}{\sin\theta} + \alpha^- \frac{\mathsf{P}^- + \mathsf{P}^+ \cos\theta - a\mathsf{N}_+}{\sin\theta}\right) \\ &+ \frac{2g^-}{a}\left(\mathsf{Q}_+\alpha^+ g + \mathsf{Q}_-\alpha^-\right) - 2\mathsf{l}_1 - \mathsf{h}_1,\end{aligned} \tag{6.37}$$

where the external loads are defined by

$$\mathsf{F}_1 = \mathbf{F}\cdot\mathbf{c}_1, \qquad \mathsf{F}_- = -\mathbf{F}\cdot\mathbf{c}_-, \qquad \mathsf{F}_+ = -\mathbf{F}\cdot\mathbf{c}_+, \qquad \text{with} \quad \mathbf{F} = \mathbf{F}^+ + \mathbf{F}^-, \tag{6.38}$$

and

$$\begin{aligned} \mathsf{H}^1 &= (\mathbf{L}^+ + \mathbf{L}^-)\cdot\mathbf{c}^1, & \mathsf{H}^- &= -(\mathbf{L}^+ + \mathbf{L}^-)\cdot\mathbf{c}^- - a\mathbf{F}^+\cdot\mathbf{c}_+, \\ \mathsf{h}_1 &= (\mathbf{L}^+ - \mathbf{L}^-)\cdot\mathbf{c}_1, & \mathsf{H}^+ &= -(\mathbf{L}^+ + \mathbf{L}^-)\cdot\mathbf{c}^+ - a\mathbf{F}^-\cdot\mathbf{c}_-. \end{aligned} \tag{6.39}$$

Note that due to the geometric constraints, we only have four equations for the six moments, the last two being determined constitutively. The removable singularity in the vector field appearing as $\theta \to 0$ is discussed in App. I.

6.3 Constitutive laws

The geometry of the birod is completely specified by 4 scalars: α^+, α^-, $\mathcal{U}$ and θ, whereas Eqs. (6.31-6.37) provide 7 equilibrium equations involving 10 mechanical quantities: $\mathbf{N}$, P^1, P^+, P^-, Q^1, Q^+, Q^- and l_1. As a result, we need (10+4)-7=7 constitutive laws.

Constitutive law for the attachment. The moment l_1 about $\mathbf{d}_1$ applied by the sub-rods on one another is transmitted by the particular fashion in with the two rods are attached and that we referred to as *the glue*.. Its dependance on the strain is therefore a constitutive property of the glue itself and must be specified. For simplicity, we assume that it is a function of θ only. In particular we shall look into both special cases of free to rotate sud-rods: the case where $\mathsf{l}_1 = 0$ and the case where the two sub-rods are rigidly attached so that $\theta(S)$ is a prescribed function. In the latter case, l_1 is no longer prescribed constitutively but we can drop (6.37) since the birod lost a degree of freedom (θ is specified).

Constitutive law for extensible sub-rods. The constitutive laws for the sub-rods provide 6 constitutive laws respectively for P^1, P^+, P^-, Q^1, Q^+ and Q^-. Indeed, if both sub-rods are extensible, the moments $\mathbf{m}^\pm$ and the tensions $\mathsf{n}_3^\pm$ appearing in (6.30) are known constitutively in function of $\alpha^\pm$ and $\mathbf{u}^\pm$. But since $\mathbf{u}^\pm$ is a function of $\alpha^\pm$, θ and $\mathcal{U}$ (see Sec. 6.1), these relations can be re-expressed in function of the latter variables. These 6 relationships together with the law for the attachment give the 7 required constitutive laws. An explicit computation of these constitutive laws in the particular case of sub-rods with linear constitutive laws for the moments $\mathbf{m}^\pm$ is given in App. H.

Constitutive law for one or two inextensible sub-rods. If one of the sub-rod is inextensible, say the + rod, then its stretch is given and the birod looses both a degree of freedom α^+ and the constitutive law for P^- so that both the total count of variables and equations are decreased by the number of inextensible sub-rods.

We have now a full system of equations for the growing birod. This system is defined by the following three components:

- **The growth laws.** A set of growth laws for the slow evolution of the attachment and reference shapes of the sub-rods is specified as explain in Sections 2.1.3 & 3.1.2.
- **The equilibrium equations.** The quasi-static equilibrium problem involving 4 kinematic variables and 10 mechanical variables for 7 equilibrium equations (6.31-6.37).
- **The constitutive laws.** A set of 7 constitutive laws as discussed in this section.

Once the solution of this system is known, the the position of the sub-rods centrelines is obtained by integration of $(\mathbf{r}^\pm)' = \alpha^\pm g^\pm \mathbf{c}_\pm$ from (6.5), (6.24), (6.25), and (6.28).

6.4 Unloaded birod and reference configuration

The first question of interest is to establish the shape of the birod when unloaded (that is in the absence of external line density of forces $\mathbf{f}$, moments $\mathbf{l}$ or loads at the ends). It is important to realise that an unloaded birod can be stressed in order to balance its internal geometry. Therefore, the unloaded shape cannot be simply obtained by imposing the vanishing of the constitutive laws (indeed, this would provide a system of 7 equations for 4 unknown strains).

More precisely, an *unloaded configuration* is defined as a configuration which solves (6.31-6.37) with $\mathbf{F} = H = \mathbf{0}$ and $\mathsf{h}_1 = 0$ and no end loads: $\mathbf{N}(0) = \mathbf{N}(L) = \mathbf{0}$ and $\mathsf{P}^1(0) = \mathsf{P}^+(0) = \mathsf{P}^-(0) = \mathsf{Q}_1(0) = \mathsf{P}^1(L) = \mathsf{P}^+(L) = \mathsf{P}^-(L) = \mathsf{Q}_1(L) = 0$. In that case, Eqs. (6.31-6.36) imply[13] $\mathbf{N} = \mathbf{0}$ together with

$$\mathsf{P}^1 = \mathsf{P}^+ = \mathsf{P}^- = 0, \tag{6.40}$$

[13] Indeed the boundary condition imply $\mathbf{A} = \mathbf{B} = \mathbf{0}$ in App. I which in turn imply $\mathsf{P}^\alpha = 0$.

while Eq. (6.37) becomes

$$\frac{1}{2}(\mathsf{Q}_1)' = \frac{g^-}{a}\left(\mathsf{Q}_+\alpha^+ g + \mathsf{Q}_-\alpha^-\right) - \mathsf{l}_1, \tag{6.41}$$

with the boundary condition $\mathsf{Q}_1(0) = \mathsf{Q}_1(L) = 0$.

This system of equations can also be written in in term of the mechanical quantities of the sub-rods. In which case, it reads

$$\begin{aligned} &\pm(\mathbf{m}^+ + \mathbf{m}^-)\cdot(\mathbf{d}_1 \times \mathbf{d}_3^\pm) = -a\mathsf{n}_3^\pm, \qquad &&(\mathbf{m}^+ + \mathbf{m}^-)\cdot\mathbf{d}_1 = 0, \\ &\left((\mathbf{m}^+ - \mathbf{m}^-)\cdot\mathbf{d}_1\right)' + \frac{2g^-}{a}\left(\alpha^-\mathbf{d}_3^-\cdot\mathbf{m}^+ + \alpha^+ g\,\mathbf{d}_3^+\cdot\mathbf{m}^-\right) + 2\mathsf{l}_1 = 0, \end{aligned} \tag{6.42}$$

With the boundary conditions $(\mathbf{m}^+ - \mathbf{m}^-)\cdot\mathbf{c}^1 = 0$ at $R = 0$ and at $R = L$.

The system (6.42) is a completely generic set of four equations for the four degrees of freedom of the unloaded birod. It is valid for any choice of constitutive laws of the sub-rods.

6.5 Unloaded configuration with linear moments

We now consider the particular but important case of sub-rods with linear diagonal constitutive laws for the moments $\mathbf{m}^\pm$ and arbitrary laws for $\mathsf{n}_3^\pm$:

$$\mathbf{m}^\pm = (EI)^\pm\left[\left(\mathsf{u}_1^\pm - \widehat{\mathsf{u}_1}^\pm\right)\mathbf{d}_1^\pm + b^\pm\left(\mathsf{u}_2^\pm - \widehat{\mathsf{u}_2}^\pm\right)\mathbf{d}_2^\pm + \Gamma^\pm\left(\mathsf{u}_3^\pm - \widehat{\mathsf{u}_3}^\pm\right)\mathbf{d}_3^\pm\right], \tag{6.43}$$

where $(EI)^\pm = [(EI)_1]^\pm$, $b^\pm = [(EI)_2]^\pm/[(EI)_1]^\pm$, and $\Gamma^\pm = (\mu J)^\pm/[(EI)_1]^\pm$. We define a measure (EI) of the total stiffness of the birod together with the total reference curvatures and twists $\widehat{\mathcal{U}}_i$ about key directions

$$(EI) = \frac{(EI)^+}{g} + (EI)^-, \qquad \mathcal{E}^+ = \frac{(EI)^+}{g(EI)}, \qquad \mathcal{E}^- = \frac{(EI)^-}{(EI)}, \tag{6.44}$$

$$\begin{aligned} &\widehat{\mathcal{U}}_0 = a\,(g\hat{\mathbf{u}}^+ - \hat{\mathbf{u}}^-)\cdot\mathbf{d}_1, \qquad &&\widehat{\mathcal{U}}_2^\pm = a\,\frac{g^\pm}{g^-}\,(\hat{\mathbf{u}}^\pm\cdot\mathbf{c}^\mp), \\ &\widehat{\mathcal{U}}_1 = a\,(g\hat{\mathbf{u}}^+ + \hat{\mathbf{u}}^-)\cdot\mathbf{d}_1, \qquad &&\widehat{\mathcal{U}}_3^\pm = a\,\frac{g^\pm}{g^-}\left(\hat{\mathsf{u}}_3^\pm + \frac{\mathrm{d}\varphi^\pm}{\mathrm{d}S^\pm}\right). \end{aligned} \tag{6.45}$$

The computation of the general constitutive laws for the components is given in App. H. We focus on the case of sub-rods having cross-sections with at least the symmetries of the square ($b^\pm = 1$) or such that one of their principal axes is along $\mathbf{c}_1$: $\varphi^\pm = k\pi$ ($k \in \mathbb{Z}$) (see the appendix for a discussion). In this case, the constitutive laws for the birod are

$$\mathsf{P}^1 = \frac{(EI)}{g^-}\left[\left(\mathcal{U} - \frac{g^-}{a}\frac{\widehat{\mathcal{U}}_1}{2}\right) + (\mathcal{E}^+ - \mathcal{E}^-)\left(\frac{\theta'}{2} - \frac{g^-}{a}\frac{\widehat{\mathcal{U}}_0}{2}\right)\right], \tag{6.46}$$

$$\begin{aligned} \mathsf{P}^+ = -a\mathsf{n}_3^-(\alpha^-) - \frac{(EI)}{a}\Big[&b^-\mathcal{E}^-\left(\alpha^- - \alpha^+ g\cos\theta - \widehat{\mathcal{U}}_2^-\right) \\ &-b^+\mathcal{E}^+\cos\theta\left(\alpha^+ g - \alpha^-\cos\theta - \widehat{\mathcal{U}}_2^+\right) \\ &+\mathcal{E}^+\Gamma^+\sin\theta\left(\alpha^-\sin\theta + \widehat{\mathcal{U}}_3^+\right)\Big], \end{aligned} \tag{6.47}$$

$$\begin{aligned} \mathsf{P}^- = -a\mathsf{n}_3^+(\alpha^+) - \frac{(EI)}{a}\Big[&b^+\mathcal{E}^+\cos\theta\left(\alpha^+ g - \alpha^-\cos\theta - \widehat{\mathcal{U}}_2^+\right) \\ &-b^-\mathcal{E}^-\cos\theta\left(\alpha^- - \alpha^+ g\cos\theta - \widehat{\mathcal{U}}_2^-\right) \\ &+\mathcal{E}^-\Gamma^-\sin\theta\left(\alpha^+ g\sin\theta + \widehat{\mathcal{U}}_3^+\right)\Big], \end{aligned} \tag{6.48}$$

$$\mathsf{Q}_1 = \frac{(EI)}{g^-}\left[\left(\frac{\theta'}{2}-\frac{g^-}{a}\frac{\widehat{\mathcal{U}}_0}{2}\right)+(\mathcal{E}^+-\mathcal{E}^-)\left(\mathcal{U}-\frac{g^-}{a}\frac{\widehat{\mathcal{U}}_1}{2}\right)\right], \tag{6.49}$$

$$\mathsf{Q}_+ = \frac{(EI)}{a}\left[\mathcal{E}^-b^-\sin\theta\left(\alpha^- - \alpha^+ g\cos\theta - \widehat{\mathcal{U}}_2^-\right)+\mathcal{E}^-\Gamma^-\cos\theta\left(\alpha^+ g\sin\theta+\widehat{\mathcal{U}}_3^-\right)\right], \tag{6.50}$$

$$\mathsf{Q}_- = \frac{(EI)}{a}\left[\mathcal{E}^+b^+\sin\theta\left(\alpha^+ g - \alpha^-\cos\theta - \widehat{\mathcal{U}}_2^+\right)+\mathcal{E}^+\Gamma^+\cos\theta\left(\alpha^-\sin\theta+\widehat{\mathcal{U}}_3^+\right)\right]. \tag{6.51}$$

These unloaded configuration is obtained by substituting these relationships in the condition (6.40,6.41) to obtain a set of four equations for $\alpha^\pm$, θ and $\mathcal{U}$. In particular, the condition $\mathsf{P}^\pm = 0$ becomes

$$\frac{a^2}{(EI)}\mathsf{n}_3^+ + \alpha^+ g\left(b^+\mathcal{E}^+ + b^-\mathcal{E}^-\cos^2\theta+\Gamma^-\mathcal{E}^-\sin^2\theta\right)-\alpha^-\cos\theta(b^+\mathcal{E}^+ + b^-\mathcal{E}^-) \tag{6.52}$$
$$= b^+\mathcal{E}^+\widehat{\mathcal{U}}_2^+ - b^-\mathcal{E}^-\widehat{\mathcal{U}}_2^-\cos\theta-\Gamma^-\mathcal{E}^-\widehat{\mathcal{U}}_3^-\sin\theta,$$

$$\frac{a^2}{(EI)}\mathsf{n}_3^- + \alpha^-\left(b^-\mathcal{E}^- + b^+\mathcal{E}^+\cos^2\theta+\mathcal{E}^+\Gamma^+\sin^2\theta\right)-\alpha^+ g\cos\theta(\mathcal{E}^+b^+ + \mathcal{E}^-b^-) \tag{6.53}$$
$$= b^-\mathcal{E}^-\widehat{\mathcal{U}}_2^- - b^+\mathcal{E}^+\widehat{\mathcal{U}}_2^+\cos\theta-\Gamma^+\mathcal{E}^+\widehat{\mathcal{U}}_3^+\sin\theta,$$

while the condition $\mathsf{P}^1 = 0$ reads

$$\mathcal{U}-\frac{g^-}{a}\frac{\widehat{\mathcal{U}}_1}{2}+(\mathcal{E}^+-\mathcal{E}^-)\left(\frac{\theta'}{2}-\frac{g^-}{a}\frac{\widehat{\mathcal{U}}_0}{2}\right)=0. \tag{6.54}$$

Finally, substituting (6.49-6.51) in (6.41) and eliminating $\mathcal{U}$ according to (6.54) gives

$$\left[\frac{(EI)}{g^-}\mathcal{E}^+\mathcal{E}^-(\theta'-\widehat{\mathcal{U}}_0)\right]'+\mathsf{l}_1(\theta) \tag{6.55}$$
$$= \frac{g^-}{a^2}(EI)\left[\sin\theta\left(b^+\mathcal{E}^+\alpha^-\left(\alpha^+ g-\alpha^-\cos\theta-\widehat{\mathcal{U}}_2^+\right)+b^-\mathcal{E}^-\alpha^+ g\left(\alpha^- - \alpha^+ g\cos\theta-\widehat{\mathcal{U}}_2^-\right)\right)\right.$$
$$\left.+\cos\theta\left(\alpha^-\mathcal{E}^+\Gamma^+\left(\sin\theta\,\alpha^- + \widehat{\mathcal{U}}_3^+\right)+\alpha^+ g\mathcal{E}^-\Gamma^-\left(\alpha^+ g\sin\theta+\widehat{\mathcal{U}}_3^-\right)\right)\right].$$

Similarly substituting (6.49) and eliminating $\mathcal{U}$ according to (6.54) in the boundary conditions $\mathsf{Q}_1(0) = \mathsf{Q}_1(L) = 0$ (see Sec. 6.4) gives

$$\theta'(0) = \widehat{\mathcal{U}}_0(0) \qquad \text{and} \qquad \theta'(L) = \widehat{\mathcal{U}}_0(L). \tag{6.56}$$

The system of equations (6.52-6.56) is a closed set of equations whose solutions make up the set of possible unloaded configurations of a birod. If the tensions $\mathsf{n}_3^\pm$ have linear constitutive laws, then (6.52,6.53) form a linear system for $\alpha^\pm$. The two streches can be substituted accordingly in (6.55) (6.55) and the problem of finding the reference state of linear birods is thus expressed as one second order differential equation with the boundary condition (6.56). Note that under our assumptions of $b^\pm = 1$ or $\varphi^\pm = k\pi$, $\mathcal{U}$ decouples from the other variables as it only appears in the linear equation (6.54).

The problem (6.52-6.56) describes many different situations of interest and different particular cases may easily be studied. From instance, in the case of a completely rigid attachment, we prescribe the function $\theta(S)$ as a constraint, then Eq. (6.55) provides an expression for the moment l_1. The unloaded states then simply obey the algebraic system of equations (6.52,6.54). Note that if either sub-rod is inextensible the corresponding stretch is fixed and the equation (6.52) or (6.53) involving the corresponding tension disappears from the problem. Finally, another particularly interesting class of structures arise when all parameters are chosen constant along the length of the structure. We will now study this case in details.

7 Homogeneous birods

7.1 A mechanical analogy

A birod is homogeneous when its sub-rods are homogeneous (the constitutive laws are independent of $S^{\pm}$), g and the $\widehat{\mathcal{U}}$s are all independent of R and l_1 does not explicitly depend on R. It is straightforward to show that in this case, (EI) is also independent of R. After solving (6.52,6.53) for α^- and $(\alpha^+ g)$, Eq. (6.55) reduces to a second-oder equation that can be written formally as a one-degree of freedom Hamiltonian system with a potential V such that

$$\theta'' = -\frac{1}{\mathcal{E}^+\mathcal{E}^-}\frac{\partial V}{\partial \theta} \qquad \text{with BC:} \quad \theta'(0,L) = \widehat{\mathcal{U}}_0, \tag{7.1}$$

where we used the boundary conditions (6.56). The function $V(\theta)$, defined up to an additive constant, together with $\widehat{\mathcal{U}}_0$ contain all the information on the possible solutions of the system. A judicious choice for the parameterisation of the birod and for the erst of this Section consists in taking $g^- = a$ which implies that $R = S^-/a$

The problem (7.1) is mathematically analogous to that of finding the trajectory of a ball sliding on a potential and such that the ball starts and ends at 'time' L with a 'velocity' $\widehat{\mathcal{U}}_0$. In particular, the quantity $\frac{\theta'^2}{2} + \frac{V}{\mathcal{E}^+\mathcal{E}^-}$, the total energy of the ball in the analogy, is a first integral along the length of the birod

$$\left(\frac{\theta'^2}{2} + \frac{V}{\mathcal{E}^+\mathcal{E}^-}\right)' = 0, \tag{7.2}$$

As a consequence, the local extrema of $V(\theta)$ lead to solutions with constant θ. Since θ is the angle between the tangents of the sub-rods, those solutions correspond to birods wrapping around helices. Also, whenever $\widehat{\mathcal{U}}_0 \neq 0$, there are no solutions with strictly constant θ.

Furthermore, the analogy with the sliding ball implies that whenever Vhas a local minimum, the problem (7.1) admits a set of discrete sets of oscillating solutions provided that the depth of the well is larger than $\mathcal{E}^+\mathcal{E}^-(\widehat{\mathcal{U}}_0)^2/2$. Similarly, if the potential V has a maximum whose height is greater than $\mathcal{E}^+\mathcal{E}^-(\widehat{\mathcal{U}}_0)^2/2$, and $\widehat{\mathcal{U}}_0 > 0$ (resp. $\widehat{\mathcal{U}}_0 < 0$), the problem (7.1) admits a solution that starts on the left (resp. right) of the maximum, goes over the local maximum and ends exactly at the same height on the other side of the maximum. We now examine these solutions further in the case of inextensible sub-rods.

7.2 Inextensible sub-rods

When the sub-rods are inextensible $\alpha^{\pm} = 1$ and from (6.52-6.56) tension $\mathsf{n}_3^{\pm}$ in each sub-rod is known. Then, Eqs. (6.55,6.56) reduce to (7.1) with

$$V = -\frac{A}{4}\cos 2\theta + B\ \cos\theta\,[g\ - \widehat{\mathcal{U}}_2] - C\ \sin\theta\,\widehat{\mathcal{U}}_3 - \psi(\theta), \tag{7.3}$$

where $\frac{\mathrm{d}\psi}{\mathrm{d}\theta} = a\mathsf{l}_1$ and

$$\widehat{\mathcal{U}}_2 = \frac{b^+\mathcal{E}^+\widehat{\mathcal{U}}_2^+ + b^-\mathcal{E}^- g\,\widehat{\mathcal{U}}_2^-}{b^+\mathcal{E}^+ + b^-\mathcal{E}^- g}, \qquad \widehat{\mathcal{U}}_3 = \Gamma^+\mathcal{E}^+\widehat{\mathcal{U}}_3^+ + g\,\Gamma^-\mathcal{E}^-\widehat{\mathcal{U}}_3^-, \tag{7.4}$$

$$A = (b^+ - \Gamma^+)\mathcal{E}^+ + g^2\,(b^- - \Gamma^-)\mathcal{E}^-, \qquad B = b^-\mathcal{E}^- + b^+\mathcal{E}^+. \tag{7.5}$$

The parameter $\widehat{\mathcal{U}}_2$ is a measure ofthe reference curvatures of the sub-rods about the respective axes along $\mathbf{d}_1 \times \mathbf{d}_3^{\pm}$. Similarly $\widehat{\mathcal{U}}_3$ is related to both the reference twist and pre-gluing twist of the sub-rods. Parameters A and B give the relative stiffnesses of the sub-rods. Note that although it is

mathematically convenient to study the system (7.1,7.3) in function of the independent parameters g, A, B, $\widehat{\mathcal{U}}_2$ an $\widehat{\mathcal{U}}_3$, when constructing a birod, the control parameters are the reference curvature of the sub-rods, their principal stiffnesses and g and all 5 parameters mentioned above actually depend on g.

7.3 Identical sub-rods with free glue

In order to show the great wealth of possible solutions for growing birods we conclude this paper by studying a simple cases of two homogeneous inextensible and identical sub-rods apart from having possibly different intrinsic curvatures. We let one of the rods grow homogeneously and we assemble the two rods as explained in Section 3.1.1. The question is then to compute possible unloaded equilibrium states. The stability of such solutions will be studied elsewhere.

In the particular case of constitutively identical sub-rods with isotropic cross-sections: $(EI)^+ = (EI)^-$, $b^+ = b^- = 1$, $\Gamma^+ = \Gamma^- = \Gamma$ (taken to be $2/3$ in all figures), the expression of the material parameters become considerably simpler: $A = (1-\Gamma)(1-g+g^2)$ and $B = 1$. If furthermore, the glue is assumed to oppose no resistance to the relative rotation of the sub-rods about $\mathbf{d}_1$, we have $\psi = 0$ for all θ. Under these hypotheses, V defined in (7.3) further simplifies to

$$V = (g - \widehat{\mathcal{U}}_2)\cos\theta - \frac{1-\Gamma}{4}(1-g+g^2)\cos 2\theta - \widehat{\mathcal{U}}_3 \sin\theta, \tag{7.6}$$

$$= \frac{g-\widehat{\mathcal{U}}_2}{\cos\phi}\cos(\theta+\phi) - \frac{1-\Gamma}{4}(1-g+g^2)\cos(2\theta), \tag{7.7}$$

where $\phi = \arctan\left(\frac{\widehat{\mathcal{U}}_3}{g-\widehat{\mathcal{U}}_2}\right)$.

We remark that $\phi = 0$ whenever $\widehat{\mathcal{U}}_3 = 0$. This phase shift encodes the effect of reference twist in the system (be it reference twist of the sub-rods $\hat{\mathfrak{u}}_3^{\pm}$ or the changes of $\varphi^{\pm}$ along the length of the structure).

The function $V(\theta)$ in Eq. (7.6) is shown in Fig. 12 for different values of the parameters. As can be seen from Fig. 12a and Fig. 12b there are two qualitatively different cases: either $V(\theta)$ is concave with one local extremum θ_m on the domain $-\frac{\pi}{2} \le \theta \le \frac{\pi}{2}$ (hill shaped) or it presents three extrema: two maxima and one minimum ('M' shaped).

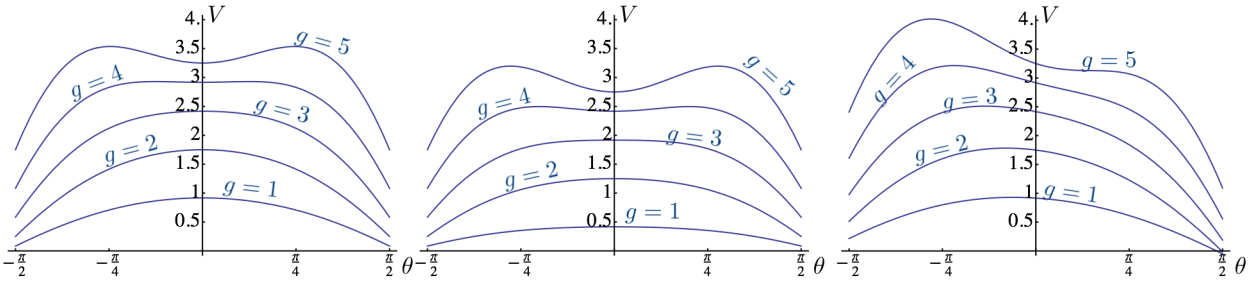

(a) $\widehat{\mathcal{U}}_2 = 0$ & $\phi = 0$ (b) $\widehat{\mathcal{U}}_2 = \frac{1}{2}$ & $\phi = 0$ (c) $\widehat{\mathcal{U}}_2 = 0$ & $\phi = \frac{\pi}{24}$

Figure 12: The function V controlling the equation (7.1) and defined in (7.6). Parameters as specified with $\Gamma = 2/3$.

This is a general feature of the system. The second form (7.7) shows that there is a competition between two terms: a $\cos\theta$ term shifted by the phase ϕ and a $\cos 2\theta$ term. If the former dominates, the potential is 'hill' shaped; if not, the potential is 'M' shaped. This transition can occur under various combination of parameter values. It is characterised by the maximum of the hill shaped

$V(\theta)$ becoming a minimum of the M shaped $V(\theta)$. The bifurcation criterion is therefore

$$\frac{\mathrm{d}^2 V}{\mathrm{d}\theta^2}\Big|_{\theta_m} = 0. \tag{7.8}$$

When $\widehat{\mathcal{U}}_3 = 0$, both the maximum of the bell shaped and the minimum of the 'M' shaped potentials lie at $\theta_m = 0$. In that case, the bifurcation condition (7.8) simplifies to

$$\frac{\mathrm{d}^2 V}{\mathrm{d}\theta^2}\Big|_0 = 0 = \widehat{\mathcal{U}}_2 - g + \big(1 - \Gamma\big)\,(1 - g + g^2). \tag{7.9}$$

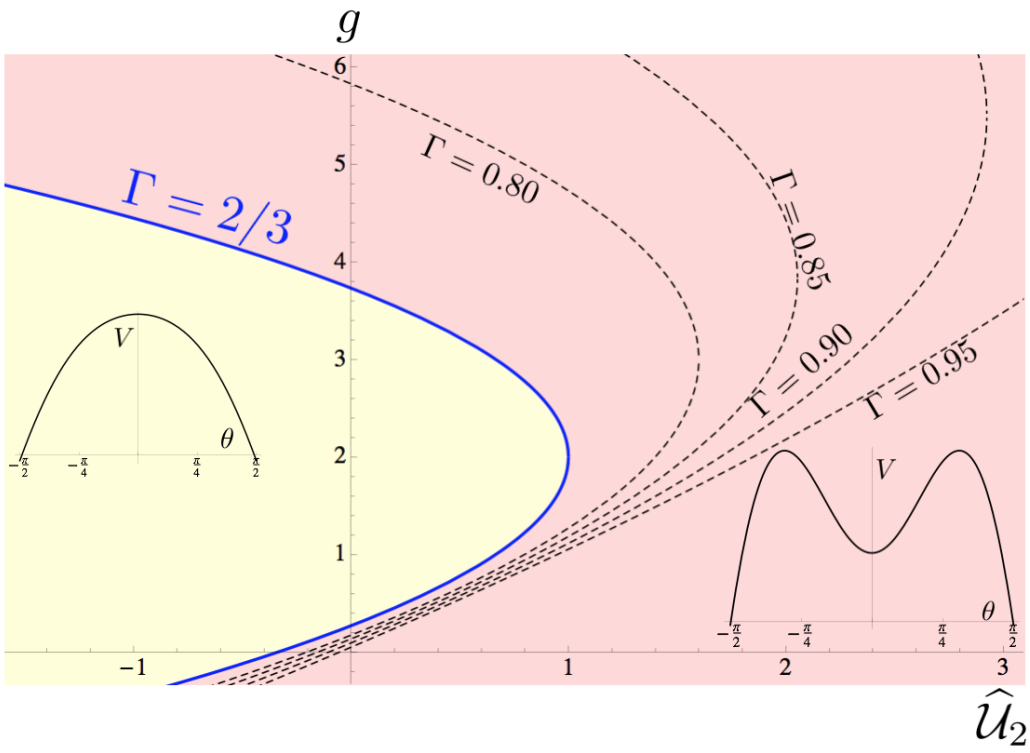

Figure 13: Boundary in parameter space between the two shapes of $V(\theta)$ as defined in (7.6) in the twist less case: $\phi = \widehat{\mathcal{U}}_3 = 0$. The full curve (blue online) shows the boundary for $\Gamma = 2/3$. The to shades of grey (yellow and red online) colour respecting regions split by that boundary. The dashed curves show the shape of the boundary for different values of Γ.

For each value of the parameter Γ, the bifurcation criterion (7.9) defines a parabola which splits the $(\widehat{\mathcal{U}}_2, g)$ plane into two regions: one in which the potential is hill shaped and the other in which it is M shaped (see Fig. 13).

The distinction between the two general shapes of V is important because it leads to qualitatively different solutions. The hill shaped potential present a single maximum and as a result the corresponding birods each have a single unloaded equilibrium. Indeed, the function $V(\theta)$ being concave, the sliding ball analogy shows that the only way to start with a velocity $\widehat{\mathcal{U}}_0$ and end with the same velocity anywhere is to have a symmetric trajectory over the maximum. On the other hand, M shaped potentials lead to a multitude of equilibria: one for each maximum and a discrete set of solutions of (7.1,7.6) oscillating about the minimum and bounded between the two maxima.

Because birods with hill shaped potentials have a single equilibrium unloaded configuration, that configuration must be stable (otherwise, by contradiction, we would have perpetual motion in

the absence of load). We observe that this stable equilibrium corresponds to either staying on the maximum of V if $\widehat{\mathcal{U}}_0 = 0$, or going over the maximum if $\widehat{\mathcal{U}}_0 \neq 0$. Although, studying the stability of the problem is beyond the scope of this paper, this fact leads us to conjecture that solutions close to maxima of V may be good candidates for stable solutions. In that sense we expect that the solutions of the M shaped potentials that are on (if $\widehat{\mathcal{U}}_0 = 0$) or close to (if $\widehat{\mathcal{U}}_0 \neq 0$) the local maxima should be stable.

Note that equilibrium solutions with $\theta = 0$ lead to planar birods (either straight or forming arcs of circle) and that equilibria with $\theta < 0$ (resp. $\theta > 0$) lead to right (resp. left) handed helical solutions. The functions $V(\theta)$ displayed in Fig. 12a and Fig. 12b correspond to $\widehat{\mathcal{U}}_3 = \phi = 0$. In Fig. 12c, we observe that ϕ shifts the maximum hill shaped V to values of θ of the opposite sign; so positive values of ϕ lead to right-handed helical birods and negative ϕ lead to left-handed helical birods.

7.4 Explicit examples

We conclude this section by solving numerically (by using a shooting method) the second order ODE problem (7.1) with Neumann-Neumann boundary conditions for a few particular choice of parameter values. Once the function $\theta(R)$ is known, we find $\mathcal{U}(R)$ using (6.54). Remembering that sub-rods are inextensible, we have $\alpha^{\pm} = 1$. We can then numerically integrate (6.24,6.25) where $\boldsymbol{\mathcal{U}}$ is substituted according to (6.28).

In Fig. 14 we display the result of this process for various parameter values leading to hill shaped potentials. We systematically show the reference shapes of the sub-rods together with the unloaded shape of the birod. Throughout we assume constitutively identical subrods with isotropic cross-sections: $(EI)^+ = (EI)^-$, $b^+ = b^- = 1$, $\Gamma^+ = \Gamma^- = 2/3$.

Next we turn to the case of M shaped potentials. According to Fig. 13, there are essentially two ways to achieve this: with large values of either $\widehat{\mathcal{U}}_2$ or g. Fig. 15 and Fig. 16 show the case of large $\widehat{\mathcal{U}}_2$ while Fig. 17 and Fig. 18 display the case for large g. Notice that both the values of V change and the qualitative behaviour of all solutions. Also, the oscillating solutions in the case $g \gg 1$ systematically involve self penetration of the attaching spokes. Finally, the helical solutions displayed in Fig. 15 and obtained for a large value of $\widehat{\mathcal{U}}_2$ and $g = 1$ qualitatively correspond to the equilibrium of the ladder described in Example 3 of Sec. 3.1.3 and observed in [48].

8 Conclusions

The aim of this paper was to derive a practical framework to study the mechanical equilibrium of structures composed of two morphoelastic rods. In particular, we wanted to obtain a set of equations describing the structure as a single macroscopic object. The constitutive properties of the two (microscopic) strands together with their growth law were to be translated into effective constitutive laws for the structure. Furthermore, we wanted to obtain equations expressing the balance of external and internal forces and moments so that the behaviour of the structure under general loads can be studied.

When the structure is constrained on a straight line or when it is planar, it is possible to describe it as a single Kirchhoff rod. A centreline is defined together with a local material frame of directors. Global forces and moments of forces applied at every point of the centreline of the macro-structure can also be defined. Expressing the equilibrium of these moments lead to the well known Kirchhoff equations. We then devised a three steps method allowing to compute the constitutive laws of the macro-structure for general growth, remodelling and constitutive laws of the (micro) sub-rods.

This method was then applied on a few examples both academic and practical. Interestingly, differential growth between the two strands may drive them to their non-linear regimes. As a result,

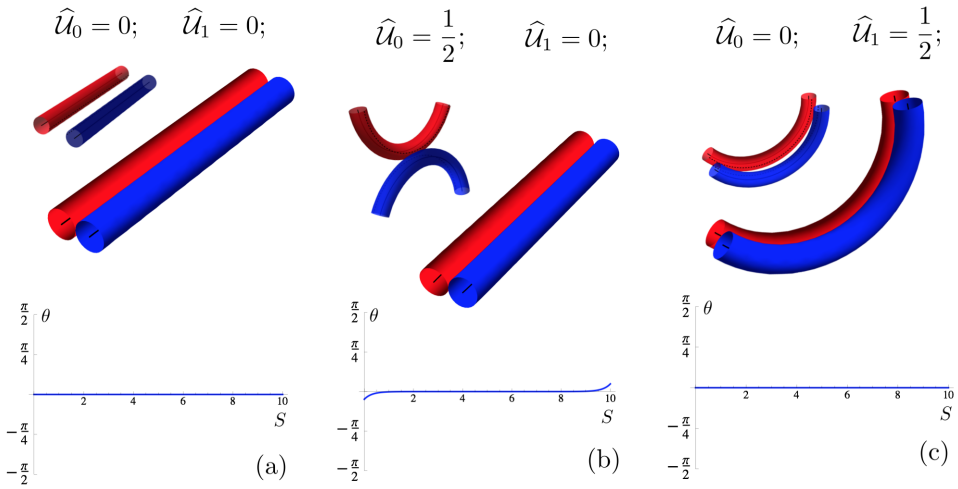

(a) Example 1: $g = 1;$ $\widehat{\mathcal{U}}_2 = 0;$ $\widehat{\mathcal{U}}_3 = 0;$ $\Gamma = 2/3.$

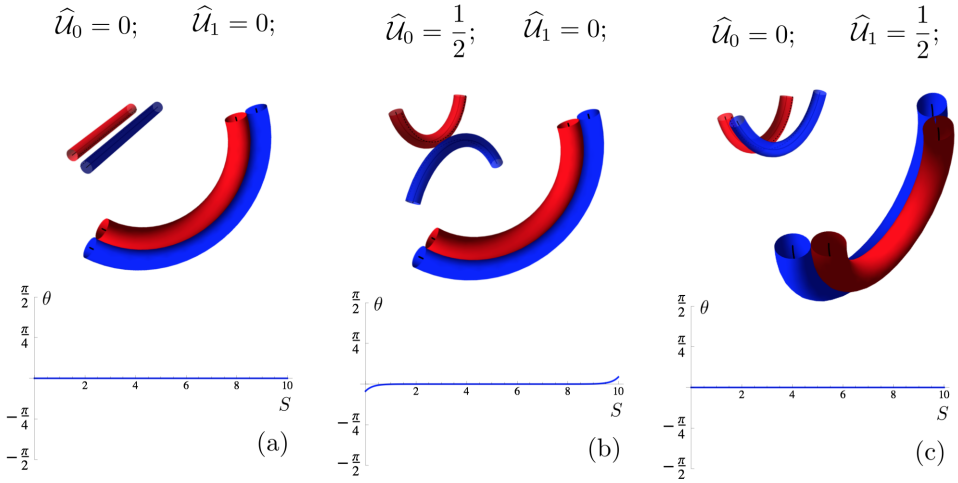

(b) Example 2: $g = 5/4;$ $\widehat{\mathcal{U}}_2 = 0;$ $\widehat{\mathcal{U}}_3 = 0;$ $\Gamma = 2/3.$

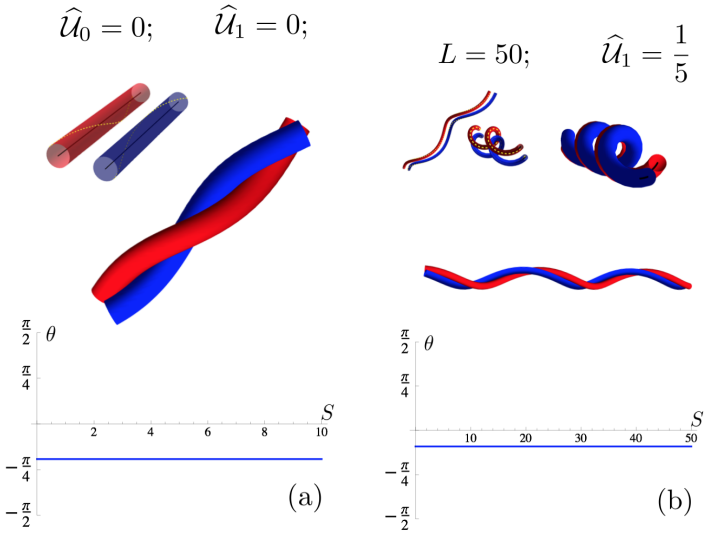

(c) Example 3: $g = 1;$ $\widehat{\mathcal{U}}_2 = 0;$ $\widehat{\mathcal{U}}_3 = \frac{1}{5};$ $\Gamma = 2/3.$

Figure 14: A few particular examples of unloaded birods with hill shaped $V(\theta)$.

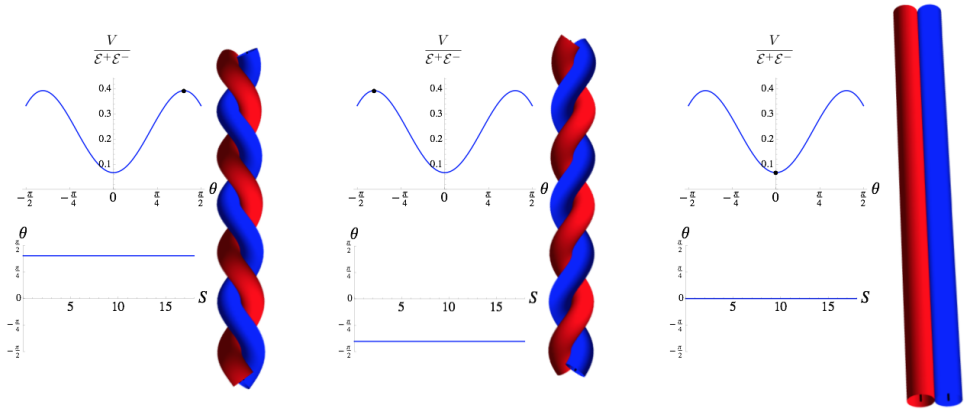

Figure 15: Equilibria with constant $\theta(S)$ of homogeneous birods with inextensible sub-rods and parameters $L^+ = L^- = 18$, $\widehat{\mathcal{U}}_0 = \widehat{\mathcal{U}}_1 = \widehat{\mathcal{U}}_3 = 0$, $g = 1$ and $\widehat{\mathcal{U}}_2 = \frac{9}{10}$. Top: the right handed helical solution. Mid: the left handed helical solution. Bottom: the neutral (probably unstable) planar solution. In each case, the function $V(\theta)$ is shown in the upper left corner together with the position at which the system stays (black dot); the function $\theta(S)$ is shown in the bottom right corner; and the shape of the resulting birod is displayed on the right.

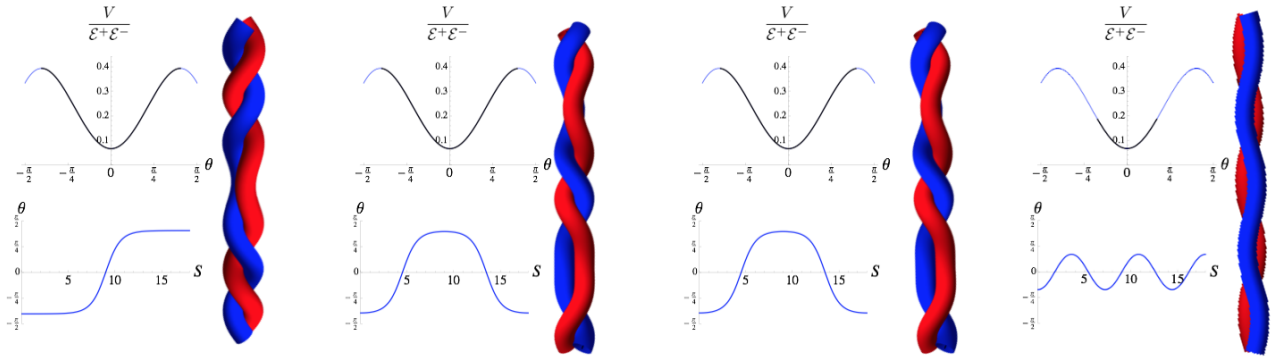

Figure 16: Equilibria with $\theta(S)$ oscillating k times about $\theta = 0$ with from left to right: $k = 1$, $k = 2$, $k = 3$ and $k = 5$; same parameters as Fig. 15. In the top left panels, the thin line (blue online) indicates the shape of the function $V(\theta)/(\mathcal{E}^+\mathcal{E}^-)$, while the thick (black online) curve shows the (k times covered) trajectory in the $(\theta, V/(\mathcal{E}^+\mathcal{E}^-))$ plane. The shapes of the resulting structures are displayed (+ rod red online and − rod blue online).

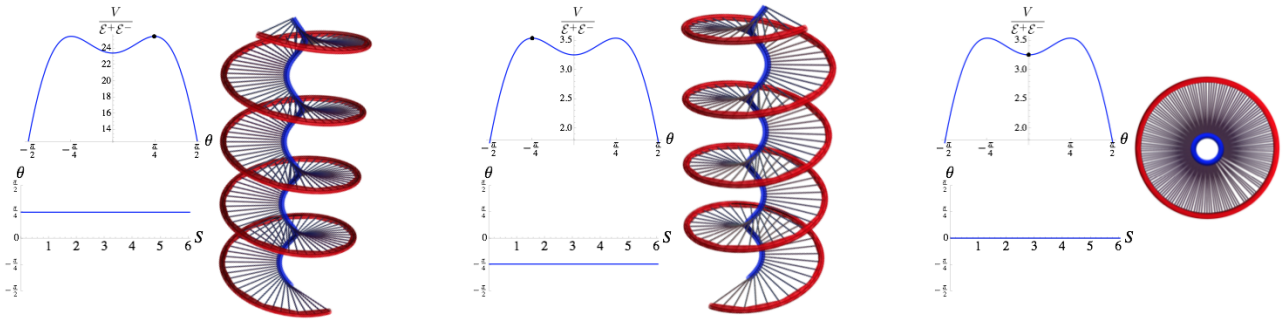

Figure 17: Equilibria with constant $\theta(S)$ of homogeneous birods with inextensible sub-rods and parameters $L^- = 6.08$, $\widehat{\mathcal{U}}_0 = \widehat{\mathcal{U}}_1 = \widehat{\mathcal{U}}_2 = \widehat{\mathcal{U}}_3 = 0$ and $g = 5$. From left to right: the left handed helical solution with $\theta > 0$, the right handed helical solution with $\theta < 0$ and the neutral (probably unstable) planar solution (multiply covered). In each case, the function $V(\theta)/(\mathcal{E}^+\mathcal{E}^-)$ is shown (blue online) in the upper left corner where the (black online) dot displays the position at which the system stays (dot); the function $\theta(S)$ is shown in the bottom left corner; and the shape of the resulting birod is displayed on the right. The shapes of the resulting structures are displayed assuming that the thin spokes (black online) are rigid (similarly to the ladder of Example 3 in Sec. 3.1.3), the + rod is the longest tube (red online) and the − rod is the shorter inner one (blue online).

the macro-structure may be considerably stiffer (or softer depending on the non-linearity of the microscopic constitutive laws) than its part, like for instance in the case of the rhubarb stalk. This is a well known phenomenon which is easily captured by our framework.

In the general three dimensional case, we showed that the structure is no longer equivalent to a Kirchhoff rod. Accordingly, we proposed a new geometric description of the macro-structure and showed why it is better suited to this structure than the traditional 'centreline equipped with a local material frame' description. We then proposed a new set of generalised moments for which we established both the relevant constitutive laws and equilibrium equations. Even computing the unloaded equilibria of these structures is a non-trivial task. We highlighted the method allowing to perform the computation for arbitrary growth, remodelling and constitutive laws of the sub-rods.

Finally, we applied this method to the particular case of an homogeneous structure composed of inextensible sub-rods with linear moments. The problem was reduced to finding the solutions of a single second-order differential equation with Neumann-Neumann boundary condition. We showed that the complete set of solutions can be computed although it may be countably infinite. The shape of some of these equilibria was then (numerically) computed and displayed.

The stability of these equilibrium solutions is another matter entirely. Indeed, we obtained a differential equation in space and it does not contain in itself sufficient information to assess the stability of the solution which is concerned with changes in function of time. The question of the stability of the unloaded solutions is outside the scope of this paper and will be studied in a sequel.

Acknowledgments: AG is a Wolfson/Royal Society Merit Award Holder and both AG and TL acknowledge support from EC Framework VII through a Reintegration Grant under and a Marie Curie Fellow.

References

[1] C. J. Benham. An elastic model of the large structure of duplex DNA. *Bioploymers*, 18:609–623, 1979.

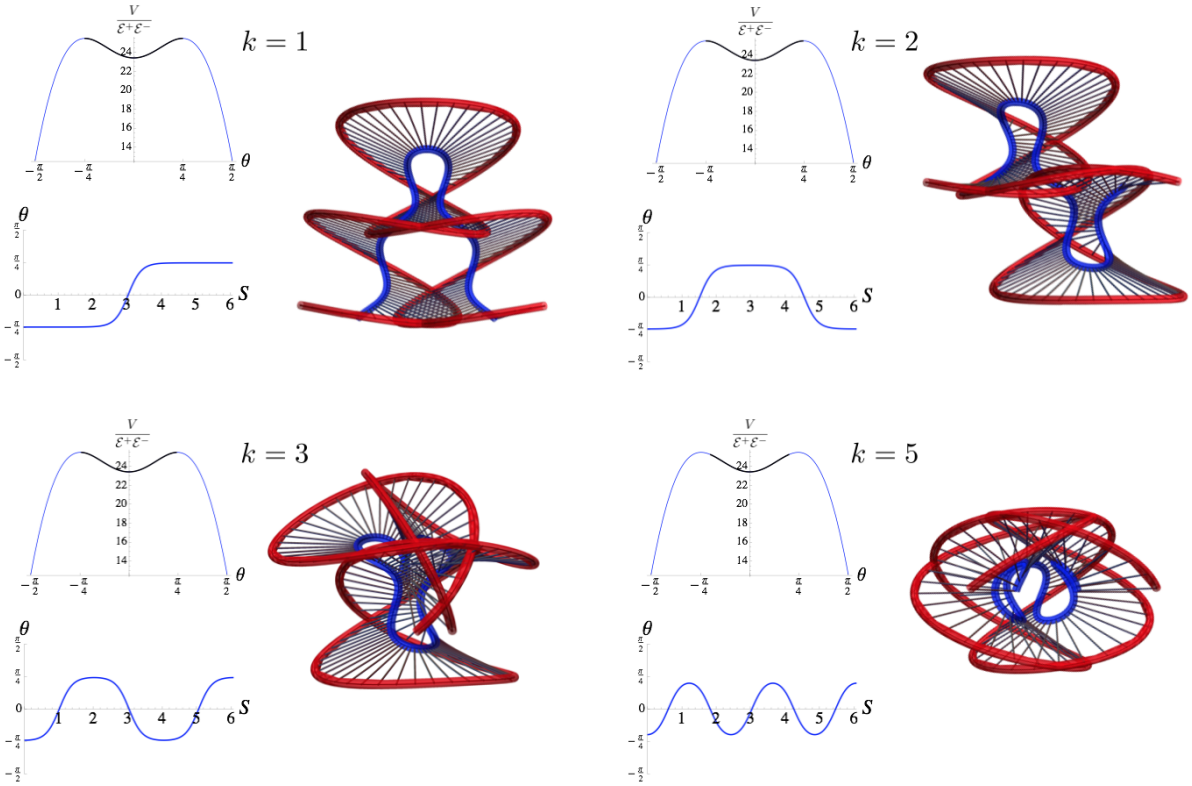

Figure 18: Equilibria with $\theta(S)$ oscillating k times about $\theta = 0$ with $k = 1$ (top left), $k = 2$ (top right), $k = 3$ (bottom left) and $k = 5$ (bottom right); same parameters as Fig. 17. In the top left panels, the thin line (blue online) indicates the shape of the function $V(\theta)$, while the thick (black online) curve shows the (k times covered) trajectory in the $V(\theta)/(\mathcal{E}^+\mathcal{E}^-)$ plane. The shapes of the resulting structures are displayed assuming that the thin spokes (black online) are rigid (similarly to the ladder of Example 3 in Sec. 3.1.3), the + rod is the longest tube (red online) and the − rod is the shorter inner one (blue online).

[2] C. J. Benham. Theoretical analysis of conformational equilibria in superhelical DNA. *Ann. Rev. Biophys. Chem.*, 14:23–45, 1985.

[3] B.D. Coleman and D. Swigon. Theory of self-contact in dna molecules modeled as elastic rods. *Atti Convegni Lincei.*, 177:281–296, 2001.

[4] K. A. Hoffman, R. S. Manning, and J. H. Maddocks. Link, twist, energy, and the stability of DNA minicircles. *Biopolymers*, 70:145–157, 2003.

[5] R. S. Manning, J. H. Maddocks, and J. D. Kahn. A continuum rod model of sequence-dependent DNA structure. *J. Chem. Phys.*, 105:5626–5646, 1996.

[6] S. Neukirch. Extracting dna twist rigidity from experimental supercoiling data. *Phys. Rev. Lett.*, 93(19):198107, 2004.

[7] S. Neukirch, A. Goriely, and A. C. Hausrath. Chirality of coiled coils: Elasticity matters. *Phys. Rev. Lett.*, 100(3):038105, 2008.

[8] S. Neukirch, A. Goriely, and A. C. Hausrath. Elastic coiled-coils act as energy buffers in the ATP synthase. *Int. J. Nonlinear Mech.*, 2008.

[9] R. E. Goldstein and A. Goriely. Dynamic buckling of morphoelastic filaments. *Phys. Rev. E*, 74:010901, 2006.

[10] A. Goriely and M. Tabor. Spontaneous helix-hand reversal and tendril perversion in climbing plants. *Phys. Rev. Lett.*, 80:1564–1567, 1998.

[11] A. Goriely and S. Neukirch. Mechanics of climbing and attachment in twining plants. *Phys. Rev. Lett.*, 97(18):184302, 2006.

[12] T. Alméras, J. Gril, and E. Costes. Bending of apricot tree branches under the weight of axillary growth: test of a mechanical model with experimental data. *Trees-Struct. Funct.*, 16(1):5–15, 2002.

[13] Basile Audoly and Yves Pomeau. *Elasticity and geometry*. Oxford Univ. Press, 2010.

[14] C Gross, J Graham, M Neuwirth, and J Pugh. Scoliosis and growth. an analysis of the literature. *Clinical orthopaedics and related research*, (175):243, 1983.

[15] Yaron Levinson and Reuven Segev. On the kinematics of the octopus's arm. *Journal of Mechanisms and Robotics*, 2(1):011008, 2010.

[16] D. Ambrosi, GA Ateshian, EM Arruda, SC Cowin, J. Dumais, A. Goriely, GA Holzapfel, JD Humphrey, R. Kemkemer, E. Kuhl, et al. Perspectives on biological growth and remodeling. *J. Mech. Phys. Solids*, 2010.

[17] A. Goriely and D. Moulton. Morphoelasticity - a theory of elastic growth. In Oxford University Press, editor, *New Trends in the Physics and Mechanics of Biological Systems*, 2010.

[18] D E Moulton, T Lessinnes, and A Goriely. Journal of the Mechanics and Physics of Solids. *Journal of the Mechanics and Physics of Solids*, 61(2):398–427, February 2013.

[19] E. K. Rodriguez, A. Hoger, and A. McCulloch. Stress-dependent finite growth in soft elastic tissue. *J. Biomech.*, 27:455–467, 1994.

[20] C. Lloyd and J. Chan. Helical microtubule arrays and spiral growth. *The Plant Cell Online*, 14(10):2319–2324, 2002.

[21] H. Buschmann, M. Hauptmann, D. Niessing, C.W. Lloyd, and A.R. Schäffner. Helical growth of the Arabidopsis mutant tortifolia2 does not depend on cell division patterns but involves handed twisting of isolated cells. *Plant Cell*, 21(7):2090, 2009.

[22] I. Furutani, Y. Watanabe, R. Prieto, M. Masukawa, K. Suzuki, K. Naoi, S. Thitamadee, T. Shikanai, and T. Hashimoto. The spiral genes are required for directional control of cell elongation in aarabidopsis thaliana. *Development*, 127(20):4443–4453, 2000.

[23] *Construction of bacterial flagellar filaments, and aspects of their conversion to different helical forms*, volume Procaryotic and eucaryotic flagella. Symp. Soc. Exp. Biol. XXXV. Cambridge Univ. Press, Cambridge, 1982.

[24] R. Kamiya, S. Asakura, K. Wakabayashi, and K. Namba. Transition of bacterial flagella from helical to straight forms with different subunits arrangements. *J. Mol. Biol.*, 131, 1979.

[25] S.V. Srigiriraju and T.R. Powers. Continuum model for polymorphism of bacterial flagella. *Phys. Rev. Lett.*, 94(24):248101, 2005.

[26] Hermes Gadêlha, Eamonn A Gaffney, and Alain Goriely. The counterbend phenomenon in flagellar axonemes and cross-linked filament bundles. *Proceedings of the National Academy of Sciences*, 110(30):12180–12185, 2013.

[27] Mohammad R K Mofrad Stephen J Peter. Computational Modeling of Axonal Microtubule Bundles under Tension. *Biophysical Journal*, 102(4):749, February 2012.

[28] R. V. Lacro, K. L. Jones, and K. Benirschke. The umbilical cord twsit: origin, direction, and relevance. *Am. J. Obstet. Gynecol.*, 157, 1987.

[29] A. Goriely. Knotted umbilical cords. In J. A. Calvo, A. Stasiak, and E. Rawdon, editors, *Physical and Numerical Models in Knot Theory Including Their Application to the Life Sciences*, pages 109–126. World Scientific, Singapore, 2004.

[30] A. Goriely and R. Vandiver. On the mechanical stability of growing arteries. *IMA journal of applied mathematics*, 75(4):549–570, 2010.

[31] G.A. Holzapfel and R.W. Ogden. Modelling the layer-specific three-dimensional residual stresses in arteries, with an application to the human aorta. *J. R. Soc. Interface*, 7(787-799), 2010.

[32] Yaron Levinson and Reuven Segev. On the Kinematics of the Octopus's Arm. *Journal of Mechanisms and Robotics*, 2(1):011008, 2010.

[33] W.M. Kier and K.K. Smith. Tongues, tentacles and trunks: the biomechanics of movement in muscular-hydrostats. *Zool. J. Linn. Soc.*, 83(4):307–324, 1985.

[34] Maher Moakher and John H Maddocks. A Double-Strand Elastic Rod Theory. *Archive for Rational Mechanics and Analysis*, 177(1):53–91, July 2005.

[35] J M T Thompson, G H M van der Heijden, and S Neukirch. Supercoiling of DNA plasmids: mechanics of the generalized ply. *Proceedings of the Royal Society A: Mathematical, Physical and Engineering Sciences*, 458(2020):959–985, April 2002.

[36] E L Starostin and G H M van der Heijden. Theory of equilibria of elastic 2-braids with interstrand interaction. *Journal of the Mechanics and Physics of Solids*, 64:83–132, March 2014.

[37] S Neukirch and G H M van der Heijden. Geometry and Mechanics of Uniform n-Plies: from Engineering Ropes to Biological Filaments . *Journal of Elasticity*, 69(1/3):41–72, 2002.

[38] EL Starostin and GHM van der Heijden. Theory of equilibria of elastic 2-braids with interstrand interaction. *Journal of the Mechanics and Physics of Solids*, 2013.

[39] Mourad Chamekh, Saloua Mani-Aouadi, and Maher Moakher. Modeling and numerical treatment of elastic rods with frictionless self-contact. *Computer Methods in Applied Mechanics and Engineering*, 198(47):3751–3764, 2009.

[40] Kasper Olsen and Jakob Bohr. Geometry of the toroidal n-helix: optimal-packing and zero-twist. *New Journal of Physics*, 14(2):023063, 2012.

[41] Christopher Prior. Helical Birods: An Elastic Model of Helically Wound Double-Stranded Rods. *Journal of elasticity*, March 2014.

[42] S Timoshenko. ANALYSIS OF BI-METAL THERMOSTATS. *JOSA*, 11(3):233–255, September 1925.

[43] R. L. Bishop. There is more than one way to frame a curve. *Amer. Math. Month.*, 82, 1975.

[44] Antman S S. *Nonlinear Problems of Elasticity*, volume 107 of *Applied Mathematical Sciences*. Springer New York, 2005.

[45] A. Goriely, M. Nizette, and M. Tabor. On the dynamics of elastic strips. *J. Nonlinear Sci.*, 11:3–45, 2001.

[46] M. Nizette and A. Goriely. Towards a classification of Euler-Kirchhoff filaments. *J. Math. Phys.*, 40:2830–2866, 1999.

[47] A. Goriely and M. Tabor. The nonlinear dynamics of filaments. *Nonlinear Dynam.*, 21(1):101–133, 2000.

[48] X Lachenal, PM Weaver, and S Daynes. Multi-stable composite twisting structure for morphing applications. *Proceedings of the Royal Society A: Mathematical, Physical and Engineering Science*, 468(2141):1230–1251, 2012.

[49] Rebecca Vandiver and Alain Goriely. Differential growth and residual stress in cylindrical elastic structures. *Philosophical Transactions of the Royal Society A: Mathematical, Physical and Engineering Sciences*, 367(1902):3607–3630, 2009.

[50] R. Vandiver and A. Goriely. Tissue tension and axial growth of cylindrical structures in plants and elastic tissues. *Europhys. Lett.*, 84(58004), 2008.

[51] M. A. Holland, T. Kosmata, A. Goriely, and E. Kuhl. On the mechanics of thin films and growing surfaces. *Mathematics and Mechanics of Solids*, 2013.

[52] A Goriely, M Destrade, and M Ben Amar. Instabilities in elastomers and in soft tissues. *The Quarterly Journal of Mechanics and Applied Mathematics*, 59(4):615–630, October 2006.

[53] YC Fung. What are the residual stresses doing in our blood vessels? *Ann. Biomed. Eng.*, 19(3):237–249, 1991.

[54] J H Waite. Quinone-tanned scleroproteins. In A S M Saleuddin and K M Wilbur, editors, *The Mollusca, Physiology*, pages 467–504. Academic Press, New York, February 1983.

A Normal frames and frame of directors

The motivation for using normal frames compared to, say, the Frenet frame, is three fold. First, it is somewhat easier to infer geometric information about the 3D curve $\mathbf{r}$ from its normal development than from a Frenet development, see Tab. 1. Second, the normal development only requires the curve $\mathbf{r}$ to be C^2 while a Frenet frame needs both C^3 and non-vanishing $\frac{\partial^2 \mathbf{r}}{\partial R^2}$. Third, it plays a particularly illuminating role in the geometric description of elastic rods (cf. below).

Shape of $\mathbf{r}$	Frenet (κ, τ)	Normal development $(\mathsf{p}_1, \mathsf{p}_2)$
Straight line	$\kappa = \tau = 0$	$\mathsf{p}_1 = \mathsf{p}_2 = 0$
Circle	κ constant, $\tau = 0$	p_1 & p_2 constant
Planar curve	$\tau = 0$	within a straight line through the origin
Curve on a sphere of radius ρ	?	within a straight line at distance $1/\rho$ from the origin

Table 1: Description of special curves by curvature and torsion vs normal development. Note that the relation between shape and normal development are bijective while the shapes only imply the Frenet development (e.g. uniformly vanishing torsion does not insure planarity). The second column contains trivial results. Proofs regarding the third column can be found in [43].

While a normal frame is a property of the centreline of the rod, the frame of directors contain also information about the orientation of cross sections. Because we focus on unshearable rods, both $\mathbf{c}_3$ and $\mathbf{d}_3$ are aligned with the tangent vector to $\mathbf{r}$. Therefore, there exists a function φ such that

$$\mathbf{d}_j = \mathbf{c}_i \, (R_{3,\varphi})_{ij} \quad \text{with} \quad R_{3,\varphi} = \begin{pmatrix} \cos\varphi & -\sin\varphi & 0 \\ \sin\varphi & \cos\varphi & 0 \\ 0 & 0 & 1 \end{pmatrix}, \tag{A.1}$$

and

$$\begin{aligned} \frac{\partial \mathbf{d}_j}{\partial R} &= \left(\frac{\partial \mathbf{c}_i}{\partial s}(R_{3,\varphi})_{ij} + \mathbf{c}_i \frac{\partial (R_{3,\varphi})_{ij}}{\partial s} \right) \frac{\partial s}{\partial R} && \text{(A.2)} \\ &= v \left(\mathbf{p} \times \mathbf{c}_i (R_{3,\varphi})_{ij} + \mathbf{c}_i (\mathbf{d}_3 \times (R_{3,\varphi})_{ij}) \frac{\partial \varphi}{\partial s} \right) && \text{(A.3)} \\ &= \left(v\mathbf{p} + \frac{\partial \varphi}{\partial R} \mathbf{d}_3 \right) \times \mathbf{d}_j && \text{(A.4)} \end{aligned}$$

Eqs. (A.4) together with Eq. (2.9) lead to the relation

$$\mathbf{u} = v\,\mathbf{p} + \frac{\partial \varphi}{\partial R} \mathbf{d}_3. \tag{A.5}$$

Because $\mathbf{p}$ is orthogonal to $\mathbf{c}_3$ and therefore to $\mathbf{d}_3$, this last relation shows that

$$\mathsf{u}_3 = \frac{\partial \varphi}{\partial R} \tag{A.6}$$

describes the twist of the rod about the centreline which corresponds to the change of angle φ between a normal frame and the frame of directors. Furthermore (A.5) implies

$$\mathsf{u}_1 \mathbf{d}_1 + \mathsf{u}_2 \mathbf{d}_2 = v(p_1 \mathbf{c}_1 + p_2 \mathbf{c}_2) \tag{A.7}$$

$$\text{so that} \quad \begin{pmatrix} \cos\varphi & -\sin\varphi \\ \sin\varphi & \cos\varphi \end{pmatrix} \begin{pmatrix} \mathsf{u}_1 \\ \mathsf{u}_2 \end{pmatrix} = v \begin{pmatrix} p_1 \\ p_2 \end{pmatrix}. \tag{A.8}$$

Eqs. (2.6,2.8,A.6,A.8) lead to

$$\kappa = \frac{1}{v}\sqrt{\mathsf{u}_1^2 + \mathsf{u}_2^2} \quad \text{and} \quad \tau = \frac{1}{v}\left(\mathsf{u}_3 + \frac{\mathsf{u}_1\partial_R\mathsf{u}_2 - \mathsf{u}_2\partial_R\mathsf{u}_1}{\mathsf{u}_1^2 + \mathsf{u}_2^2}\right). \tag{A.9}$$

These relations (A.9) compared with Eqs. (20,21) of part I [18] prove that the curvature and torsion defined in the context of the normal development in Eqs. (2.6,2.8) are indeed the same quantities as those defined in the usual Frenet Frame. Furthermore, because p_1 and p_2 describe the bending of the centreline about $\mathbf{c}_1$ and $\mathbf{c}_2$, Eq. (A.8) shows that u_1 and u_2 respectively describe the bending of the rod about $\mathbf{d}_1$ and $\mathbf{d}_2$.

B Geometry of the 3D birod as slender structure themselves

The objective of this appendix is to show how the shape of the sub-rods can be recovered from the centreline of the birod $\mathbf{r}$ and its local frame $\{\mathbf{d}_1, \mathbf{d}_2, \mathbf{d}_3\}$. In other terms we show that under the definitions of Sec. 3.1.2 and after the functions $g^\pm$ have been computed, upon knowing the stretch α and Darboux vectors $\mathbf{u}$ of the birod, we can recover the stretches $\alpha^\pm$ of the sub-rods, the angle θ between their tangents $\mathbf{d}_3^\pm$ and their respective Darboux vectors $\mathbf{u}^\pm$.

We open by recalling the definition and assumptions listed in Sec. 3.1.2, most of which is summarised in Fig. 19a. Then we introduce the angles θ and τ shown in Fig. 19b and consider separately the relations concerning $\alpha^\pm$ and θ (Sec. B.1) and the relations involving $\mathbf{u}^\pm$ (Sec. B.2). The former are concisely gathered in Fig. 20 while the latter lead to (B.45-B.47).

In Sec. 3.1.2, a birod was defined as a composite object made of two sub-rods the centrelines $\mathbf{r}^\pm$, assumed to be at constant distance a from one another, were equipped with the local material frames $\{\mathbf{d}_1, \mathbf{d}_2, \mathbf{d}_3\}$. Their local stretch $\alpha^\pm$ and Darboux vector $\mathbf{u}^\pm$ were defined as

$$\alpha^\pm = \left|\frac{\partial \mathbf{r}^\pm}{\partial S^\pm}\right|, \qquad \frac{\partial \mathbf{d}_i}{\partial S^\pm} = \mathbf{u}^\pm \times \mathbf{d}_i, \tag{B.1}$$

where $S^\pm$ are the reference arc lengthes along $\mathbf{r}^\pm$.

Furthermore, it was assumed that there exists a mapping G pairing points along both centreline. Intuitively, G pairs centre-points belonging to glued cross-sections.

Finally, choosing a point on the centreline χ (with $\chi = +$ or $-$ labelling the sub-rods), the azimuth of the paired point (on $-\chi$) in the local frame of χ is recorded by the material angle φ^χ (cf. Fig. 19a).

The vector field $\mathbf{d}_1$ was defined as the unit vector pointing from the point $\mathbf{r}^-$ to its paired point in the $+$ centreline cf. (3.16) recalled here

$$\mathbf{r}^+ = \mathbf{r}^- + a\mathbf{d}_1. \tag{B.2}$$

Because the centrelines are at constant distance a, each of them lies on a cylinder of radius a centred on the other. It follows that the tangent vectors $\mathbf{d}_3^\pm$ are perpendicular to the radial unit vector $\mathbf{d}_1$.

The centreline of the birod $\mathbf{r}$ was defined by (**??**) which we recall here

$$\mathbf{r} = \mathbf{r}^- + a\beta\mathbf{d}_1. \tag{B.3}$$

The vector field $\mathbf{d}_3$ was defined as unit tangent to $\mathbf{r}$. Furthermore, we defined S as the reference arc length $\mathbf{r}$ and we defined $g^\pm = \frac{\partial S^\pm}{\partial S}$. Taking the derivative of (B.3) by S proves that $\mathbf{d}_3$ is perpendicular to $\mathbf{d}_1$ since $\mathbf{d}_3^- \perp \mathbf{d}_1$ and $\partial_S\mathbf{d}_1 \perp \mathbf{d}_1$ (as $\mathbf{d}_1$ is a unit vector). We also defined

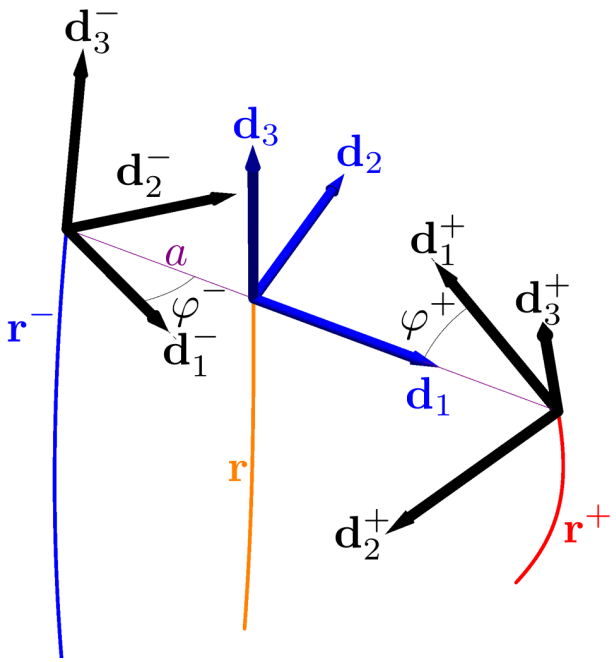

(a) A subfigure

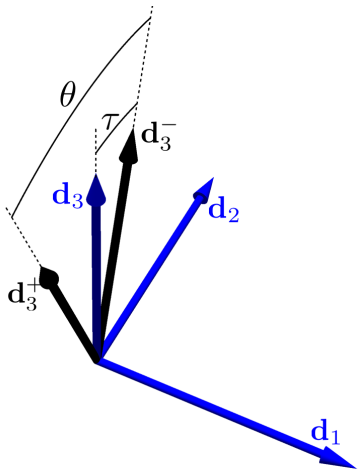

(b) A subfigure

Figure 19: A figure with two subfigures

$\mathbf{d}_2 = \mathbf{d}_3 \times \mathbf{d}_1$ so that $\{\mathbf{d}_1, \mathbf{d}_2, \mathbf{d}_3\}$ forms a right handed orthonormal frame. In any configuration, the stretch α of the birod and its Darboux vector $\mathbf{u}$ were defined as

$$\alpha = \left|\frac{\partial \mathbf{r}}{\partial S}\right|; \qquad \frac{\mathrm{d}\mathbf{d}_i}{\mathrm{d}S} = \mathbf{u} \times \mathbf{d}_i. \tag{B.4}$$

B.1 Stretches $\alpha^\pm$ and angle θ

All four unit vectors $\mathbf{d}_3^\pm$, $\mathbf{d}_3$ and $\mathbf{d}_2$ are coplanar as they are orthogonal to $\mathbf{d}_1$. We therefore define θ the angle from $\mathbf{d}_3^-$ to $\mathbf{d}_3^+$ and τ the angle from $\mathbf{d}_3^-$ to $\mathbf{d}_3$ such that

$$\mathbf{d}_3^- = \cos\tau \quad \mathbf{d}_3 + \sin\tau \quad \mathbf{d}_2, \tag{B.5}$$

$$\mathbf{d}_3^+ = \cos(\tau - \theta)\, \mathbf{d}_3 + \sin(\tau - \theta)\, \mathbf{d}_2. \tag{B.6}$$

It is possible to compute the angles τ and $\tau - \theta$ in function of $\alpha^\pm$ and θ as follows. Eqs. (B.2,B.3) imply

$$\mathbf{r} = (1-\beta)\mathbf{r}^- + \beta\mathbf{r}^+, \tag{B.7}$$

the derivative by S of which leads to

$$\alpha\mathbf{d}_3 = \alpha^- g^- (1-\beta)\mathbf{d}_3^- + \alpha^+ g^+ \beta \mathbf{d}_3^+. \tag{B.8}$$

Substituting $\mathbf{d}_3^\pm$ according to (B.5,B.6) in (B.8) and projecting on $\mathbf{d}_3$ and $\mathbf{d}_2$ leads to the following linear system in $\cos\tau$ and $\sin\tau$

$$\begin{cases} \alpha = \left[\alpha^- g^- (1-\beta) + \alpha^+ g^+ \beta\cos\theta\right] \cos\tau + \left[\alpha^+ g^+ \beta \sin\theta\right] \sin\tau, \\ 0 = -\left[\alpha^+ g^+ \beta \sin\theta\right] \cos\tau + \left[\alpha^- g^- (1-\beta) + \alpha^+ g^+ \beta\cos\theta\right] \sin\tau, \end{cases} \tag{B.9}$$

the inversion of which gives

$$\begin{pmatrix}\cos\tau\\ \sin\tau\end{pmatrix} = \frac{\alpha\begin{pmatrix}\alpha^- g^-(1-\beta)+\alpha^+ g^+\beta\cos\theta\\ \alpha^+ g^+\beta\sin\theta\end{pmatrix}}{(\alpha^- g^-(1-\beta))^2+(\alpha^+ g^+\beta)^2+2\alpha^- g^-\alpha^+ g^+\beta(1-\beta)\cos\theta}. \tag{B.10}$$

Taking the norm of (B.8), we obtain

$$\alpha = \sqrt{(\alpha^- g^-(1-\beta))^2+(\alpha^+ g^+\beta)^2+2\alpha^- g^-\alpha^+ g^+\beta(1-\beta)\cos\theta}, \tag{B.11}$$

and (B.10) simplifies to

$$\begin{pmatrix}\cos\tau\\ \sin\tau\end{pmatrix} = \frac{1}{\alpha}\begin{pmatrix}\alpha^- g^-(1-\beta)+\alpha^+ g^+\beta\cos\theta\\ \alpha^+ g^+\beta\sin\theta\end{pmatrix} = \frac{1}{\alpha}\begin{pmatrix}\alpha^- g^-(1-\beta)\\ 0\end{pmatrix} + \frac{1}{\alpha}R_\theta\begin{pmatrix}\alpha^+ g^+\beta\\ 0\end{pmatrix}, \tag{B.12}$$

where R_χ is the 2D rotation matrix of angle χ. The second formulation in (B.12) is practical as we can directly obtain

$$\begin{pmatrix}\cos(\tau-\theta)\\ \sin(\tau-\theta)\end{pmatrix} = R_{-\theta}\begin{pmatrix}\cos\tau\\ \sin\tau\end{pmatrix} = \frac{1}{\alpha}\begin{pmatrix}\alpha^+ g^+\beta+\alpha^- g^-(1-\beta)\cos\theta\\ -\alpha^- g^-(1-\beta)\sin\theta\end{pmatrix}. \tag{B.13}$$

We are now ready to express the components of $\mathbf{u}$ as function of $\alpha^\pm$ and θ. The derivative of (B.2) by S yields

$$\alpha^+ g^+\mathbf{d}_3^+ = \alpha^- g^-\mathbf{d}_3^- + a(\mathsf{u}_3\mathbf{d}_2 - \mathsf{u}_2\mathbf{d}_3). \tag{B.14}$$

Substituting $\mathbf{d}_3^\pm$ according to (B.5,B.6) in (B.8) and projecting on $\mathbf{d}_3$ and $\mathbf{d}_2$ gives

$$a\begin{pmatrix}\mathsf{u}_2\\ \mathsf{u}_3\end{pmatrix} = M_1\begin{pmatrix}\alpha^- g^-\\ \alpha^+ g^+\end{pmatrix}; \qquad \text{where } M_1 = \begin{pmatrix}\cos\tau & -\cos(\tau-\theta)\\ -\sin\tau & \sin(\tau-\theta)\end{pmatrix}. \tag{B.15}$$

Substituting in turn (B.12,B.13) in (B.15), we obtain

$$a\mathsf{u}_2 = \frac{(\alpha^- g^-)^2(1-\beta)-(\alpha^+ g^+)^2\beta+(\alpha^- g^-)(\alpha^+ g^+)\cos\theta(2\beta-1)}{\sqrt{(\alpha^- g^-(1-\beta))^2+(\alpha^+ g^+\beta)^2+2\alpha^- g^-\alpha^+ g^+\beta(1-\beta)\cos\theta}}, \tag{B.16}$$

$$a\mathsf{u}_3 = \frac{-\alpha^- g^-\alpha^+ g^+\sin\theta}{\sqrt{(\alpha^- g^-(1-\beta))^2+(\alpha^+ g^+\beta)^2+2\alpha^- g^-\alpha^+ g^+\beta(1-\beta)\cos\theta}}. \tag{B.17}$$

Relations (B.16,B.17) together with (B.11) prove that once the functions $g^\pm$ are known, the three variables $\alpha^\pm$, θ are in one-to-one correspondence with the three variables α, u_2 & u_3. Indeed, Eqs. (B.11,B.16,B.17) can be inverted (since $\alpha^\pm > 0$ and $\cos\theta > 0$) to obtain:

$$\alpha^- = \frac{1}{g^-}\sqrt{a^2\mathsf{u}_3^2\beta^2+(a\beta\mathsf{u}_2+\alpha)^2}, \tag{B.18}$$

$$\alpha^+ = \frac{1}{g^+}\sqrt{a^2(1-\beta)^2\mathsf{u}_3^2+(\alpha-a(1-\beta)\mathsf{u}_2)^2}, \tag{B.19}$$

$$\sin\theta = \frac{-a\alpha\mathsf{u}_3}{\sqrt{a^2\beta^2\mathsf{u}_3^2+(\alpha+a\beta\mathsf{u}_2)^2}\sqrt{a^2(1-\beta)^2\mathsf{u}_3^2+(\alpha-a(1-\beta)\mathsf{u}_2)^2}}. \tag{B.20}$$

Although Eqs. (B.16-B.20) appear tedious, these results can be brought together in a relatively simple geometric construction (see Fig. 20) which allows to find the variables α, u_2 and u_3 in function of the angle θ and of $\alpha^\pm g^\pm$ (represented by the positions of points $A^\pm$ along $\mathbf{d}_3^\pm$). We readily observe on Fig. 20 that

- if $\theta \to 0$, then

$$\begin{aligned} a\mathsf{u}_2 &\to \alpha^- g^- - \alpha^+ g^+, && \text{(B.21)}\\ a\mathsf{u}_3 &\to 0, && \text{(B.22)}\\ \alpha &\to \alpha^- g^- (1-\beta) + \alpha^+ g^+ \beta. && \text{(B.23)} \end{aligned}$$

  so that we recover the geometric relations (5.3) of the 2D case;

- if $\beta \to 0$, then $B^+ \to A^-$, $\tau \to 0$, and

$$\begin{aligned} &\alpha \to \alpha^- g^-, && \text{(B.24)}\\ &a\mathsf{u}_2 \to \alpha^- g^- - \cos\theta \alpha^+ g^+, && \text{(B.25)}\\ &a\mathsf{u}_3 \to -\alpha^+ g^+ \sin\theta. && \text{(B.26)} \end{aligned}$$

- similarly, if $\beta \to 1$, then $B^+ \to A^+$, $\tau \to \theta$ and

$$\begin{aligned} &\alpha \to \alpha^+ g^+, && \text{(B.27)}\\ &a\mathsf{u}_2 \to \alpha^- g^- \cos\theta - \alpha^+ g^+, && \text{(B.28)}\\ &a\mathsf{u}_3 \to -\alpha^- g^- \sin\theta. && \text{(B.29)} \end{aligned}$$

The one-to-one correspondence between $\alpha^\pm$, θ and α, u_2, u_3 implies we can work with either set of variables to solve problems. While the latter gives direct geometrical information on the birod, we shall see that in some practical cases, working with the former can be easier. In the derivations of App. **??** we extensively use the matrices R_τ, $R_{\tau-\theta}$ and M_1. It is therefore practical to be able to express them in function of our two sets of variables (no explicit dependance on τ). Following from (B.12,B.13):

$$\begin{aligned} \alpha R_{\pm\tau} &= \alpha^+ g^+ \beta R_{\pm\theta} + \alpha^- g^- (1-\beta)\, \mathbb{I}_2, && \text{(B.30)}\\ \alpha R_{\pm(\tau-\theta)} &= \alpha^+ g^+ \beta \mathbb{I}_2 + \alpha^- g^- (1-\beta)\, R_{\mp\theta}. && \text{(B.31)} \end{aligned}$$

Next we observe from the definition of M_1 that

$$\begin{aligned} &M_1 = R_{-(\tau-\theta)} M_2 = R_{-\tau} M_3, && \text{(B.32)}\\ &R_\theta M_2 = M_3, && \text{(B.33)} \end{aligned}$$

where $M_2 = \begin{pmatrix} \cos\theta & -1 \\ -\sin\theta & 0 \end{pmatrix}$, $M_3 = \begin{pmatrix} 1 & -\cos\theta \\ 0 & -\sin\theta \end{pmatrix}$.

Substituting (B.30-B.31) in (B.32) and using (B.33), we obtain

$$M_1 = \beta \frac{\alpha^+ g^+}{\alpha} M_2 + (1-\beta) \frac{\alpha^- g^-}{\alpha} M_3. \qquad \text{(B.34)}$$

Substitutions according to (B.18-B.20) lead to

$$M_1 = \begin{pmatrix} \frac{\alpha+\beta\ a\mathsf{u}_2}{\sqrt{(\alpha+\beta a\mathsf{u}_2)^2+(\beta a\mathsf{u}_3)^2}} & \frac{\alpha-(1-\beta)\ a\mathsf{u}_2}{\sqrt{(\alpha-(1-\beta)a\mathsf{u}_2)^2+((1-\beta)a\mathsf{u}_3)^2}} \\ \frac{\beta\ a\mathsf{u}_3}{\sqrt{(\alpha+\beta a\mathsf{u}_2)^2+(\beta a\mathsf{u}_3)^2}} & \frac{(1-\beta)\ a\mathsf{u}_3}{\sqrt{(\alpha-(1-\beta)a\mathsf{u}_2)^2+((1-\beta)a\mathsf{u}_3)^2}} \end{pmatrix}. \qquad \text{(B.35)}$$

Similarly, substituting $\alpha^\pm$ and θ in (B.12,B.13) according to (B.18-B.20), we obtain

$$\begin{aligned} R_\tau &= \frac{1}{\sqrt{(\alpha+\beta a\mathsf{u}_2)^2+(\beta a\mathsf{u}_3)^2}} \begin{pmatrix} \alpha+\beta\ a\mathsf{u}_2 & \beta\ a\mathsf{u}_3 \\ -\beta\ a\mathsf{u}_3 & \alpha+\beta\ a\mathsf{u}_2 \end{pmatrix}, \\ R_{\tau-\theta} &= \frac{1}{\sqrt{(\alpha-(1-\beta)a\mathsf{u}_2)^2+((1-\beta)a\mathsf{u}_3)^2}} \begin{pmatrix} -(\alpha-(1-\beta)\ a\mathsf{u}_2 & (1-\beta)\ a\mathsf{u}_3 \\ -(1-\beta)\ a\mathsf{u}_3 & \alpha-(1-\beta)\ a\mathsf{u}_2 \end{pmatrix}. \end{aligned} \qquad \text{(B.36)}$$

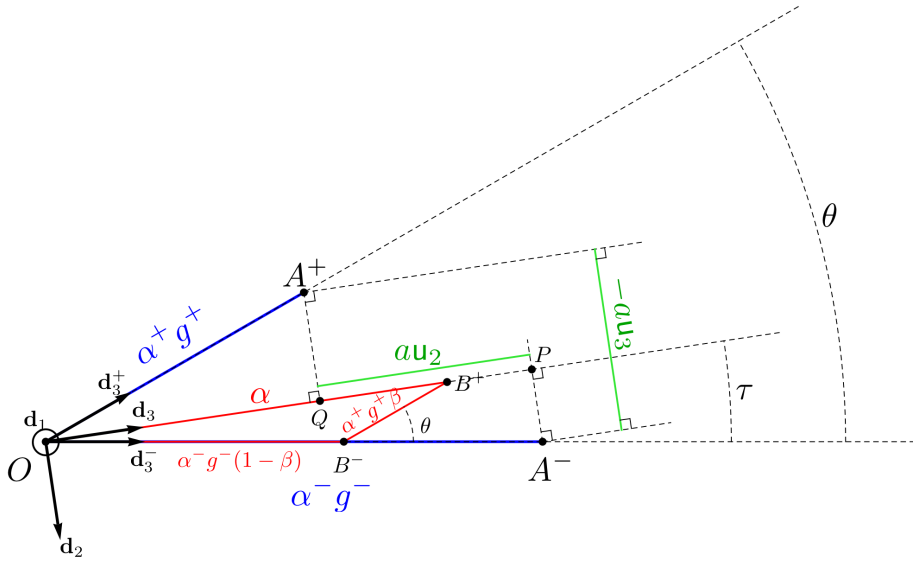

Figure 20: This geometric construction allows to find α, $a\mathsf{u}_2$ and $a\mathsf{u}_3$ in function of $\alpha^\pm$ and θ once the functions $g^\pm$ are known. The construction, built in the plane perpendicular to $\mathbf{d}_1$, proceeds as follow. Define a unit reference length, an arbitrary reference point O and an arbitrary unit vector $\mathbf{d}_3^-$ thourgh O. Find $\mathbf{d}_3^+$ by rotating the the vector $\mathbf{d}_3^-$ by the oriented angle θ. Find points $A^\pm$ so that $\mathbf{OA}^\pm \parallel \mathbf{d}_3^\pm$ and $|OA^\pm| = \alpha^\pm g^\pm$, where $\mathbf{AB}$ and $|AB|$ are respectively the vector and the distance from the point A to the point B in units of our reference length. Find the point B^- on the straight line OA^- such that $\frac{|OB^-|}{|OA^-|} = (1-\beta)$. Draw the parallel to OA^- through B^- on which we find the point B^+ such that $\frac{|B^-B^+|}{|OA^-|} = \beta$. By virtue of Eq. (B.8), $\alpha = |OB^+|$ and $\mathbf{d}_3$ is the unit vector on the oriented line OB^+. Define the points P and Q as the intersections of the perpendicular to OB^+ through A^- and A^+ respectively. By virtue of Eq. (B.15), $a\mathsf{u}_2 = |OP| - |OQ|$, and $a\mathsf{u}_3 = -|A^+Q| - |PA^-|$.

Finally, for any 2×2 matrix A, defining $\widetilde{A} = \begin{pmatrix} 0 & 1 \\ -1 & 0 \end{pmatrix} A \begin{pmatrix} 0 & -1 \\ 1 & 0 \end{pmatrix}$ so that $A^{-1} = \frac{1}{\det(A)}\widetilde{A}^T$, we note that

$$M_1 = \begin{pmatrix} \cos\tau & -\cos(\tau-\theta) \\ -\sin\tau & \sin(\tau-\theta) \end{pmatrix}; \quad \widetilde{M_1} = \begin{pmatrix} \sin(\tau-\theta) & \sin\tau \\ \cos(\tau-\theta) & \cos\tau \end{pmatrix};$$
$$M_1^{-1} = \frac{-1}{\sin\theta}\begin{pmatrix} \sin(\tau-\theta) & \cos(\tau-\theta) \\ \sin\tau & \cos\tau \end{pmatrix}. \tag{B.37}$$

B.2 Deriving the Darboux vectors of the sub-rods

Next we derive the geometric relations between $\mathbf{u}^\pm$ and $\mathbf{u}$. By definition of φ^- (cf. Fig. 19a) and τ (cf. Fig. 19b),

$$\begin{aligned} \begin{pmatrix} \mathbf{d}_1 & \mathbf{d}_2 & \mathbf{d}_3 \end{pmatrix} &= \begin{pmatrix} \mathbf{d}_1 & \mathbf{d}_3^- \times \mathbf{d}_1 & \mathbf{d}_3^- \end{pmatrix} \mathsf{R}_{1,\tau} && \text{(B.38)} \\ &= \begin{pmatrix} \mathbf{d}_1^- \mathbf{d}_2^- \mathbf{d}_3^- \end{pmatrix} \mathsf{R}_{3,\varphi^-}\mathsf{R}_{1,\tau}, && \text{(B.39)} \\ \Leftrightarrow \mathbf{D} &= \mathbf{D}^-\mathsf{R}_{3,\varphi^-}\mathsf{R}_{1,\tau}, && \text{(B.40)} \\ \text{and similarly} \quad \mathbf{D} &= \mathbf{D}^+\mathsf{R}_{3,\varphi^+ + \pi}\mathsf{R}_{1,\tau-\theta}. && \text{(B.41)} \end{aligned}$$

where $\mathsf{R}_{3,\chi} = \begin{pmatrix} \cos\chi & -\sin\chi & 0 \\ \sin\chi & \cos\chi & 0 \\ 0 & 0 & 1 \end{pmatrix}$ and $\mathsf{R}_{1,\chi} = \begin{pmatrix} 1 & 0 & 0 \\ 0 & \cos\chi & -\sin\chi \\ 0 & \sin\chi & \cos\chi \end{pmatrix}$.

Using the matrix form of $\mathbf{u}$ defined in (2.13), remembering that $\partial_S = g^- \partial_{S^-}$ and invoking (B.40), we obtain

$$
\begin{aligned}
g^- \mathbf{U}^- &= \mathbf{D}^{-T} \frac{\partial \mathbf{D}^-}{\partial S} && \text{(B.42)} \\
&= \left(\mathsf{R}_{3,\varphi^-} \cdot \mathsf{R}_{1,\tau}\right) \mathbf{D}^T \frac{\partial}{\partial S} \left[\mathbf{D} \left(\mathsf{R}_{3,\varphi^-} \cdot \mathsf{R}_{1,\tau}\right)^T\right], && \text{(B.43)} \\
&= \left(\mathsf{R}_{3,\varphi^-} \cdot \mathsf{R}_{1,\tau}\right) \mathbf{U} \left(\mathsf{R}_{3,\varphi^-} \cdot \mathsf{R}_{1,\tau}\right)^T \\
&\quad - \begin{pmatrix} 0 & 0 & \sin\varphi^- \\ 0 & 0 & -\cos\varphi^- \\ -\sin\varphi^- & \cos\varphi^- & 0 \end{pmatrix} \tau' - \begin{pmatrix} 0 & -1 & 0 \\ 1 & 0 & 0 \\ 0 & 0 & 0 \end{pmatrix} \varphi^{-\prime}, && \text{(B.44)}
\end{aligned}
$$

where $' = \frac{\partial}{\partial S}$.

After developing (B.44) in components, we obtain

$$
g^- \begin{pmatrix} \mathsf{u}_1^- \\ \mathsf{u}_2^- \\ \mathsf{u}_3^- \end{pmatrix} = \mathsf{R}_{3,\varphi^-} \mathsf{R}_{1,\tau} \begin{pmatrix} \mathsf{u}_1 \\ \mathsf{u}_2 \\ \mathsf{u}_3 \end{pmatrix} - \tau' \mathsf{R}_{3,\varphi^-} \begin{pmatrix} 1 \\ 0 \\ 0 \end{pmatrix} - \varphi^{-\prime} \begin{pmatrix} 0 \\ 0 \\ 1 \end{pmatrix}. \tag{B.45}
$$

The same procedure can be applied to $\mathbf{U}^+$ after which we obtain

$$
g^+ \begin{pmatrix} \mathsf{u}_1^+ \\ \mathsf{u}_2^+ \\ \mathsf{u}_3^+ \end{pmatrix} = \mathsf{R}_{3,\varphi^+ + \pi} \mathsf{R}_{1,\tau-\theta} \begin{pmatrix} \mathsf{u}_1 \\ \mathsf{u}_2 \\ \mathsf{u}_3 \end{pmatrix} - (\tau - \theta)' \, \mathsf{R}_{3,\varphi^+ + \pi} \begin{pmatrix} 1 \\ 0 \\ 0 \end{pmatrix} - \varphi^{+\prime} \begin{pmatrix} 0 \\ 0 \\ 1 \end{pmatrix}. \tag{B.46}
$$

Applying $\mathbf{D}^-$ and $\mathbf{D}^+$ respectively to (B.45) and (B.46), we obtain

$$
\begin{aligned}
g^- \mathbf{u}^- &= \mathbf{u} - \tau' \mathbf{d}_1 - \varphi^{-\prime} \mathbf{d}_3^-, \\
g^+ \mathbf{u}^+ &= \mathbf{u} - (\tau - \theta)' \mathbf{d}_1 - \varphi^{+\prime} \mathbf{d}_3^+.
\end{aligned} \tag{B.47}
$$

C The unloaded 2D ring

Consider a planar, extensible rod, with constant reference curvature $\hat{\mathsf{u}}_2$ and linear constitutive laws. Form a closed ring by joining the ends of the rod such that the tangents to the centreline are aligned. What stable configuration does the ring assume when no external loads are applied?

Suppose the rod has length L and constitutive laws

$$
\begin{aligned}
\mathsf{n}_3 &= k(\alpha - 1), \\
\mathsf{m}_2 &= K(\mathsf{u}_2 - \hat{\mathsf{u}}_2),
\end{aligned} \tag{C.1}
$$

Define one point of the ring as $S = 0$ and $\mathbf{d}_{30}$ the tangent to the centreline at that point. Then define $\theta(S)$ the oriented angle from $\mathbf{d}_{30}$ to the tangent at that point $\mathbf{d}_3(S)$. By definition of θ, $\theta(0) = 0$. Furthermore, imposing $\theta(S)$ to be continuous on $S \in [0, L]$ yields $\theta(L) = 2\pi$ on a ring. Finally, note that $\mathsf{u}_2 = \frac{\mathrm{d}\theta}{\mathrm{d}S}$.

The current configuration is completely specified provided we know the two functions $\alpha(S)$ and $\theta(S)$. Equilibrium configurations can be found by finding extrema of the energy functional $\mathcal{E}$:

$$
\mathcal{E}[\alpha(S), \theta(S)] = \int_0^L \frac{K_1}{2} (\alpha(S) - 1)^2 + \frac{K_2}{2} \left(\theta'(S) - \hat{\mathsf{u}}_2\right)^2 \mathrm{d}S, \tag{C.2}
$$

under the constraints

$$\int_0^L \alpha(S)\cos\theta(S)\mathrm{d}S = 0, \qquad \int_0^L \alpha(S)\sin\theta(S)\mathrm{d}S = 0. \tag{C.3}$$

which ensure that the extremities of the rod meet ($\frac{\mathrm{d}\mathbf{r}\cdot\mathbf{d}_{30}}{\mathrm{d}S} = \alpha\cos\theta$, $\frac{\mathrm{d}\mathbf{r}\cdot(\mathbf{d}_2\times\mathbf{d}_{30})}{\mathrm{d}S} = \alpha\sin\theta$), the constraint (C.3) ensures the tangent are aligned and that the rod makes a full turn.

Consider the easier problem of minimizing (C.2) with the boundary conditions $\theta(0) = 0$ and $\theta(L) = 2\pi$ alone. The Euler-Lagrange equations derived from for the integrand $\mathcal{E}$ are

$$\left(\frac{\partial\mathcal{E}}{\partial\alpha'}\right)' - \frac{\partial\mathcal{E}}{\partial\alpha} = K_1(\alpha-1) = 0, \qquad \left(\frac{\partial\mathcal{E}}{\partial\theta'}\right)' - \frac{\partial\mathcal{E}}{\partial\theta} = K_2\theta'' = 0. \tag{C.4}$$

From this and the boundary conditions we conclude $\alpha = 1$ and $\theta = \frac{2\pi}{L}S$. This solution also satisfies the constraints (C.3).

As this is the only extremum of (C.2) with adequate boundary conditions but no constraints, it is a global minimum of the constrained problem. Finding all equilibria of the constrained problem is a much harder task that we will not undertake here. In any case, this simple exercise demonstrates that if a rod with constant intrinsic curvature is closed into a circular ring, *the length does not change during the deformation*, and thus the energy minimizing ring is the one with radius $\frac{L}{2\pi}$.

D Constitutive laws for n, M and m for 3D extensible birod

D.1 Constitutive law for n

Assuming that the sub-rods are extensible and unshearable so that $\mathsf{n}_3^+ = \mathbf{n}^+\cdot\mathbf{d}_3^+$ and $\mathsf{n}_3^- = \mathbf{n}^-\cdot\mathbf{d}_3^-$ are known constitutively in function of $\alpha^\pm$ (and possibly $\mathbf{u}^\pm$). Using the result of the previous appendix, we can therefore infer constitutive laws for $\mathsf{n}_3^\pm$ in function of α and $\mathbf{u}$:

$$\begin{aligned}\mathsf{n}_3^+ &= \mathsf{n}_3^+(\alpha,\mathbf{u}),\\ \mathsf{n}_3^- &= \mathsf{n}_3^-(\alpha,\mathbf{u}).\end{aligned} \tag{D.1}$$

Because the mechanical balance of the birod (3.28-3.32) involve $\mathbf{N}$ and $\mathbf{n}$ rather than the stresses $\mathbf{n}^\pm$ in the sub-rods, we need to translate the constitutive information contained in (D.1) into constitutive relations for $\mathbf{N}$ and $\mathbf{n}$. To this intend, we first note that (3.28,3.30) can be inverted to

$$\mathbf{n}^\pm = \frac{1}{2}(\mathbf{N}\pm\mathbf{n}). \tag{D.2}$$

Next, we invoke the geometric relations (B.5,B.6) so that

$$\begin{aligned}\mathsf{n}_3^+ = \mathbf{n}^+\cdot\mathbf{d}_3^+ &= \frac{1}{2}\left(\mathbf{N}+\mathbf{n}\right)\cdot\left(\cos\left(\tau-\theta\right)\mathbf{d}_3 + \sin\left(\tau-\theta\right)\mathbf{d}_2\right),\\ \mathsf{n}_3^- = \mathbf{n}^-\cdot\mathbf{d}_3^- &= \frac{1}{2}\left(\mathbf{N}-\mathbf{n}\right)\cdot\left(\cos\tau\mathbf{d}_3 + \sin\tau\mathbf{d}_2\right),\end{aligned} \tag{D.3}$$

These two equations can be gathered in matricidal form (see Eq. (B.37))

$$2\begin{pmatrix}\mathsf{n}_3^+\\ \mathsf{n}_3^-\end{pmatrix} = \widetilde{M}_1^T\begin{pmatrix}\mathsf{N}_2\\ \mathsf{N}_3\end{pmatrix} + \begin{pmatrix}1 & 0\\ 0 & -1\end{pmatrix}\widetilde{M}_1^T\begin{pmatrix}\mathsf{n}_2\\ \mathsf{n}_3\end{pmatrix}. \tag{D.4}$$

When $\theta = 0$, the tangents are aligned $\mathbf{d}_3^\pm = \mathbf{d}_3$ such that $\mathsf{N}_3 = \mathsf{n}_3^+ + \mathsf{n}_3^-$ and $\mathsf{n}_3 = \mathsf{n}_3^+ - \mathsf{n}_3^-$. When $\theta \neq 0$, we obtain

$$\begin{pmatrix}\mathsf{n}_2\\ \mathsf{n}_3\end{pmatrix} = \frac{-2}{\sin\theta}M_1\begin{pmatrix}1 & 0\\ 0 & -1\end{pmatrix}\begin{pmatrix}\mathsf{n}_3^+\\ \mathsf{n}_3^-\end{pmatrix} - M_1\begin{pmatrix}1 & 0\\ 0 & -1\end{pmatrix}M_1^{-1}\begin{pmatrix}\mathsf{N}_2\\ \mathsf{N}_3\end{pmatrix}. \tag{D.5}$$

This generic form for the constitutive laws of n_2 and n_3 is practical since M_1 and $\sin\theta$ can either be expressed in function of $\alpha^\pm$ and θ using (B.34) or in function of α, u_2 and u_3 using (B.18,B.35).

Although we have not been able to express n_2 and n_3 in function of kinematic variable only, the relation (D.5) still plays the role of a constitutive law in the theory of the three-dimensional birod as it eliminates two mechanical variables from the problem. It's important to note that we have no constitutive law for any component of $\mathbf{N}$.

D.2 Constitutive law for M and m

The definitions3.27Defm of both these global moments involves components of $\mathbf{n}^\pm$ for which no constitutive laws exists. As discussed in Sec. 3.2.3, we propose here one way around that problem. An alternative approach is discussed in Sec. 6 where we define different global strains; see also App. I. In the definitions (3.27,3.31) of $\mathbf{M}$ and $\mathbf{m}$, let us substitutive $\mathbf{n}^\pm$ according to (D.2):

$$\mathbf{M} = \mathbf{m}^+ + \mathbf{m}^- + \frac{a}{2}\mathbf{d}_1 \times \mathbf{n} + \frac{c^+ - c^-}{2}\mathbf{d}_1 \times \mathbf{N}, \tag{D.6}$$

$$\mathbf{m} = \mathbf{m}^+ - \mathbf{m}^- + \frac{a}{2}\mathbf{d}_1 \times \mathbf{N} + \frac{c^+ - c^-}{2}\mathbf{d}_1 \times \mathbf{n}. \tag{D.7}$$

We already know from (D.5) that we have a constitutive laws for the n_2 and n_3 components of $\mathbf{n}$ in function of $\mathbf{N}$ and the birods geometric variables (α and $\mathbf{u}$ for instance). Similarly, Eqs. (D.6,D.7) are constitutive laws for $\mathbf{M}$ and $\mathbf{m}$ in function of the strain of the birod (e.g. α and $\mathbf{u}$) and of $\mathbf{N}$. While this construction allows to make progress regarding the count of variables vs count of equations discussed in Sec 3.2.3 (after all Eqs. (D.5-D.7) provide 9 equations at the cost of adding 5 variables to the theory (2 for n_2 and n_3 and 3 for $\mathbf{m}$), it does so at the cost of making the moments of forces in the structure a direct explicit function of the force applied on the structure.

Finally to actually obtain an explicit version of the constitutive laws mentioned in the previous paragraph, we need to be able to express the constitutive laws of $\mathbf{m}^\pm$ and $\mathsf{n}_3^\pm$ in function of α and $\mathbf{u}$. While the latter usually poses little problem, we would also like to be able to express the constitutive laws for $\mathbf{m}$ in the frame of director of the birod (they are originally known in the frame of director of the sub-rods). In the next subsection, we show how this can be done in the case of linear constitutive laws for the moments $\mathbf{m}^\pm$.

D.3 Constitutive laws for $\mathbf{m}^\pm$ in function of the kinematic variables of the birod

To be able to treat both the '+' and the '−' rod at once, we introduce

- the angles $\tau^- = \tau$ and $\tau^+ = \tau - \theta$;
- the matrices $\mathsf{R}^+ = \mathsf{R}_{3,\varphi^+ + \pi}\mathsf{R}_{1,\tau-\theta}$ and $\mathsf{R}^- = \mathsf{R}_{3,\varphi^-}\mathsf{R}_{1,\tau}$ so that according to (B.40,B.41), we have $\mathbf{D} = \mathbf{D}^\pm\mathsf{R}^\pm$;
- $M^+ = M_2$ and $M^- = M_3$.

According to (2.20) with the definitions listed below (6.43), linear constitutive laws for the sub-rods can be expressed in the following matricidal form:

$$\mathbf{m}^{\pm} = (EI)^{\pm}\mathbf{D}^{\pm}\begin{pmatrix}1&0&0\\0&b^{\pm}&0\\0&0&\Gamma^{\pm}\end{pmatrix}\left[\begin{pmatrix}\mathsf{u}_1^{\pm}\\ \mathsf{u}_2^{\pm}\\ \mathsf{u}_3^{\pm}\end{pmatrix}-\begin{pmatrix}\hat{\mathsf{u}}_1^{\pm}\\ \hat{\mathsf{u}}_2^{\pm}\\ \hat{\mathsf{u}}_3^{\pm}\end{pmatrix}\right]. \tag{D.8}$$

$$\overset{(B.45,B.46),\ (B.40,B.41)}{=} \frac{(EI)}{g^{-}}\mathcal{E}^{\pm}\mathbf{D}\mathsf{R}^{\pm-1}\left(\mathbb{I}+(b^{\pm}-1)\begin{pmatrix}0&0&0\\0&1&0\\0&0&0\end{pmatrix}+(\Gamma^{\pm}-1)\begin{pmatrix}0&0&0\\0&0&0\\0&0&1\end{pmatrix}\right)$$
$$\mathsf{R}^{\pm}\left[\begin{pmatrix}\mathsf{u}_1-\tau^{\pm\prime}\\ \mathsf{u}_2\\ \mathsf{u}_3\end{pmatrix}-\mathsf{R}^{\pm-1}\begin{pmatrix}g^{\pm}\hat{\mathsf{u}}_1^{\pm}\\ g^{\pm}\hat{\mathsf{u}}_2^{\pm}\\ g^{\pm}\hat{\mathsf{u}}_3^{\pm}+\varphi^{\pm\prime}\end{pmatrix}\right], \tag{D.9}$$

where $(EI)=(EI)^{-}+\frac{1}{g}(EI)^{+}$, $\mathcal{E}^{+}=\frac{(EI)^{+}}{g(EI)}$ and $\mathcal{E}^{-}=\frac{(EI)^{-}}{(EI)}$. Furthermore,

$$\begin{aligned}\mathbf{m}^{\pm} &= \frac{(EI)}{g^{-}}\mathcal{E}^{\pm}\mathbf{d}_1\left[\mathsf{u}_1-\tau^{\pm\prime}\pm g^{\pm}(\cos\varphi^{\pm}\hat{\mathsf{u}}_1^{\pm}+\sin\varphi^{\pm}\hat{\mathsf{u}}_2^{\pm})\right]\\ &\quad+\frac{(EI)}{g^{-}}\mathcal{E}^{\pm}\begin{pmatrix}\mathbf{d}_2&\mathbf{d}_3\end{pmatrix}\left(\mathbb{I}+(\Gamma^{\pm}-1)R_{-\tau^{\pm}}\begin{pmatrix}0&0\\0&1\end{pmatrix}R_{\tau^{\pm}}\right)\\ &\quad\left[\begin{pmatrix}\mathsf{u}_2\\ \mathsf{u}_3\end{pmatrix}-R_{-\tau^{\pm}}\begin{pmatrix}\mp g^{\pm}(\cos\varphi^{\pm}\hat{\mathsf{u}}_2^{\pm}-\sin\varphi^{\pm}\hat{\mathsf{u}}_1^{\pm})\\ g^{\pm}\hat{\mathsf{u}}_3^{\pm}+\varphi^{\pm\prime}\end{pmatrix}\right]\\ &\quad+(b^{\pm}-1)\frac{(EI)}{g^{-}}\mathcal{E}^{\pm}\mathbf{D}\mathsf{R}_{1,-\tau^{\pm}}\mathsf{B}^{\pm}\left[\mathsf{R}_{1,\tau^{\pm}}\begin{pmatrix}\mathsf{u}_1-\tau^{\pm\prime}\\ \mathsf{u}_2\\ \mathsf{u}_3\end{pmatrix}-R_{3,-(\varphi^{\pm}+\frac{\pi}{2}\pm\frac{\pi}{2})}\begin{pmatrix}g^{\pm}\hat{\mathsf{u}}_1^{\pm}\\ g^{\pm}\hat{\mathsf{u}}_2^{\pm}\\ g^{\pm}\hat{\mathsf{u}}_3^{\pm}+\varphi^{\pm\prime}\end{pmatrix}\right],\end{aligned} \tag{D.10}$$

where the matrices $\mathsf{B}^{\pm}$ are defined as

$$\mathsf{B}^{\pm}=\mathsf{R}_{3,-(\varphi^{\pm}+\frac{\pi}{2}\pm\frac{\pi}{2})}\begin{pmatrix}0&0&0\\0&1&0\\0&0&0\end{pmatrix}\mathsf{R}_{3,(\varphi^{\pm}+\frac{\pi}{2}\pm\frac{\pi}{2})}. \tag{D.11}$$

Next, let us define

$$\widehat{\boldsymbol{\mathcal{U}}}^{\pm}=\mp\mathbf{d}_1\left(\cos\varphi^{\pm}\hat{\mathsf{u}}_1^{\pm}+\sin\varphi^{\pm}\hat{\mathsf{u}}_2^{\pm}\right)\mp\mathbf{d}_2\left(\cos\varphi^{\pm}\hat{\mathsf{u}}_2^{\pm}-\sin\varphi^{\pm}\hat{\mathsf{u}}_1^{\pm}\right)+\mathbf{d}_3\left(\hat{\mathsf{u}}_3^{\pm}+\frac{\mathrm{d}\varphi^{\pm}}{\mathrm{d}S^{\pm}}\right). \tag{D.12}$$

Furthermore, recalling (B.32): $R_{\tau^{\pm}}=M^{\pm}\left(M_1\right)^{-1}$, we note that

$$R_{-\tau^{\pm}}\begin{pmatrix}0&0\\0&1\end{pmatrix}R_{\tau^{\pm}}=M_1\left(M^{\pm}\right)^{-1}\begin{pmatrix}0&0\\0&1\end{pmatrix}M^{\pm}{M_1}^{-1}=\begin{cases}M_1\begin{pmatrix}0&\cos\theta\\0&1\end{pmatrix}M_1^{-1}\text{ when }\pm=\text{-},\\ M_1\begin{pmatrix}1&0\\\cos\theta&0\end{pmatrix}M_1^{-1}\text{ when }\pm=+.\end{cases} \tag{D.13}$$

With (D.13) and the notations (D.11,D.12), Eq. (D.10) becomes

$$
\begin{aligned}
\mathbf{m}^{\pm} \;=\; & \frac{(EI)}{g^-}\mathcal{E}^{\pm}\mathbf{d}_1\,\left(\mathsf{u}_1-\tau^{\pm\prime}-g^{\pm}\widehat{\mathcal{U}}_1^{\pm}\right)\\
& +\frac{(EI)}{g^-}\mathcal{E}^{\pm}\begin{pmatrix}\mathbf{d}_2 & \mathbf{d}_3\end{pmatrix}M_1\left(\begin{pmatrix}1&0\\0&1\end{pmatrix}+(\Gamma^{\pm}-1)\left\{\begin{matrix}\begin{pmatrix}1&0\\\cos\theta&0\end{pmatrix}\\ \begin{pmatrix}0&\cos\theta\\0&1\end{pmatrix}\end{matrix}\right\}\right)\\
& \qquad\left[(M_1)^{-1}\begin{pmatrix}\mathsf{u}_2\\\mathsf{u}_3\end{pmatrix}-g^{\pm}\left(M^{\pm}\right)^{-1}\begin{pmatrix}\widehat{\mathcal{U}}_2^{\pm}\\\widehat{\mathcal{U}}_3^{\pm}\end{pmatrix}\right] \qquad\qquad (D.14)\\
& +(b^{\pm}-1)\frac{(EI)}{g^-}\mathcal{E}^{\pm}\mathbf{D}\begin{pmatrix}1&0&0\\0&M_1\end{pmatrix}\left[\begin{pmatrix}1&0&0\\0&(M^{\pm})^{-1}\end{pmatrix}\mathsf{B}^{\pm}\begin{pmatrix}1&0&0\\0&M^{\pm}\end{pmatrix}\right]\\
& \qquad\left[\begin{pmatrix}1&0&0\\0&(M_1)^{-1}\end{pmatrix}\begin{pmatrix}\mathsf{u}_1-\tau^{\pm\prime}\\\mathsf{u}_2\\\mathsf{u}_3\end{pmatrix}-g^{\pm}\begin{pmatrix}1&0&0\\0&(M^{\pm})^{-1}\end{pmatrix}\begin{pmatrix}\widehat{\mathcal{U}}_1^{\pm}\\\widehat{\mathcal{U}}_2^{\pm}\\\widehat{\mathcal{U}}_3^{\pm}\end{pmatrix}\right].
\end{aligned}
$$

The two matrices superposed in the second line of (D.14), mean that the top one must be used for $\mathbf{m}^+$ and the bottom one for $\mathbf{m}^-$.

The expression (D.14) gives the constitutive laws of $\mathbf{m}^{\pm}$ in the orthonormal frame of director of the birod and in function of α and $\mathbf{u}$. Indeed, see (B.30-B.37) for expressions of all the matrices involved in function of α and $\mathbf{u}$. Similarly, τ' could be substituted (although the expression would become very lengthy) for α and $\mathbf{u}$ by using Eqs. (B.12,B.18-refappsinthgeom).

The complexity of the expression (D.14) and the difficulty to use it to solve practical birods is one of the major motivations behind the development of the alternative geometric description of the birod in Sec. 6.1. For comparison, we then obtain the fully explicit constitutive laws (H.6) for $\mathbf{m}^{\pm}$.

E Linear approximation to the constitutive laws of 2D morphoelastic birods

The constitutive laws (5.8) can be linearised around the reference state of the birod, giving

$$
\begin{aligned}
\mathsf{N}_3 \;=\; & \left.\frac{\partial k(\alpha,\mathsf{u}_2)}{\partial\alpha}\right|_{\substack{\alpha=1\\ \mathsf{u}_2=\hat{\mathsf{u}}_2}}(\alpha-1)+\left.\frac{\partial k(\alpha,\mathsf{u}_2)}{\partial\mathsf{u}_2}\right|_{\substack{\alpha=1\\ \mathsf{u}_2=\hat{\mathsf{u}}_2}}(\mathsf{u}_2-\hat{\mathsf{u}}_2)+\text{h.o.t.}\\
\;=\; & \frac{1}{gg^-}\left[\partial_{\alpha^+}k^+ + g\partial_{\alpha^-}k^-\right]\Big|_{\mathcal{B}_0}(\alpha-1)+\\
& \frac{1}{gg^-}\left[-a(1-\beta)\partial_{\alpha^+}k^+ + ag\beta\partial_{\alpha^-}k^-\right]\Big|_{\mathcal{B}_0}(\mathsf{u}_2-\hat{\mathsf{u}}_2)+\\
& \frac{1}{gg^-}\left[\partial_{u^+}k^+ + g\partial_{u^-}k^-\right]\Big|_{\mathcal{B}_0}(\mathsf{u}_2-\hat{\mathsf{u}}_2)+\text{h.o.t.}, \qquad\qquad (E.1)
\end{aligned}
$$

and

$$\begin{aligned}
\mathsf{M}_2 &= \left.\frac{\partial K(\alpha,\mathsf{u}_2)}{\partial\alpha}\right|_{\substack{\alpha=1\\ \mathsf{u}_2=\hat{\mathsf{u}}_2}}(\alpha-1)+\left.\frac{\partial K(\alpha,\mathsf{u}_2)}{\partial \mathsf{u}_2}\right|_{\substack{\alpha=1\\ \mathsf{u}_2=\hat{\mathsf{u}}_2}}(\mathsf{u}_2-\hat{\mathsf{u}}_2)+\text{h.o.t}\\
&= \frac{1}{gg^-}\left[\partial_{\alpha^+}K^+ + g\partial_{\alpha^-}K^-\right]\Big|_{\mathcal{B}_0}(\alpha-1)\\
&\quad+\frac{1}{gg^-}\left[\partial_{u^+}K^+ + g\partial_{u^-}K^-\right]\Big|_{\mathcal{B}_0}(\mathsf{u}_2-\hat{\mathsf{u}}_2)\\
&\quad+\frac{1}{gg^-}\left[-a(1-\beta)\partial_{\alpha^+}k^+ + ag\beta\partial_{\alpha^-}k^-\right]\Big|_{\mathcal{B}_0}(\alpha-1)\\
&\quad+\frac{1}{gg^-}\left[a^2(1-\beta)^2\partial_{\alpha^+}k^+ + ga^2\beta^2\partial_{\alpha^-}k^-\right]\Big|_{\mathcal{B}_0}(\mathsf{u}_2-\hat{\mathsf{u}}_2)\\
&\quad+\frac{1}{gg^-}\left[-a(1-\beta)\partial_{\mathsf{u}_2^+}k^+ + ag\beta\partial_{\mathsf{u}_2^-}k^-\right]\Big|_{\mathcal{B}_0}(\mathsf{u}_2-\hat{\mathsf{u}}_2)+\text{h.o.t.},
\end{aligned}\tag{E.2}$$

where we have defined the reference state of the birod $\mathcal{B}_0$ as $\alpha^+ = (1-a(1-\beta)\hat{\mathsf{u}}_2)/gg^-$, $\mathsf{u}_2^+ = \hat{\mathsf{u}}_2/gg^-$, $\alpha^- = (1+a\beta\hat{\mathsf{u}}_2)/g^-$ and $\mathsf{u}_2^- = \hat{\mathsf{u}}_2/g^-$.

This linearisation is particularly useful if the sub-rods are uniform and uniformly glued so that $k^\pm$, $K^\pm$ and g are independent of S. If furthermore their constitutive laws are diagonal so that $\partial_{\mathsf{u}_2^\pm}k^\pm = 0$ and $\partial_{\alpha^\pm}K^\pm = 0$, we choose

$$\beta = \beta^\star := \left.\frac{\partial_{\alpha_+}k^+}{\partial_{\alpha_+}k^+ + g\partial_{\alpha_-}k^-}\right|_{\mathcal{B}_0}.\tag{E.3}$$

With this choice, the birod also has diagonal constitutive laws at first order,

$$\mathsf{N}_3 = \frac{-1}{gg^-}\left[\partial_{\alpha^+}k^+ + g\partial_{\alpha^-}k^-\right]\Big|_{\mathcal{B}_0}(\alpha-1)+\text{h.o.t.},\tag{E.4}$$

$$\mathsf{M}_2 = \frac{1}{gg^-}\left[\partial_{\mathsf{u}_2^+}K^+ + g\partial_{\mathsf{u}^-}K^- + a^2\frac{g\partial_{\alpha^-}k^-\partial_{\alpha_+}k^+}{\partial_{\alpha_+}k^+ + g\partial_{\alpha_-}k^-}\right]\Big|_{\mathcal{B}_0}(\mathsf{u}_2-\hat{\mathsf{u}}_2)+\text{h.o.t.}.\tag{E.5}$$

Finally, note that although β explicitly appears in the R.H.S. of (E.3), the derivatives are to be evaluated in the reference state of the birod, in which the values of $\alpha^\pm$ are independent of β. Explicitly, the reference stretches can be found either by solving (5.7) and using (5.3) or by directly inverting

$$\begin{aligned}
&\mathsf{N}_3 = k^+(\hat{\alpha}^+) + k^-(\hat{\alpha}^-) = 0,\\
&\mathsf{M}_2 = K^+(\mathsf{u}_2^+) + K^-(\mathsf{u}_2^-) + ak^-(\hat{\alpha}^-)\\
&\qquad = K^+\left(\frac{\hat{\alpha}^- - g\hat{\alpha}^+}{ag}\right) + K^-\left(\frac{\hat{\alpha}^- - g\hat{\alpha}^+}{a}\right) + ak^-(\hat{\alpha}^-) = 0.
\end{aligned}\tag{E.6}$$

F Proof of (6.7)

In this section, for any vector $\mathbf{u}\in\mathbb{R}^3$, we note $[\mathbf{u}]_\times$ the operator:

$$[\mathbf{u}]_\times : \mathbb{R}^3 \to \mathbb{R}^3 : \mathbf{w} \to \mathbf{u}\times\mathbf{w}.\tag{F.1}$$

Let $\{\mathbf{d}_1,\mathbf{d}_2,\mathbf{d}_3\}$ be a right-handed orthonormal bases of $\mathbb{R}^3$ and D the matrix, the ith column of which are the components of $\{\mathbf{d}_i\}$ in the fix right handed orthonormal lab frame $\{\mathbf{e}_1,\mathbf{e}_2,\mathbf{e}_3\}$. Let R

be an orthogonal matrix of determinant 1 (i.e. a rotation matrix). Let U be a the skew symmetric matrix defined by $\mathsf{u}_1, \mathsf{u}_2$ and u_3:

$$\mathsf{U} = \begin{pmatrix} 0 & -\mathsf{u}_3 & \mathsf{u}_2 \\ \mathsf{u}_3 & 0 & -\mathsf{u}_1 \\ -\mathsf{u}_2 & \mathsf{u}_1 & 0 \end{pmatrix}.$$

Finally, define $\{\mathbf{c}_1, \mathbf{c}_2, \mathbf{c}_3\}$ the right-handed orthnormal frame such that $\begin{pmatrix} \mathbf{c}_1 & \mathbf{c}_2 & \mathbf{c}_3 \end{pmatrix} = \begin{pmatrix} \mathbf{d}_1 & \mathbf{d}_2 & \mathbf{d}_3 \end{pmatrix} \mathsf{R}^T$.

Lemma 1. *In the basis $\{\mathbf{d}_i\}$, the matrix $R^T U R$ is the matrix of the operator $[\mathbf{c}_i u_i]_\times$.*

Proof. Applying standard change of basis formula, the operator A, the matrix of which is $\mathsf{R}^T\mathsf{U}\mathsf{R}$ in the basis $\{\mathbf{d}_i\}$ has the matrix $\mathsf{R}(\mathsf{R}^T\mathsf{U}\mathsf{R})\mathsf{R}^T = \mathsf{U}$ in the basis $\{\mathbf{c}_i\}$. Direct expansion of $\mathbf{u} \times \mathbf{w}$ in components in the basis $\{\mathbf{c}_i\}$ shows that U is indeed the matrix of the operator $[\mathsf{u}_i\mathbf{c}_i]_\times$ in that basis. Hence $A = [\mathsf{u}_i\mathbf{c}_i]_\times$.

Next let us define the short hands $\mathsf{R}_{i,\omega}$ for the matrices:

$$\mathsf{R}_{1,\omega} = \begin{pmatrix} 1 & 0 & 0 \\ 0 & \cos\omega & -\sin\omega \\ 0 & \sin\omega & \cos\omega \end{pmatrix}, \qquad \mathsf{R}_{2,\omega} = \begin{pmatrix} \cos\omega & 0 & \sin\omega \\ 0 & 1 & 0 \\ -\sin\omega & 0 & \cos\omega \end{pmatrix}, \qquad \mathsf{R}_{3,\omega} = \begin{pmatrix} \cos\omega & -\sin\omega & 0 \\ \sin\omega & \cos\omega & 0 \\ 0 & 0 & 1 \end{pmatrix}. \tag{F.2}$$

Note that (as can be checked by direct expansion)

$$\frac{\mathrm{d}}{\mathrm{d}S}\mathsf{R}_{i,\omega(S)} = \mathsf{R}_{i,\omega(S)} \underbrace{\begin{pmatrix} 0 & -\delta_{3,i} & \delta_{2,i} \\ \delta_{3,i} & 0 & -\delta_{1,i} \\ -\delta_{2,i} & \delta_{1,i} & 0 \end{pmatrix}}_{\mathsf{U}_i} \frac{\mathrm{d}\omega}{\mathrm{d}S}, \tag{F.3}$$

where there is no summation over repeated indices and $\delta_{i,j} = 1$ if $i = j$ and 0 otherwise.

We are now ready to prove (6.7). Introducing the matrices $\mathbf{D}^\pm = \begin{pmatrix} \mathbf{d}_1^\pm & \mathbf{d}_2^\pm & \mathbf{d}_3^\pm \end{pmatrix}$, we can rewrite (6.6) as

$$\mathbf{D}^+ = \mathbf{D}^- \underbrace{\mathsf{R}_{3,\varphi^-} \overbrace{\mathsf{R}_{1,\theta}\, \mathsf{R}_{3,-\varphi^+-\pi}}^{\mathsf{Q}}}_{\mathsf{R}}. \tag{F.4}$$

Taking the derivative of (F.4) by S an arbitrary parameterisation of the sections of the birod:

$$\begin{aligned} g^+\mathbf{D}^+\mathsf{U}^+ &= g^-\mathbf{D}^-\mathsf{U}^-\mathsf{R}_{3,\varphi^-}\, \mathsf{R}_{1,\theta}\, \mathsf{R}_{3,-\varphi^+-\pi} + \frac{\mathrm{d}\varphi^-}{\mathrm{d}S}\, \mathbf{D}^-\mathsf{R}_{3,\varphi^-}\, \mathsf{U}_3\, \mathsf{R}_{1,\theta}\, \mathsf{R}_{3,-\varphi^+-\pi} \\ &\quad + \frac{\mathrm{d}\theta}{\mathrm{d}S}\, \mathbf{D}^-\mathsf{R}_{3,\varphi^-}\, \mathsf{R}_{1,\theta}\, \mathsf{U}_1\, \mathsf{R}_{3,-\varphi^+-\pi} - \frac{\mathrm{d}\varphi^+}{\mathrm{d}S}\, \mathbf{D}^-\mathsf{R}_{3,\varphi^-}\, \mathsf{R}_{1,\theta}\, \mathsf{R}_{3,-\varphi^+-\pi}\, \mathsf{U}_3 \\ &= \mathbf{D}^+\left(g^-\mathsf{R}^T\mathsf{U}^-\mathsf{R} + \frac{\mathrm{d}\varphi^-}{\mathrm{d}S}\, \mathsf{Q}^T\mathsf{U}_3\mathsf{Q} + \frac{\mathrm{d}\theta}{\mathrm{d}S}\, \mathsf{R}^T_{3,-\varphi^+-\pi}\mathsf{U}_1\mathsf{R}_{3,-\varphi^+-\pi} + -\frac{\mathrm{d}\varphi^+}{\mathrm{d}S}\, \mathsf{U}_3 \right) \end{aligned} \tag{F.5}$$

where the first equality comes from applying (F.3) to the derivative of the LHS of (F.4); and the second equality comes from substituting $\mathbf{D}^-$ according to (F.4).

Next we compute

$$\mathbf{D}^+\mathsf{R}^T_{3,-\varphi^+-\pi} = \begin{pmatrix} \mathbf{d}_1 & \mathbf{d}_3^+ \times \mathbf{d}_1 & \mathbf{d}_3^+ \end{pmatrix}, \quad \mathbf{D}^+\mathsf{Q}^T = \begin{pmatrix} \mathbf{d}_1 & \mathbf{d}_3^- \times \mathbf{d}_1 & \mathbf{d}_3^- \end{pmatrix}. \tag{F.6}$$

Applying Lemma 1, the equality (F.5) between matrices can be translated into an equality between operators:

$$\begin{aligned} & g^+[\mathbf{u}^+]_\times = g^-[\mathbf{u}^-]_\times + \frac{\mathrm{d}\varphi^-}{\mathrm{d}S}\,[\mathbf{d}_3^-]_\times + \frac{\mathrm{d}\theta}{\mathrm{d}S}\,[\mathbf{d}_1]_\times - \frac{\mathrm{d}\varphi^+}{\mathrm{d}S}\,[\mathbf{d}_3^+]_\times, \\ \Leftrightarrow\quad & [g^+\mathbf{u}^+]_\times = \left[g^-\mathbf{u}^- + \frac{\mathrm{d}\varphi^-}{\mathrm{d}S}\,\mathbf{d}_3^- + \frac{\mathrm{d}\theta}{\mathrm{d}S}\,\mathbf{d}_1 - \frac{\mathrm{d}\varphi^+}{\mathrm{d}S}\,\mathbf{d}_3^+\right]_\times. \\ \Leftrightarrow\quad & g^+\mathbf{u}^+ = g^-\mathbf{u}^- + \frac{\mathrm{d}\varphi^-}{\mathrm{d}S}\,\mathbf{d}_3^- + \frac{\mathrm{d}\theta}{\mathrm{d}S}\,\mathbf{d}_1 - \frac{\mathrm{d}\varphi^+}{\mathrm{d}S}\,\mathbf{d}_3^+. \end{aligned} \tag{F.7}$$

G Calculus for Section 6.2

In this section we derive equilibrium equations (6.31-6.37).

Next we project (3.28) along $\mathbf{c}_-$. Since

$$\begin{aligned} \big(\mathbf{N}'+\mathbf{F}\big)\cdot\mathbf{c}_- &= (\mathbf{N}\cdot\mathbf{c}_-)' - \mathbf{N}\cdot(\mathbf{c}_-)' + \mathbf{F}\cdot\mathbf{c}_- \\ &= -(\mathsf{N}_-)' - \left[\mathsf{N}_1\mathbf{c}^1 + \mathsf{N}_+\frac{\mathbf{c}^+}{\sin\theta} + \mathsf{N}_-\frac{\mathbf{c}^-}{\sin\theta}\right]\cdot\left[\left(\boldsymbol{\mathcal{U}} - \frac{\theta'}{2}\mathbf{c}_1\right)\times\mathbf{c}_-\right] + \mathbf{F}\cdot\mathbf{c}_-, \end{aligned}$$

we obtain

$$(\mathsf{N}_-)' = \left(\widehat{\mathcal{U}}_1 - \frac{\theta'}{2}\right)\left(\frac{\mathsf{N}_+ - \mathsf{N}_-\cos\theta}{\sin\theta}\right) - \frac{g^-}{a}(\alpha^- - \alpha^+ g\cos\theta)\mathsf{N}_1 + \mathbf{F}\cdot\mathbf{c}_-, \tag{G.1}$$

where we substituted $\boldsymbol{\mathcal{U}}$ according to (6.28). Similarly, $(\mathbf{N}'+\mathbf{F})\cdot\mathbf{c}_+ = 0$ leads to

$$(\mathsf{N}_+)' = -\left(\widehat{\mathcal{U}}_1 + \frac{\theta'}{2}\right)\left(\frac{\mathsf{N}_- - \mathsf{N}_+\cos\theta}{\sin\theta}\right) - \frac{g^-}{a}(\alpha^-\cos\theta - \alpha^+ g)\mathsf{N}_1 + \mathbf{F}\cdot\mathbf{c}_+, \tag{G.2}$$

and $(\mathbf{N}'+\mathbf{F})\cdot\mathbf{c}_1 = 0$ gives (6.31).

It turns out that (6.34-6.36) can be recovered in a similar fashion by projecting Eq. (3.29) on $\mathbf{c}^\pm$ and $\mathbf{c}^1$. Before we proceed, we however need to express $\mathbf{M}$ in function of $\mathbf{P}$.

First, we project (D.2) on $\mathbf{d}_3^\pm = \mathbf{c}_\pm$ (cf. Eq. (6.8)):

$$\mathsf{n}_3^+ = -\frac{1}{2}(\mathsf{N}_+ + \mathsf{n}_+), \qquad \text{and} \qquad \mathsf{n}_3^- = -\frac{1}{2}(\mathsf{N}_- - \mathsf{n}_-), \tag{G.3}$$

where the vector $\mathbf{n}$ was defined in App. D as $\mathbf{n} = \mathbf{n}^+ - \mathbf{n}^-$. Eqs. (G.3) can be reorganised as

$$\mathsf{n}_+ = -\mathsf{N}_+ - 2\,\mathsf{n}_3^+, \qquad \text{and} \qquad \mathsf{n}_- = \mathsf{N}_- + 2\,\mathsf{n}_3^-. \tag{G.4}$$

Second, we recall (D.6) where we expand $\mathbf{N}$ and $\mathbf{n}$ according to (6.17) and remember that the scalars $c^+ = a(1-\beta)$ and $c^- = a\beta$:

$$\mathbf{M} = \mathbf{m}^+ + \mathbf{m}^- + \frac{a}{2}\mathbf{d}_1\times\left(\mathsf{n}_1\mathbf{c}^1 + \mathsf{n}_+\frac{\mathbf{c}^+}{\sin\theta} + \mathsf{n}_-\frac{\mathbf{c}_-}{\sin\theta}\right) + \frac{a}{2}(1-2\beta)\mathbf{d}_1\times\left(\mathsf{N}_1\mathbf{c}^1 + \mathsf{N}_+\frac{\mathbf{c}^+}{\sin\theta} + \mathsf{N}_-\frac{\mathbf{c}_-}{\sin\theta}\right). \tag{G.5}$$

Substituting $\mathsf{n}_\pm$ according to (G.4) in (G.5) and remembering according to (6.9) that $\mathbf{d}_1 = \mathbf{c}^1$, we obtain

$$\mathbf{M} = \mathbf{m}^+ + \mathbf{m}^- + \frac{a}{2}\mathbf{c}^1\times\left(-2\,\mathsf{n}_3^+\frac{\mathbf{c}^+}{\sin\theta} + 2\,\mathsf{n}_3^-\frac{\mathbf{c}^-}{\sin\theta} - 2\beta\,\mathsf{N}_+\frac{\mathbf{c}^+}{\sin\theta} + 2\,(1-\beta)\mathsf{N}_-\frac{\mathbf{c}^-}{\sin\theta}\right). \tag{G.6}$$

Finally, we expand $\mathbf{m}^+ + \mathbf{m}^-$ according to (6.17) and use the relations (6.13,6.15) to obtain the following expression in which we recognise the components P^1, P^+ and P^- defined in (6.30)

$$\begin{aligned}\mathbf{M} &= \Big((\mathbf{m}^+ + \mathbf{m}^-)\cdot\mathbf{c}^1\Big)\mathbf{c}_1 - \Big((\mathbf{m}^+ + \mathbf{m}^-)\cdot\mathbf{c}^+\Big)\frac{\mathbf{c}_+}{\sin\theta} - \Big((\mathbf{m}^+ + \mathbf{m}^-)\cdot\mathbf{c}^-\Big)\frac{\mathbf{c}_-}{\sin\theta} \\ &\quad -a\mathsf{n}_3^-\frac{\mathbf{c}_+}{\sin\theta} - a\mathsf{n}_3^+\frac{\mathbf{c}_-}{\sin\theta} - a\,(1-\beta)\mathsf{N}_-\frac{\mathbf{c}_+}{\sin\theta} - a\,\beta\mathsf{N}_+\frac{\mathbf{c}_-}{\sin\theta} \\ &= \mathbf{P} - a(1-\beta)\frac{\mathsf{N}_-\mathbf{c}_+}{\sin\theta} - a\beta\frac{\mathsf{N}_+\mathbf{c}_-}{\sin\theta}, \end{aligned} \tag{G.7}$$

We are now ready to project (3.29) on $\mathbf{c}^-$. To this intend, let us compute

$$\begin{aligned}&\big(\mathbf{M}' + \mathbf{r}'\times\mathbf{N}\big)\cdot\mathbf{c}^- \\ &= \big(\mathbf{M}\cdot\mathbf{c}^-\big)' - \mathbf{M}\cdot(\mathbf{c}^-)' + (\mathbf{c}^-\times\mathbf{r}')\cdot\mathbf{N} \\ &= (-\mathsf{P}^- + a\beta\mathsf{N}_+)' \\ &\quad - \left(\mathsf{P}^1\mathbf{c}_1 + \mathsf{P}^+\frac{\mathbf{c}_+}{\sin\theta} + \mathsf{P}^-\frac{\mathbf{c}_-}{\sin\theta} - a\,(1-\beta)\frac{\mathsf{N}_-\mathbf{c}_+}{\sin\theta} - a\,\beta\frac{\mathsf{N}_+\mathbf{c}_-}{\sin\theta}\right)\cdot\left[\left(\mathcal{U} + \frac{\theta'}{2}\mathbf{c}_1\right)\times\mathbf{c}^-\right] \\ &\qquad +g^-\left(\mathbf{c}^-\times\left((1-\beta)\alpha^-\mathbf{c}_- + \beta\alpha^+ g\mathbf{c}_+\right)\right)\cdot\mathbf{N}. \end{aligned} \tag{G.8}$$

Next, in Eq. (G.8), substitute $(\mathsf{N}_+)'$ according to (G.2) and use (6.28) to compute the factor in the square bracket:

$$\begin{aligned}&\big(\mathbf{M}' + \mathbf{r}'\times\mathbf{N}\big)\cdot\mathbf{c}^- \\ &= -(\mathsf{P}^-)' - a\beta\left(\mathcal{U} + \frac{\theta'}{2}\right)\left(\frac{\mathsf{N}_- - \mathsf{N}_+\cos\theta}{\sin\theta}\right) - g^-\beta(\alpha^-\cos\theta - \alpha^+ g)\mathsf{N}_1 + a\beta\mathbf{F}\cdot\mathbf{c}_+ \\ &\quad +\mathsf{P}_1\frac{g^-}{a}\sin\theta\alpha^- + \left(\mathcal{U} + \frac{\theta'}{2}\right)\frac{\mathsf{P}^+ + \mathsf{P}^-\cos\theta}{\sin\theta} - \left(\mathcal{U} + \frac{\theta'}{2}\right)a\frac{(1-\beta)\mathsf{N}_- + \beta\mathsf{N}_+\cos\theta}{\sin\theta} \\ &\qquad -\frac{g^-}{a}a\mathsf{N}_1\left((1-\beta)\alpha^-\cos\theta + \beta\alpha^+ g\right), \end{aligned} \tag{G.9}$$

$$\begin{aligned}&= -(\mathsf{P}^-)' - a\left(\mathcal{U} + \frac{\theta'}{2}\right)\frac{\mathsf{N}_-}{\sin\theta} - \frac{g^-}{a}\alpha^-\cos\theta\, a\,\mathsf{N}_1 + +a\beta\mathbf{F}\cdot\mathbf{c}_+ \\ &\quad +\frac{g^-}{a}\alpha^-\sin\theta\mathsf{P}_1 + \left(\mathcal{U} + \frac{\theta'}{2}\right)\frac{\mathsf{P}^+ + \mathsf{P}^-\cos\theta}{\sin\theta}. \end{aligned} \tag{G.10}$$

Finally substituting (G.10) in (3.29) gives

$$(\mathsf{P}^-)' = \frac{g^-}{a}\alpha^-\left(\mathsf{P}^1\sin\theta - a\mathsf{N}_1\cos\theta\right) + \left(\frac{\theta'}{2} + \mathcal{U}\right)\frac{\mathsf{P}^+ + \mathsf{P}^-\cos\theta - a\mathsf{N}_-}{\sin\theta} + a\beta\mathbf{F}\cdot\mathbf{c}_+ + \mathbf{L}\cdot\mathbf{c}^-, \tag{G.11}$$

which the balance equation (6.35).

Similarly, projecting (3.29) on $\mathbf{c}^1$ and on $\mathbf{c}^+$ gives (6.34,6.36) and projecting (3.32) on $\mathbf{c}_1$ gives (6.37) after a similar sequence of steps.

H Linear constitutive laws for moments $\mathbf{m}^\pm$

As mentioned in Sec. 6.3, the constitutive laws for $\mathbf{m}^\pm$ can be written in function of $\alpha^\pm$, θ and $\mathcal{U}$. Here we carry out this computation in the most common case of linear constitutive laws for $\mathbf{m}^\pm$. Note that practically, not only do we need to express the laws in function of the adequate variable but also to project them on the frames $\{\mathbf{c}^1, \mathbf{c}^+, \mathbf{c}^-\}$ in which we intend to perform further computations.

$$
\begin{aligned}
\mathbf{m}^{\pm} &= (EI)^{\pm}\left[(\mathsf{u}_1^{\pm}-\widehat{\mathsf{u}}_1^{\pm})\mathbf{d}_1^{\pm}+b^{\pm}(\mathsf{u}_2^{\pm}-\widehat{\mathsf{u}}_2^{\pm})\mathbf{d}_2^{\pm}+\Gamma^{\pm}(\mathsf{u}_3^{\pm}-\widehat{\mathsf{u}}_3^{\pm})\mathbf{d}_3^{\pm}\right]\\
&= (EI)^{\pm}\left[\mathbf{u}^{\pm}-\widehat{\mathbf{u}}^{\pm}+(b^{\pm}-1)\left[(\mathbf{u}^{\pm}-\widehat{\mathbf{u}}^{\pm})\cdot\mathbf{d}_2^{\pm}\right]\,\mathbf{d}_2^{\pm}+(\Gamma^{\pm}-1)\left[(\mathbf{u}^{\pm}-\widehat{\mathbf{u}}^{\pm})\cdot\mathbf{d}_3^{\pm}\right]\,\mathbf{d}_3^{\pm}\right]\\
&= \frac{(EI)^{\pm}}{g^{\pm}}\Big\{\boldsymbol{\mathcal{U}}\pm\frac{\theta'}{2}\mathbf{c}^1-\left(\varphi^{\pm}\right)'\mathbf{c}_{\pm}-g^{\pm}\widehat{\mathbf{u}}^{\pm}-(\Gamma^{\pm}-1)\left[\sin\theta\alpha^{\mp}g^{\mp}+\left(\varphi^{\pm}\right)'+g^{\pm}\widehat{\mathsf{u}}_3^{\pm}\right]\mathbf{c}_{\pm}\\
&\qquad +(b^{\pm}-1)\left(\cos\varphi^{\pm}\;\mathbf{c}^{\mp}\mp\sin\varphi^{\pm}\;\mathbf{c}^1\right)\\
&\qquad\qquad\left(\left[\boldsymbol{\mathcal{U}}\pm\frac{\theta'}{2}\mathbf{c}^1-\left(\varphi^{\pm}\right)'\mathbf{c}_{\pm}\right]\cdot\left(\cos\varphi^{\pm}\;\mathbf{c}^{\mp}\mp\sin\varphi^{\pm}\;\mathbf{c}^1\right)-g^{\pm}\widehat{\mathsf{u}}_2^{\pm}\right)\Big\}\\
&= \frac{(EI)^{\pm}}{ag^{\pm}}\left[a\left[\mathcal{U}\pm\frac{\theta'}{2}\pm g^{\pm}(\widehat{\mathsf{u}}_1^{\pm}\cos\varphi^{\pm}+\widehat{\mathsf{u}}_2^{\pm}\sin\varphi^{\pm})\right]\mathbf{c}^1+\alpha^{-}g^{-}\mathbf{c}^{+}+\alpha^{+}g^{+}\mathbf{c}^{-}\right.\\
&\qquad -ag^{\pm}\left(\widehat{\mathsf{u}}_2^{\pm}\cos\varphi^{\pm}-\widehat{\mathsf{u}}_1^{\pm}\sin\varphi^{\pm}\right)\mathbf{c}^{\mp}-ag^{\pm}\left(\widehat{\mathsf{u}}_3^{\pm}+\frac{\mathrm{d}\varphi^{\pm}}{\mathrm{d}S^{\pm}}\right)\mathbf{c}_{\pm}\\
&\qquad -(\Gamma^{\pm}-1)\left[\sin\theta\;\alpha^{\mp}g^{\mp}+a\,g^{\pm}\left(\widehat{\mathsf{u}}_3^{\pm}+\frac{\mathrm{d}\varphi^{\pm}}{\mathrm{d}S^{\pm}}\right)\right]\mathbf{c}_{\pm}\\
&\qquad +(b^{\pm}-1)\left(\cos\varphi^{\pm}\;\mathbf{c}^{\mp}\mp\sin\varphi^{\pm}\;\mathbf{c}^1\right)\\
&\qquad\qquad\left.\left[\mp\sin\varphi^{\pm}\;a\,(\mathcal{U}\pm\frac{\theta'}{2})-\cos\varphi^{\pm}\;(\alpha^{\mp}g^{\mp}\cos\theta-\alpha^{\pm}g^{\pm})-ag^{\pm}\widehat{\mathsf{u}}_2^{\pm}\right]\right]
\end{aligned}
\tag{H.1}
$$

Next let us define a measure (EI) of the total stiffness of the birod together with the total reference curvatures and twists $\widehat{\mathcal{U}}_i$ about key directions

$$
\begin{aligned}
(EI)&=\frac{(EI)^{+}}{g}+(EI)^{-}, & \widehat{\mathcal{U}}_0&=a\,(g\hat{\mathbf{u}}^{+}-\hat{\mathbf{u}}^{-})\cdot\mathbf{d}_1,\\
\mathcal{E}^{+}&=\frac{(EI)^{+}}{g(EI)}, & \widehat{\mathcal{U}}_1&=a\,(g\hat{\mathbf{u}}^{+}+\hat{\mathbf{u}}^{-})\cdot\mathbf{d}_1,\\
\mathcal{E}^{-}&=\frac{(EI)^{-}}{(EI)}, & \widehat{\mathcal{U}}_2^{\pm}&=a\,\frac{g^{\pm}}{g^{-}}\,(\hat{\mathbf{u}}^{\pm}\cdot\mathbf{c}^{\mp}),\\
& & \widehat{\mathcal{U}}_3^{\pm}&=a\,\frac{g^{\pm}}{g^{-}}\,\left(\hat{\mathsf{u}}_3^{\pm}+\frac{\mathrm{d}\varphi^{\pm}}{\mathrm{d}S^{\pm}}\right).
\end{aligned}
\tag{H.2}
$$

which can be inverted to obtain

$$
\begin{aligned}
\hat{\mathsf{u}}_1^{\pm} &= \frac{-g^{-}}{ag^{\pm}}\left(\cos\varphi^{\pm}\,(\widehat{\mathcal{U}}_0\pm\widehat{\mathcal{U}}_1)+\sin\varphi^{\pm}\widehat{\mathcal{U}}_2^{\pm}\right),\\
\hat{\mathsf{u}}_2^{\pm} &= \frac{g^{-}}{ag^{\pm}}\left(-\sin\varphi^{\pm}\,(\widehat{\mathcal{U}}_0\pm\widehat{\mathcal{U}}_1)+\cos\varphi^{\pm}\widehat{\mathcal{U}}_2^{\pm}\right),\\
\hat{\mathsf{u}}_3^{\pm} &= \frac{g^{-}}{a\,g^{\pm}}\widehat{\mathcal{U}}_3^{\pm}-\frac{\mathrm{d}\varphi^{\pm}}{\mathrm{d}S^{\pm}}.
\end{aligned}
\tag{H.3}
$$

In particular,

$$
\hat{\mathsf{u}}_1^{\pm}\cos\varphi^{\pm}+\hat{\mathsf{u}}_2^{\pm}\sin\varphi^{\pm}=-\frac{g^{-}}{ag^{\pm}}\left(\frac{\widehat{\mathcal{U}}_0}{2}\pm\frac{\widehat{\mathcal{U}}_1}{2}\right),
\tag{H.4}
$$

$$
\hat{\mathsf{u}}_2^{\pm}\cos\varphi^{\pm}-\hat{\mathsf{u}}_1^{\pm}\sin\varphi^{\pm}=\frac{g^{-}}{a\,g^{\pm}}\widehat{\mathcal{U}}_2^{\pm}.
\tag{H.5}
$$

The substitution of (H.3-H.5) in (H.1) gives

$$\begin{aligned}\mathbf{m}^{\pm} &= \frac{(EI)^{\pm}}{ag^{\pm}}\left\{a\left[\left(\mathcal{U}-\frac{g^{-}}{a}\frac{\widehat{\mathcal{U}}_1}{2}\right)\pm\left(\frac{\theta'}{2}-\frac{g^{-}}{a}\frac{\widehat{\mathcal{U}}_0}{2}\right)\right]\mathbf{c}^1+\alpha^{-}g^{-}\mathbf{c}^{+}+\alpha^{+}g^{+}\mathbf{c}^{-}\right.\\ &\quad -(\Gamma^{\pm}-1)\sin\theta\ \alpha^{\mp}g^{\mp}\mathbf{c}_{\pm}-g^{-}\widehat{\mathcal{U}}_2^{\pm}\mathbf{c}^{\mp}-g^{-}\Gamma^{\pm}\widehat{\mathcal{U}}_3^{\pm}\mathbf{c}_{\pm}\\ &\quad -(b^{\pm}-1)\left(\cos\varphi^{\pm}\ \mathbf{c}^{\mp}\mp\sin\varphi^{\pm}\ \mathbf{c}^1\right)\\ &\quad \left(a\sin\varphi^{\pm}\left[\left(\frac{\theta'}{2}-\frac{g^{-}}{a}\frac{\widehat{\mathcal{U}}_0}{2}\right)\pm\left(\mathcal{U}-\frac{g^{-}}{a}\frac{\widehat{\mathcal{U}}_1}{2}\right)\right]\right.\\ &\quad \left.\left.+\cos\varphi^{\pm}\left(\alpha^{\mp}g^{\mp}\cos\theta-\alpha^{\pm}g^{\pm}+g^{-}\widehat{\mathcal{U}}_2^{\pm}\right)\right)\right\}. \end{aligned}\tag{H.6}$$

The last term in (H.6) is by far the most complicated one. It accounts for the fact that if one of the sub-sections does not have the symmetries of the square ($b^{\chi}=1$), and if the common chord $\mathbf{d}_1$ is not aligned with a principal axis of that sub-section, their is a coupling between the birod bending about $\mathbf{d}_1$ and the stretches in the sub rods. For the sake of clarity, we ignore that case (a mere algebraic complication) and focus on either of two cases: $b^{\chi}=1$ or $\varphi^{\chi}=k\,\pi$ ($k\in\mathbb{Z}$), both for $\chi=+$ and $\chi=-$.

Under these restrictions (H.6) simplifies to

$$\begin{aligned}\mathbf{m}^{\pm} &= \frac{(EI)^{\pm}}{ag^{\pm}}\left\{a\left[\left(\mathcal{U}-\frac{g^{-}}{a}\frac{\widehat{\mathcal{U}}_1}{2}\right)\pm\left(\frac{\theta'}{2}-\frac{g^{-}}{a}\frac{\widehat{\mathcal{U}}_0}{2}\right)\right]\mathbf{c}^1+\alpha^{-}g^{-}\mathbf{c}^{+}+\alpha^{+}g^{+}\mathbf{c}^{-}\right.\\ &\quad -(\Gamma^{\pm}-1)\sin\theta\ \alpha^{\mp}g^{\mp}\mathbf{c}_{\pm}-g^{-}\widehat{\mathcal{U}}_2^{\pm}\mathbf{c}^{\mp}-g^{-}\Gamma^{\pm}\widehat{\mathcal{U}}_3^{\pm}\mathbf{c}_{\pm}\\ &\quad \left.-(b^{\pm}-1)\left(\alpha^{\mp}g^{\mp}\cos\theta-\alpha^{\pm}g^{\pm}+g^{-}\widehat{\mathcal{U}}_2^{\pm}\right)\mathbf{c}^{\mp}\right\}. \end{aligned}\tag{H.7}$$

Substituting Eq. (H.7) in the definitions (6.30) allows to find the constitutive laws for P^1, P^{+},

P^-, Q^1, Q^+ and Q^-:

$$\mathsf{P}^1 = \left(\mathbf{m}^+ + \mathbf{m}^-\right)\cdot\mathbf{c}^1 = \frac{(EI)}{g^-}\left[\left(\mathcal{U} - \frac{g^-}{a}\frac{\widehat{\mathcal{U}}_1}{2}\right) + \left(\mathcal{E}^+ - \mathcal{E}^-\right)\left(\frac{\theta'}{2} - \frac{g^-}{a}\frac{\widehat{\mathcal{U}}_0}{2}\right)\right], \tag{H.8}$$

$$\begin{aligned}\mathsf{P}^+ &= -\left(\mathbf{m}^+ + \mathbf{m}^-\right)\cdot\mathbf{c}^+ - a\mathsf{n}_3^- \\ &= -a\mathsf{n}_3^-(\alpha^-) - \frac{(EI)}{a}\left[b^-\mathcal{E}^-\left(\alpha^- - \alpha^+ g\cos\theta - \widehat{\mathcal{U}}_2^-\right)\right. \\ &\qquad -b^+\mathcal{E}^+\cos\theta\left(\alpha^+ g - \alpha^-\cos\theta - \widehat{\mathcal{U}}_2^+\right) \\ &\qquad \left.+\mathcal{E}^+\Gamma^+\sin\theta\left(\alpha^-\sin\theta + \widehat{\mathcal{U}}_3^+\right)\right],\end{aligned} \tag{H.9}$$

$$\begin{aligned}\mathsf{P}^- &= -\left(\mathbf{m}^+ + \mathbf{m}^-\right)\cdot\mathbf{c}^- - a\mathsf{n}_3^+ \\ &= -a\mathsf{n}_3^+(\alpha^+) - \frac{(EI)}{a}\left[b^+\mathcal{E}^+\cos\theta\left(\alpha^+ g - \alpha^-\cos\theta - \widehat{\mathcal{U}}_2^+\right)\right. \\ &\qquad -b^-\mathcal{E}^-\cos\theta\left(\alpha^- - \alpha^+ g\cos\theta - \widehat{\mathcal{U}}_2^-\right) \\ &\qquad \left.+\mathcal{E}^-\Gamma^-\sin\theta\left(\alpha^+ g\sin\theta + \widehat{\mathcal{U}}_3^+\right)\right],\end{aligned} \tag{H.10}$$

$$\mathsf{Q}_1 = \left(\mathbf{m}^+ - \mathbf{m}^-\right)\cdot\mathbf{c}_1 = \frac{(EI)}{g^-}\left[\left(\frac{\theta'}{2} - \frac{g^-}{a}\frac{\widehat{\mathcal{U}}_0}{2}\right) + \left(\mathcal{E}^+ - \mathcal{E}^-\right)\left(\mathcal{U} - \frac{g^-}{a}\frac{\widehat{\mathcal{U}}_1}{2}\right)\right], \tag{H.11}$$

$$\mathsf{Q}_+ = -\mathbf{m}^-\cdot\mathbf{c}_+ = \frac{(EI)}{a}\left[\mathcal{E}^- b^-\sin\theta\left(\alpha^- - \alpha^+ g\cos\theta - \widehat{\mathcal{U}}_2^-\right) + \mathcal{E}^-\Gamma^-\cos\theta\left(\alpha^+ g\sin\theta + \widehat{\mathcal{U}}_3^-\right)\right], \tag{H.12}$$

$$\mathsf{Q}_- = -\mathbf{m}^+\cdot\mathbf{c}_- = \frac{(EI)}{a}\left[\mathcal{E}^+ b^+\sin\theta\left(\alpha^+ g - \alpha^-\cos\theta - \widehat{\mathcal{U}}_2^+\right) + \mathcal{E}^+\Gamma^+\cos\theta\left(\alpha^-\sin\theta + \widehat{\mathcal{U}}_3^+\right)\right]. \tag{H.13}$$

We also note that in the simplified case where the cross-sections of the sub-rods have at least the symmetries of the square: $b^\pm = 1$ and after defining

I A computationally friendly version of the birod equilibrium equations

We note that $\{\mathbf{c}_1, \mathbf{c}^+, \mathbf{c}_-\}$ and $\{\mathbf{c}_1, -\mathbf{c}^-, \mathbf{c}_+\}$ form right handed bases which are simply the bases $\{\mathbf{d}_1^-, \mathbf{d}_2^-, \mathbf{d}_3^-\}$ rotated by φ^- about $\mathbf{d}_3^-$ and $\{\mathbf{d}_1^+, \mathbf{d}_2^+, \mathbf{d}_3^+\}$ rotated by $\varphi^+ + \pi$ about $\mathbf{d}_3^+$ respectively. According to (6.24,6.25), their Darboux vectors are $\left(\mathcal{U} - \frac{\theta'}{2}\right)\mathbf{c}_1 + \frac{g^-}{a}\alpha^-\mathbf{c}^+ + \frac{g^-}{a}\alpha^+ g\mathbf{c}^-$ and $\left(\mathcal{U} + \frac{\theta'}{2}\right)\mathbf{c}_1 + \frac{g^-}{a}\alpha^-\mathbf{c}^+ + \frac{g^-}{a}\alpha^+ g\mathbf{c}^-$ respectively.

In Sections 6.1, 6.2 & 6.3 we established that the equilibria of birods may be described by the four scalars $\alpha^\pm$, θ and $\mathcal{U}$ and the 7 equations (6.31-6.37) involving 10 momenta 7 of which have constitutive laws. While the previous discussions suggest that this is actually a minimal description of the system, some factors in Eqs. (6.31-6.37) involve divisions by $\sin\theta$. Not only this poses an obvious numerical issue, but also it makes it difficult to recover a 2D theory for which $\theta = 0$ along the whole length of the birod. The current section addresses those issues by proving that the 7 equilibrium equations (6.31-6.37) can be replaced by the 11 equilibrium equations (I.23-I.33) with

4 extra mechanical variables. The latter system presents the advantage that it no longer involves division by $\sin\theta$.

Before we proceed, a geometrical property must be highlighted. Let $\{\mathbf{d}_1(R), \mathbf{d}_2(R), \mathbf{d}_3(R)\}$ be a smooth one-parameter family of right handed orthonormal frames (like for instance the frame of directors of a single Kirchhoff rod), the Darboux vector of which is $\mathbf{u}$. For any vector field $\mathbf{v}$ depending on R, we have

$$\mathbf{v}(R) = \mathsf{v}_1(R)\mathbf{d}_1(R) + \mathsf{v}_2(R)\mathbf{d}_2(R) + \mathsf{v}_3(R)\mathbf{d}_3(R),$$

the derivative of which is

$$\begin{aligned} \mathbf{v}' &= (\mathsf{v}_i)'\mathbf{d}_i + \mathsf{v}_i(\mathbf{u}\times\mathbf{d}_i), \\ &= (\mathsf{v}_i)'\mathbf{d}_i + \mathbf{u}\times\mathbf{v}. \end{aligned}$$

Furthermore, the projection of this derivative on one of the basis vector gives

$$\mathbf{v}'\cdot\mathbf{d}_j = \mathsf{v}_j' + (\mathbf{d}_j\times\mathbf{u})\cdot\mathbf{v}. \tag{I.1}$$

We are now ready to proceed. First the factors involving division by $\sin\theta$ in (6.32,6.33) can easily be substituted for $\mathsf{N}^\pm$ according to (6.19). By so doing, we however add two variables, namely $\mathsf{N}^\pm$, to the theory. Accordingly, two more equations must be provided. This could be achieved by projecting (3.28) on $\mathbf{c}^\pm$ in a similar fashion to what we did in App. G to obtain (6.32,6.33). Let us however outline an alternative approach.

At the end of Sec. 6.1 we remarked that $\{\mathbf{c}_1, \mathbf{c}^+, \mathbf{c}_-\}$ form a right handed orthonormal basis. Hence for any vector $\mathbf{v}$, we obtain $\mathbf{v} = \mathsf{v}_1\mathbf{c}_1 - \mathsf{v}^+\mathbf{c}^+ - \mathsf{v}_-\mathbf{c}_-$ where the unfamiliar signs are due to the definitions (6.16). The Darboux vector of $\{\mathbf{c}_1(S), \mathbf{c}^+(S), \mathbf{c}_-(S)\}$ is

$$\mathbf{q}^- = \left(\mathcal{U} - \frac{\theta'}{2}\right)\mathbf{c}_1 + \frac{g^-}{a}\alpha^-\mathbf{c}^+ + \frac{g^-}{a}\alpha^+ g\mathbf{c}^-. \tag{I.2}$$

Making use of (I.1), we can easily project (3.28) on $\{\mathbf{c}_1, \mathbf{c}^+, \mathbf{c}_-\}$. As a result, we obtain

$$\begin{cases} \mathsf{N}_1' + (\mathbf{c}_1\times\mathbf{q}^-)\cdot\mathbf{N} + \mathsf{F}_1 = 0, \\ (\mathsf{N}^+)' - (\mathbf{c}^+\times\mathbf{q}^-)\cdot\mathbf{N} + \mathsf{F}^+ = 0, \\ \mathsf{N}_-' - (\mathbf{c}_-\times\mathbf{q}^-)\cdot\mathbf{N} + \mathsf{F}_- = 0. \end{cases} \tag{I.3}$$

Substituting (I.2) in (I.3), we obtain

$$\mathsf{N}_1' + \frac{g^-}{a}\left(\alpha^+ g\mathsf{N}_+ - \alpha^-\mathsf{N}_-\right) + \mathsf{F}_1 = 0, \tag{I.4}$$

$$(\mathsf{N}^+)' + \frac{g^-}{a}\alpha^+ g\,\sin\theta\,\mathsf{N}_1 - \left(\mathcal{U} - \frac{\theta'}{2}\right)\mathsf{N}_- + \mathsf{F}^+ = 0, \tag{I.5}$$

$$\mathsf{N}_-' + \frac{g^-}{a}\left(\alpha^- - \alpha^+ g\,\cos\theta\right)\mathsf{N}_1 + \left(\mathcal{U} - \frac{\theta'}{2}\right)\mathsf{N}^+ + \mathsf{F}_- = 0. \tag{I.6}$$

With (I.4) and (I.6), we recover (6.31) and (6.32) after making use of (6.19). The equation (I.5) however was not part of (6.31-6.37) and is one of the two equations we are looking for. The second one can be obtained by repeating the steps highlighted here but this time projecting (3.28) on the orthonormal basis $\{\mathbf{c}_1, -\mathbf{c}^-, \mathbf{c}_+\}$, the Darboux vector of which is

$$\mathbf{q}^+ = \left(\mathcal{U} + \frac{\theta'}{2}\right)\mathbf{c}_1 + \frac{g^-}{a}\alpha^-\mathbf{c}^+ + \frac{g^-}{a}\alpha^+ g\mathbf{c}^-. \tag{I.7}$$

As a result, we obtain (6.31) a third time together with

$$(\mathsf{N}^-)' + \left(\mathcal{U} + \frac{\theta'}{2}\right)\mathsf{N}_+ - \frac{g^-}{a}\alpha^- \sin\theta\,\mathsf{N}_1 + \mathsf{F}^- = 0, \tag{I.8}$$

$$\mathsf{N}'_+ - \frac{g^-}{a}\left(\alpha^+ g - \alpha^- \cos\theta\right)\mathsf{N}_1 - \left(\mathcal{U} + \frac{\theta'}{2}\right)\mathsf{N}^- + \mathsf{F}_+ = 0, \tag{I.9}$$

where (I.9) is equivalent to (6.33) after making use of (6.19) and Eq. (I.8) is new. The system of five equations (I.4-I.6,I.8-I.9) with the five unknown N_1, $\mathsf{N}_\pm$, $\mathsf{N}^\pm$ has been obtained by projecting the vectorial equation (3.28) on various unit vectors[14]. In that sense, it leads to the same set of solutions (under suitable initial or boundary conditions) as the system (6.31-6.32) which was obtained by projecting the same vectorial equations on a different set of unit vectors[14].

Next let us define the total moment $\mathbf{A}$ about $\mathbf{r}^-$ according to (3.27) with $c^+ = a$ and $c^- = 0$ and the total moment $\mathbf{B}$ about $\mathbf{r}^+$ according to (3.27) with $c^+ = 0$ and $c^- = a$:

$$\mathbf{A} = \mathbf{m}^+ + \mathbf{m}^- + a\,\mathbf{d}_1 \times \mathbf{n}^+, \qquad \& \qquad \mathbf{B} = \mathbf{m}^+ + \mathbf{m}^- - a\,\mathbf{d}_1 \times \mathbf{n}^-. \tag{I.10}$$

It is not surprising that $\mathbf{A}$ and $\mathbf{B}$ being the total moments due to the same system of forces but about different points, we have (as can be proven by substituting $\mathbf{n}^+ = \mathbf{N} - \mathbf{n}^-$ in the definition of $\mathbf{A}$):

$$\mathbf{A} = \mathbf{B} + a\,\mathbf{d}_1 \times \mathbf{N}. \tag{I.11}$$

We observe that P^1 and $\mathsf{P}^\pm$ defined in (6.30) can be expressed as some components of $\mathbf{A}$ and $\mathbf{B}$ respectively:

$$\mathsf{P}^1 = \mathbf{A}\cdot\mathbf{c}^1 = \mathsf{A}^1 = \mathbf{B}\cdot\mathbf{c}^1 = \mathsf{B}^1, \qquad \mathsf{P}^+ = -\mathbf{B}\cdot\mathbf{c}^+ = \mathsf{B}^+, \qquad \text{and} \qquad \mathsf{P}^- = -\mathbf{A}\cdot\mathbf{c}^- = \mathsf{A}^-. \tag{I.12}$$

Furthermore, according to Eqs. (3.28,3.29), if the birod is in equilibrium $\mathbf{A}$ and $\mathbf{B}$ obey (3.29):

$$\mathbf{A}' + (\mathbf{r}^-)' \times \mathbf{N} + \mathbf{L}_A = \mathbf{0}, \tag{I.13}$$

$$\mathbf{B}' + (\mathbf{r}^+)' \times \mathbf{N} + \mathbf{L}_B = \mathbf{0}, \tag{I.14}$$

where $\mathbf{L}_A$ and $\mathbf{L}_B$ are defined according to (3.23) with $c^+ = a$, $c^- = 0$ and with $c^+ = 0$, $c^- = a$ respectively.

Projecting (I.13,I.14) on both the orthonormal bases $\{\mathbf{c}_1, -\mathbf{c}^-, \mathbf{c}_+\}$ and $\{\mathbf{c}_1, \mathbf{c}^+, \mathbf{c}_-\}$ the Darboux vectors of which are $\mathbf{q}^\pm$ defined in (I.2,I.7), we find

$$\mathsf{A}'_1 + \frac{g^-}{a}\left(\alpha^+ g\,\mathsf{A}_+ - \alpha^-\,\mathsf{A}_-\right) + \alpha^- g^- \mathsf{N}^+ + \mathsf{L}_1 = 0, \tag{I.15}$$

$$(\mathsf{A}^-)' + \left(\mathcal{U} + \frac{\theta'}{2}\right)\mathsf{A}_+ + \frac{g^-}{a}\alpha^-\left(\cos\theta\, a\mathsf{N}_1 - \sin\theta\,\mathsf{A}_1\right) + (\mathsf{L}_A)^- = 0, \tag{I.16}$$

$$\mathsf{A}'_+ - \frac{g^-}{a}\left(\alpha^+ g - \alpha^- \cos\theta\right)\mathsf{A}_1 - \left(\mathcal{U} + \frac{\theta'}{2}\right)\mathsf{A}^- + \frac{g^-}{a}\alpha^- a\mathsf{N}_1 + (\mathsf{L}_A)_+ = 0, \tag{I.17}$$

and

$$\mathsf{B}'_1 + \frac{g^-}{a}\left(\alpha^+ g\mathsf{B}_+ - \alpha^-\mathsf{B}_-\right) - \frac{g^-}{a}\alpha^+ g\, a\mathsf{N}^- + \mathsf{L}_1 = 0, \tag{I.18}$$

$$(\mathsf{B}^+)' + \frac{g^-}{a}\alpha^+ g\left(\sin\theta\,\mathsf{B}_1 - \cos\theta\, a\mathsf{N}_1\right) - \left(\mathcal{U} - \frac{\theta'}{2}\right)\mathsf{B}_- + (\mathsf{L}_B)^+ = 0, \tag{I.19}$$

$$\mathsf{B}'_- + \frac{g^-}{a}\left(\alpha^- - \alpha^+ g\cos\theta\right)\mathsf{B}_1 + \left(\mathcal{U} - \frac{\theta'}{2}\right)\mathsf{B}^+ - \frac{g^-}{a}\alpha^+ g\, a\mathsf{N}_1 + (\mathsf{L}_B)_- = 0. \tag{I.20}$$

[14] So that the set of these unit vectors generate $\mathbb{R}^3$.

Next, projecting (I.11) on $\mathbf{c}_\pm$, it is straightforward to show that $\mathsf{A}_- - a\mathsf{N}^+ = \mathsf{B}_-$ and $\mathsf{B}_+ - a\mathsf{N}^- = \mathsf{A}_+$ the substitution of which together with (I.12) in (I.15,I.18) show that both equations are equivalent and both read

$$(\mathsf{P}^1)' + \frac{g^-}{a}(\alpha^+ g\,\mathsf{A}_+ - \alpha^-\,\mathsf{B}_-) + \mathsf{L}_1 = 0. \tag{I.21}$$

Finally, using the definitions (3.26,6.30), the identites (6.18) and the relations (6.12-6.15), it is a matter of straightforward algebra to show that

$$\frac{\mathsf{P}^+ + \mathsf{P}^- \cos\theta - a\,\mathsf{N}_-}{\sin\theta} = -\mathsf{A}_+, \qquad \text{and} \qquad \frac{\mathsf{P}^- + \mathsf{P}^+ \cos\theta - a\,\mathsf{N}_+}{\sin\theta} = -\mathsf{B}_-. \tag{I.22}$$

Substituting (I.22) in (I.21) allows to recover equations (6.34). Similarly, the substitution of (I.22) in (I.19,I.16) leads to Eqs. (6.36,6.35). In conclusion, Eqs. (6.34-6.36) can be viewed as a sub-set of the projection of (I.13) and (I.14) on $\{\mathbf{c}_1, -\mathbf{c}^-, \mathbf{c}_+\}$ and $\{\mathbf{c}_1, \mathbf{c}^+, \mathbf{c}_-\}$ respectively.

Gathering the equations (I.4-I.6,I.16-I.17,I.19-I.20,I.21,6.37) in which we we substitute (I.22) and (I.12) as necessary, the full projection of $\mathbf{N}' + \mathbf{F} = \mathbf{0}$ and (I.13,I.14) together with (6.37) reads:

$$\mathsf{N}_1' + \frac{g^-}{a}\left(\alpha^+ g \mathsf{N}_+ - \alpha^- \mathsf{N}_-\right) + \mathsf{F}_1 = 0, \tag{I.23}$$

$$(\mathsf{N}^+)' + \frac{g^-}{a}\alpha^+ g\,\sin\theta\,\mathsf{N}_1 - \left(\mathcal{U} - \frac{\theta'}{2}\right)\mathsf{N}_- + \mathsf{F}^+ = 0, \tag{I.24}$$

$$\mathsf{N}_-' + \frac{g^-}{a}\left(\alpha^- - \alpha^+ g\,\cos\theta\right)\mathsf{N}_1 + \left(\mathcal{U} - \frac{\theta'}{2}\right)\mathsf{N}^+ + \mathsf{F}_- = 0, \tag{I.25}$$

$$(\mathsf{N}^-)' + \left(\mathcal{U} + \frac{\theta'}{2}\right)\mathsf{N}_+ - \frac{g^-}{a}\alpha^-\,\sin\theta\,\mathsf{N}_1 + \mathsf{F}^- = 0, \tag{I.26}$$

$$\mathsf{N}_+' - \frac{g^-}{a}\left(\alpha^+ g - \alpha^-\,\cos\theta\right)\mathsf{N}_1 - \left(\mathcal{U} + \frac{\theta'}{2}\right)\mathsf{N}^- + \mathsf{F}_+ = 0, \tag{I.27}$$

$$(\mathsf{P}^1)' + \frac{g^-}{a}(\alpha^+ g\,\mathsf{A}_+ - \alpha^-\,\mathsf{B}_-) + \mathsf{L}_1 = 0, \tag{I.28}$$

$$(\mathsf{A}^-)' + \left(\mathcal{U} + \frac{\theta'}{2}\right)\mathsf{A}_+ + \frac{g^-}{a}\alpha^-\left(\cos\theta\, a\mathsf{N}_1 - \sin\theta\,\mathsf{P}_1\right) + (\mathsf{L}_A)^- = 0, \tag{I.29}$$

$$\mathsf{A}_+' - \frac{g^-}{a}\left(\alpha^+ g - \alpha^-\,\cos\theta\right)\mathsf{P}_1 - \left(\mathcal{U} + \frac{\theta'}{2}\right)\mathsf{A}^- + \frac{g^-}{a}\alpha^- a\mathsf{N}_1 + (\mathsf{L}_A)_+ = 0, \tag{I.30}$$

$$(\mathsf{B}^+)' + \frac{g^-}{a}\alpha^+ g\left(\sin\theta\,\mathsf{P}_1 - \cos\theta\, a\mathsf{N}_1\right) - \left(\mathcal{U} - \frac{\theta'}{2}\right)\mathsf{B}_- + (\mathsf{L}_B)^+ = 0, \tag{I.31}$$

$$\mathsf{B}_-' + \frac{g^-}{a}\left(\alpha^- - \alpha^+ g\,\cos\theta\right)\mathsf{P}_1 + \left(\mathcal{U} - \frac{\theta'}{2}\right)\mathsf{B}^+ - \frac{g^-}{a}\alpha^+ g\, a\mathsf{N}_1 + (\mathsf{L}_B)_- = 0, \tag{I.32}$$

$$(\mathsf{Q}_1)' + \frac{g^-}{a}\left(\alpha^+ g\mathsf{A}_+ + \alpha^-\mathsf{B}_-\right) - \frac{2g^-}{a}\left(\mathsf{Q}_+\alpha^+ g + \mathsf{Q}_-\alpha^-\right) + 2\mathsf{l}_1 + \mathsf{h}_1 = 0, \tag{I.33}$$

where $\mathbf{F}$ is the line density of external forces applied on the birod, $\mathbf{L}_A$ and $\mathbf{L}_B$ are the line density of the total moment of external forces respectively about $\mathbf{r}^-$ and $\mathbf{r}^+$, and h_1 is the difference of line density of moment of external forces along $\mathbf{c}_1$. The set of 7 equations (6.31-6.37) expressing the equilibrium of forces and momenta of the birod can be replaced by the set of 11 equations (I.23-I.33). According to (I.12), the constitutive laws that were found for the components P^1, P^- and P^+ – see discussion in Sec. 6.3, or explicitly (6.46-6.48) – translate to constitutive laws respectively for P^1, A^- and B^+.

Regarding the variable count, the 4 extra equations in (I.23-I.33) compared to (6.31-6.37) are balanced by the additional 4 mechanical variables N^+, N^-, A_+ and B_-.